A MULTI-WELL CONCENTRATION GRADIENT DRUG DELIVERY MICROFLUIDIC DEVICE FOR HIGH-CONTENT AND HIGH-THROUGHPUT SCREENING

A MULTI-WELL CONCENTRATION GRADIENT DRUG DELIVERY MICROFLUIDIC DEVICE FOR HIGH-CONTENT AND HIGH-THROUGHPUT SCREENING

By

Michael Nelson

B.Eng (Lakehead University, Ontario, Canada)

A Thesis
Submitted to the School of Graduate Studies
in Partial Fulfillment of the Requirements for the Degree of
Master of Applied Science
McMaster University

MASTER OF APPLIED SCIENCE (2014) McMaster University

(Biomedical Engineering) Hamilton, Ontario

TITLE: A Multi-Well Concentration Gradient Drug Delivery Microfluidic Device for High-Content and High-Throughput Screening

AUTHOR: Michael Nelson,

B.Eng (Lakehead University, Ontario, Canada)

SUPERVISOR: Dr. Qiyin Fang,

Associate Professor (Engineering Physics, McMaster University)

Number of Pages: XI, 88

Abstract

A microfluidic device capable of drug delivery to multiple wells in a concentration gradient was designed for automated high content and high throughput screening. The design was proposed to utilize a nanoporous polycarbonate membrane to spatially and temporally control drug dosage from the microchannels below to the wells above. Microchannels were to hold to the drugs or reagents, while wells were to culture cells. An array of 16 wells was to fit in the equivalent area of a single well of a 96 well plate. Two simpler devices were created to validate electrokinetic drug delivery to a single well and to characterize cell proliferation and viability in micro-wells. The first device tested drug delivery to a single well with methylene blue dye at applied voltages of 100V, 125V, and 150V; diffusion times of the dye to reach extents of the well were also measured. It was validated that the dosage of dye could be controlled by increasing the voltage and by increasing the duration the voltage was applied; for a constant voltage, the dosage increased linearly with the duration that the voltage was applied (1, 2, and 3 minutes). The dye molecules had reached the extents of the well within 5 minutes after the voltage was turned off. The second devices were a series of 9-well arrays, each testing a different diameter (1.2 mm – 0.35 mm). These devices were cultured with MCF-7 breast cancer cells over 5 days. At the end of the 5 day study, all diameters except for 0.5 mm and 0.35 mm measured a cell viability of 99% and exhibited cell growth patterns similar to coverslip glass controls. The proposed integrated cell culture and drug delivery device could have application towards early stage drug discovery and could have compatibility with lab equipment originally designed for well plates.

Acknowledgements

This interdisciplinary project and thesis could not have been completed without the expertise and guidance of my research supervisor, Dr. Qiyin Fang. I would also like to thank my co-supervisors, Dr. Ravi Selvaganapathy and Dr. David Andrews, for their invaluable advice throughout my project. Much needed assistance was provided by Dr. Hanna Budz for cell culture and growth studies; graduate student Pouya Rezai provided help with clean room protocols and general advice on microfluidics. I would like to thank my parents for their unending support. I'd also like to sincerely thank all lab-mates, laboratory staff, and friends whom I've had the privilege of knowing.

Table of Contents

Title **Page**

List of Figures

Figure Page

Figure Page

List of Tables

Table **Page**

Nomenclature

BSC - Biosafety Cabinet

°C - Degrees Celsius

∇C - Concentration Gradient

DC - Direct Current

DI - De-Ionized

DNA - Deoxyribonucleic Acid

DRIE - Deep Reactive Ion Etching

g - Gram

HB - Hydrophobic

HCS - High-Content Screening

hr - Hour

HTS - High-Throughput Screening

in - Inch

IPA - Isopropyl Alcohol

J - Joule

$\vec{J}$ - Flux Vector

K^{-1} - Debye Length

L - Liter

M - Molar Concentration

m - Meter

min - Minute

mol - Mole

PBS - Phosphate Buffered Saline

PC - Polycarbonate

PCTE - PC Track-Etched

PD - Pharmacodynamics

PDMS - Polydimethylsiloxane

PE - Polyester

PK - Pharmacokinetics

PVP - polyvinylpyrrolidone

RE - Reynold's Number

RNA - Ribonucleic Acid

RNAi - RNA Interference

mRNA - Messenger RNA

siRNA - Short Interfering RNA

rpm - Revolutions-Per-Minute

s - Second

t - Time

V - Volt

% v/v - Volume Concentration

W - Watt

z - Ionic Charge

Chapter 1: Introduction

1.1 Motivation

Since the 1990s there have been increasing costs in drug discovery due to longer average drug approval times an increased rate of drug candidates being rejected of approval. One major factor of increased drug candidate rejection may be due to lack of relevant biological information gathered during the early phases of drug development. [Dickson M, 2004] As such there exists a need for new *in-vitro* drug testing technologies to potentially provide high-quality biological information in order to better predict what might possibly occur *in-vivo*; one such technology is microfluidics which contains channels and reservoirs on a size-scale similar to that of mammalian cells, can provide rapid spatial and temporal fluid flow control, and can perform several tasks in parallel. Conversely, current *in-vitro* drug screening is currently performed in well plates; high density well plates, usually at 1532 wells and greater, can have difficulties with cell culture because of high capillary and surface tension forces that liquids can exert on cells. To address these problems, we have proposed to design and construct a microfluidic lab-on-a-chip device capable of delivering drug reagents, in a dosage gradient, to mammalian cells growing in micro-wells.

1.2 Organization of Thesis

The thesis is divided into three main chapters: multi-well drug delivery design, electrokinetic drug delivery validation of a single well, and cell seeding in PDMS micro-wells. Chapter 2 describes the design, proposed fabrication, and proposed experimental procedures for an integrated multi-well drug delivery microfluidic device with cell culture; the chapter concludes by stating that drug delivery and cell seeding need to be validated separately, before fabrication of an integrated device can begin. Chapter 3 outlines the validation for electrokinetic drug delivery, through a nanoporous membrane, into a single well. The validation study for Chapter 3 was based off the previous work by R. Selvaganapathy *et. al.*, in which drug delivery was characterized by measuring rate of dye spot size increase, and measuring dye dosage with input voltage. Chapter 3 concludes by confirming dye spot size and dye dosage can be control with input voltage and with the length of time the voltage was applied; however, it is addressed that there is still a need for dye delivery validation studies on devices with multiple wells. Chapter 4 describes the design, fabrication, and experimental procedure of several multi-well devices for testing cell

attachment, proliferation, and viability; the chapter concludes with stating that, with the exception of 0.35 mm and 0.5 mm diameters, all parameters tested had similar cell viability and similar cell proliferation to those found in the controls. The 5th and final Chapter summarizes the entire thesis and concludes that drug delivery and cell seeding in PDMS micro-wells looks promising when looked at individually, however these two modalities must still be integrating into a single device before any cellular assays can be implemented.

1.3 Drug Discovery

Drug discovery is the process of investigating a therapeutic effect from known or unknown biomolecules on a human disease or pathological condition. The disease under investigation can either be acute or chronic. If successful, the entire drug discovery process can typically last between 10 to 20 years, depending upon the disease and target. [Dickson M, 2004] Potential drugs must go through several steps of investigation: *in-vitro* laboratory trials of cells in culture, animal *in-vivo* laboratory trials, and clinical trials in humans (Figure 1.1).

Laboratory trials first start with *in-vitro* experiments on cells in culture. A large number of potential drugs are created from combinatorial chemistry, and are delivered to cells in culture to see their effect against a certain biomolecule such as a protein. Any potential drugs that have produced the desired effect, and at the desired range of concentrations, are then labeled as a hit; generated hits are then put through more rigorous testing than before. Any hits that pass these trials are then labeled as potentials drug leads. These drug leads are then tested in *in-vivo* animal trials to provide a systemic biological context.

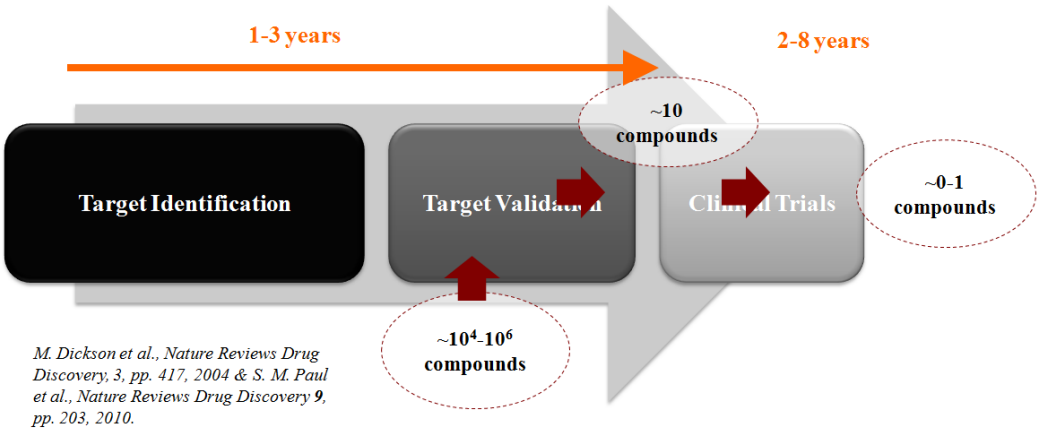

Figure 1.1: Stages in the drug discovery process. Potential target compounds are tested and validated through *in-vitro* trials, usually taking up to 3 years. Around 10 compounds are then subjected to animal trials, then clinical trials. Effective testing of drug candidates during *in-vitro* trials can lead to a greater chance of success that they will pass the later stages of drug development.

Once drug leads have been established, they are to undergo *in-vivo* trials in animal models. Hopefully the *in-vitro* trials will be able to predict the behaviour of the drug leads *in-vivo*. However, this may not always be so because of several complexities in *in-vivo* cancer tumors. Tumors are complex tissues, meaning that multiple cell types are interacting together. Cell types in tumors that aren't tested *in-vitro* can have an effect on anti-cancer drug leads. For example, stromal cells can release anti-apoptotic agents such as insulin-like growth factor-1 (IGF-1). [Weinberg NA, 2007] Furthermore, *in-vitro* cell lines may not behave like cancer cells in patients. *In-vitro* cancer cell lines are usually very robust and may have adapted over time to *in-vitro* conditions. Rats are a common animal model used for testing. However, rat tumors are usually not like human tumors; as such, human cell lines are grafted into the rats, where they will eventually grow into tumors. Even so, these grafted human tumors may still not behave like tumors in patients due to reasons explained above. Two major factors in determining the *in-vivo* success of a drug lead are its pharmacokinetics (PK) and pharmacodynamics (PD). Pharmacokinetics determines the efficacy of a drug lead *in-vivo*. PK can quantify how a drug is absorbed into tissues, how the drug is metabolized by tissues, and how the drug is excreted by tissues. Another parameter of PK is the total drug dosage the observed tissue has accumulated. Pharmacodynamics of a drug lead is important because it quantifies how the drug targets a biochemical function of *in-vivo* cancerous tissues. If the drug lead(s) are found to meet all the testing criteria, despite the potential challenges, then clinical trials

may commence. In the United States, the drug lead(s) are submitted as an Investigational New Drug Application (IND) to the Food and Drug Administration (FDA) and await approval of a 30-day review. [Weinberg NA, 2007] In all, the typical time taken for *in-vitro* and *in-vivo* pre-clinical trials is between 1 to 3 years. After pre-clinical trials, long-term animal testing continues along-side clinical trials in humans. [Dickson M, 2004]

Clinical trials sequentially go through 3 phases; the process can typically take between 2 to 10 years. Phase 1 tests the toxicity of the drug by incrementally increasing the dosage to small groups of human volunteers who may not necessarily exhibit the target symptom to be treated. Once an unacceptable dose is reached, it is then designated as the Maximum Tolerated Dose (MTD). Another purpose of Phase 1 trials is to determine if there are any toxicities or side-effects that were not predicted in pre-clinical trials. Phase 1 trials do not represent data that is statistically significant; as such, Phase 2 and Phase 3 trials must fulfill that role. An important factor in determining whether a drug moves onto Phase 2 trials is the therapeutic window, which takes into account the pharmacokinetics, the pharmacodynamics, and the maximum tolerated dose. The therapeutic window is a range of drug doses that must be below the MTD and must be above the dose required to produce any beneficial outcomes in patients; a mark for a better for the drug's success is if the therapeutic window is wide enough to anticipate any side-effects in patients. [Weinberg NA, 2007]

The purpose of Phase 2 trials is to determine the efficacy of the drug on larger groups of patients that do exhibit the symptom to be treated. These trials must determine the indications of drug efficacy on specific types of cancers based on the biomolecular target, such as lung carcinomas or gastric carcinomas. [Weinberg NA, 2007] If the drug proves to be effective against a type of cancer, then Phase 3 trials will commence.

Phase 3 trials further assess the efficacy of a drug by testing on very large groups of cancer patients. These trials cost the most, but are the ones that yield results that are statistically significant. [Weinberg NA, 2007] Patients tested on have robust tumors, since the drug candidate(s) must be more therapeutically effective than a control drug that is currently on the market. If by chance the drug candidate(s) passes Phase 3 trials, then a New Drug Application (NDA) may be submitted to the FDA for approval, in which the review process can take up to an average of 2 years. [Dickson M, 2004]

1.4 High Throughput and High Content Screening

High throughput screening (HTS) is the process of performing many parallel measurements or experiments in a short period of time (~1 day). Since its inception in the early 1990s, HTS has been used to measure molecular interactions ranging from small molecules, proteins, DNA, and RNA. HTS is typically performed in well plates, and samples are dispensed with liquid robotic handlers. Well plates consist of small wells ranging in number from 96 to 1532, are typically made from polystyrene, and have either clear or opaque bottoms (Figure 1.2). Other technologies used in HTS are micro-arrays and microfluidics. Over the years, HTS has been successfully applied to functional genomics, functional proteomics, and drug discovery. The actual measurements are taken in the form of average absorbance or fluorescence signals per well, taken from automated plate readers (Figure 1.3). More detailed measurements can be performed by imaging through a microscope. Measurements by imaging are typically used on cellular assays, such as small molecule binding and selectivity within the cells. [Alanine AI, 2003] Aside from small molecule screening [Eggert US, 2006], imaging tools can be used to screen RNA interference (RNAi) and measure the resulting inactivation of the target protein. If the RNAi does not fully compliment the messenger RNA (mRNA), it may off-target other kinds of mRNA molecules; consequentially, these off-targets are a subject of interest to researchers to turn them into potential therapeutic targets.

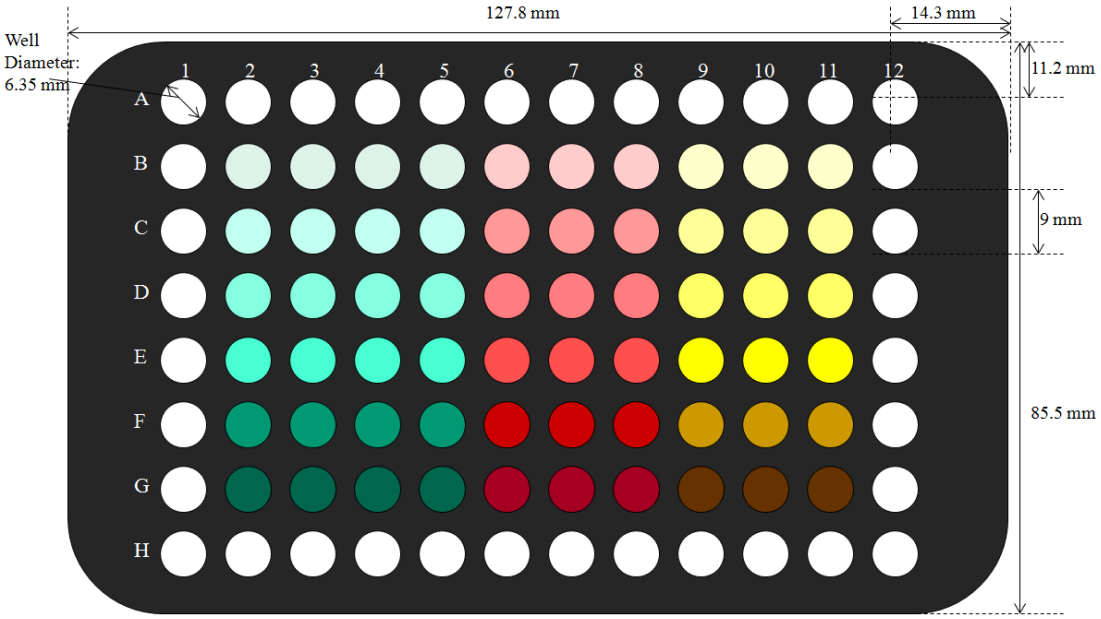

Figure 1.2: A 96 well plate, used in traditional high-throughput and high-content screening. Cells with media are dispensed into each well. Each well represents a separate test, as different compounds and concentrations can applied to each. For example as shown, 3 compounds and 6 concentrations are being tested; since the outer wells tend to evaporate rapidly in the incubator, these are usually left empty. Dimensions shown are not to scale.

In drug discovery, pharmaceutical companies have a wide range of targets for therapeutic intervention such as enzymes, receptors, hormones, and ion channels. HTS can initiate the drug discovery process by identifying small molecules that modulate a target biomolecule. The amount of potential targets for intervention is continuously expanding, which puts a greater demand on HTS for target identification. [Alanine AI, 2003] Such refinement of these drug leads can be more effectively accomplished through high content screening (HCS) assays. Early refinement of drug hits is crucial to success since it will better predict the drug lead's properties *in-vivo*.

A)

http://www.biotek.com/resources/articles/artels-multichannel-volume-verification.html; July 2012

B)

http://www.mtxlsi.com/platereaders.htm; July 2012

C)

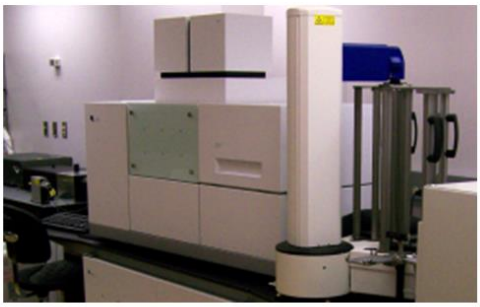

http://www.macbiophotonics.ca/screening.htm; July 2012

Figure 1.3: Apparatus used in HTS and HCS. A) Liquid dispensing robot. B) Well plate reader, with absorbance and fluorescence measurements. C) Automated confocal microscope suite, along with image processing software.

HCS is the combination of automated processes, ranging from sample dispensing, image acquisition, and data analysis to take multiple measurements of cells in parallel. [Abraham VC, 2004] Since its components are automated, HCS can be utilized in a high-throughput format. HCS can potentially produce highly biologically relevant information in the early drug discovery stages by spatially and temporally characterizing cellular functions. For example, J.R. Haskins *et. al.* used HCS to measure nuclear morphology and size, cytoplasmic calcium levels, mitochondrial membrane integrity, and integrity of the plasma membrane in parallel. [Abraham VC, 2004] In recent years, additional technologies have been integrated into HCS such as microfluidics and cell-printed micro-arrays. It is predicted that HCS will have greater importance in the drug discovery process, since it is able to provide a higher-quality biological context in the early (and less costly) stages.

1.5 Well Plates

Well plates are compartmentalized liquid storage and cell culture tools that are capable of performing many separate assays and tests in parallel. The plates are typically manufactured by injection moulding and are made from hard plastics such as polystyrene, polypropylene, and cyclo-olefin. Ranges of configurations exist in terms of well, number, well dimensions and shape, well spacing, bottom material, material colour, and surface treatment. Most commonly, well plates are classified in terms of the numbers of wells per plate: 96, 384, 1536, and 3456 wells per plate. Diameters of the wells are typically on the millimeter scale, ranging from around 6.3 mm for 96 well plates (Figure 1.2) to around 0.9 mm for 3456 well plates. The materials of well plates are usually hydrophobic, but can be surface-treated to become hydrophilic which can aid in cell attachment and liquid dispensing.

Liquids, biomolecules, cell suspensions, and other reagents are dispensed into well plates either manually by multi-tip pipettes or automatically by robotic liquid dispensers and flying reagent dispensers. Instrumentation includes plate readers to measure absorbance and fluorescence levels, and microscopes (widefield and confocal) to analyze brightfield and fluorescent images of cultured cells.

Compared with conventional methods, well plates are capable of using less reagent volumes, reduce total experiment time, and perform several different assays in parallel; the advantages become increasingly apparent as the well density increases. However, higher density well plates can suffer from liquid evaporation from the wells, and higher surface tension forces that liquids can impose onto confined spaces. Nevertheless, there are specially designed lids to aid in preventing evaporation. To reduce surface tension forces in high density well plates, the surfaces can be treated to be hydrophilic; there are also specialized equipment to dispense liquids into high-density well plates such as flying reagent dispensers and pieso-tip applicators. [Zuck P, 2004]

Because of their many advantages over conventional methods, well plates are used in many applications: reagent storage, genomics, proteomics, HTS of biomolecular assays, HTS and HCS of cell-based assays, cell biology studies, and early drug discovery. An example of the application of well plates is of the work by Y.G. Shellman *et. al.*, who used 96-well plates to simultaneously quantify apoptosis and necrosis in treated Jurakat suspension cells and in treated A375 adherent cells. [Shellman YG, 2005] Another example is of the work by P. Zuck *et. al.*, who screened compound libraries to identify hits that inhibited Hepatitis C virus replication using 384-well plates; P. Zuck *et. al.* also scaled-down the assay to 3456-well plates and had found that the results were comparable to the results of the 384-well plates. [Zuck P, 2004]

With their capability of performing multiple assays at once, their range of configurations, and their transferability from conventional protocols, well plates have become and essential tool in cell biology and in biochemistry.

1.6 Microfluidic Liquid Handling

Generally speaking, microfluidics is the manipulation of microlitre to nanolitre-scale volumes through channels, mixers, valves, and pumps that typically have feature sizes at the millimeter scale and less. Microfluidic systems, also called lab-on-a-chip and micro total analysis systems (microTAS), take up a fairly small area, usually in the range of 2 to 4 cm^2. Early devices were made from silicon wafers, and any microchannels and reservoirs were chemically-etched into the bulk material; soon after, microfluidic devices were made from transparent elastomers such as polydimethylsiloxane (PDMS) via a process called soft-lithography. Soft-lithography involves a liquid pre-polymer being poured on a master mould, which contains the microfluidic features, and then cured and peeled off; this process can yield many microfluidic devices from one master mould and hence is a quick and inexpensive method for prototyping devices. Because microfluidic devices have millimeter and micrometer scale features, and perform multiple controlled functions in parallel, they are usually applied towards aiding biomedical research.

A highly desirable function of microfluidic devices towards biomedical applications is spatially and temporally controlled liquid handling. Precise delivery of liquids can control the environmental conditions of cells in culture, such as analyte concentration and pH levels. There are different mechanisms to control fluid delivery, ranging from PDMS valves, changes in fluidic flow resistance, to nanoporous membranes. The device designed by Lee L.P. *et. al.* [Lee LP, 2005] cultured mammalian cells in 64 separate chambers, each with a diameter of 280 μm and 50 μm in height. 8 different concentrations of a drug or analyte could be created via a microfluidic mixer situated upstream from the culture chambers, with a single concentration being delivered to each of the 8 columns. The cells were loaded by microchannels that were perpendicular to the drug delivery channels. Drug delivery and cell loading were controlled by increasing flow resistance into each chamber via a specially designed ring that left a 2μm-high opening into the middle of the chambers, while letting liquids flow around the outer perimeter of the chambers. Cell numbers in each chamber could be controlled by varying the initial cell density, the flow rate, and the delivery time. Drug or analytes entered the middle of the chambers by diffusion; this was desired since shear flows and shear forces could negatively impact cell physiology. By

controlling diffusion through microfluidic pressure flow resistance, cell media and analytes could be delivered to each chamber within 10 seconds. L.P. Lee *et. al.* conclude that their design can be applied to measure several dynamic processes within cells, and that the number of chambers can potentially be scaled up to 96 and 384 chambers. Main capabilities of this device are: a drug delivery mechanism similar to physiological conditions by diffusion, low shear forces acting on the cells, and establishing a concentration gradient of 8 different concentrations. This device's main deficiencies are: incompatibility with robotic liquid handlers since it is a closed system, required continued perfusion of cell media due to nanolitre-scale chamber volumes, and only one concentration of drug or analyte could be made per column.

Another example of a microfluidic cell culture array is by S.R. Quake *et. al.* [Quake SR, 2007], whose design consisted of a 96-well array with micro-environment control for each individual well. To control fluid flow into each well, a second PDMS valve layer was bonded on top of the liquid handling layer. The microchannel in the valve layer crossed perpendicular to the channels of the well below; any liquid flowing through a microchannel in the valve layer would push down and block any crossing microchannels in the liquid handling layer. The liquid handling layer could mix up to 16 separate fluidic inputs, which were sent through a multiplexer via a peristaltic pump and then sent to the desired chambers; waste materials were pumped out through an output multiplexer (Figure 1.4). Since the delivery and cell culture processes are automated with a customized MatLAB program, the device is capable of HTS and HCS. S.R. Quake *et. al.* demonstrated this functionality by culturing human mesanchymal stem cells and monitoring differentiation and motility. Main capabilities of this device are: automated operation, direct compatibility with established 96 well plate assays, low shear forces acting on cells, and each chamber could have a different concentration of drug or analyte. The main deficiencies of this device are: required continuous perfusion of cell media due to the nanolitre-scale chamber volume, complicated operation due to the requirement of automated software, and incompatibility with robotic liquid handlers.

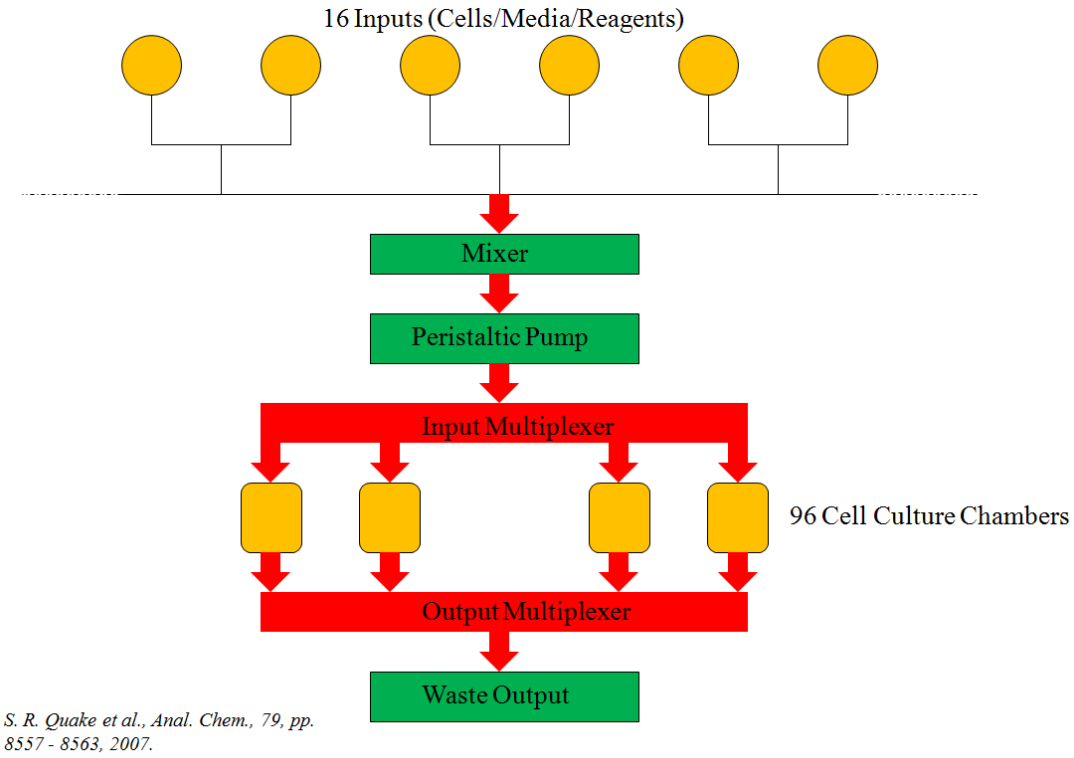

Figure 1.4: A simplified schematic of a HTS/cell culture microfluidic device, developed by S.R. Quake *et al*., 16 inputs, containing cell media or test reagents are sent to a mixer for user defined concentrations. Specified reagent concentrations are pumped through a multiplexer to address any of 96 cell culture chambers. Waste is periodically discarded via and output multiplexer.

Besides liquid handling with only microchannels and pressure flows, other groups have utilized interconnections with nanochannels and controlled fluid delivery via electrokinetic flows. An example of this is by P.W. Bohn *et. al.* [Bohn PW, 2003], whose design consisted of two perpendicularly crossed PDMS microchannels, separated by a hydrophilic nanoporous polycarbonate membrane at the area of overlap. The dimensions of both microchannels were 14 mm in length, 100 μm in width, and 60 μm in height; the polycarbonate membrane was 6 to 10 μm in height, and several pore diameters were tested: 15, 30, 50, 100, and 200 nm. To implement electrokinetic flows, a platinum electrode was inserted into each microchannel reservoir, and the applied voltage was controlled by a program in LabVIEW. With a fluorescent dye, the flow direction into either microchannel was controlled by varying the pore size and the applied voltage. S.R. Quake *et. al.* also designed, in a later study, a microfluidic device that consisted of 3 crossing microchannels made from

polymethylmethacrylate (PMMA) which were separated by 2 hydrophilic nanoporous polycarbonate membranes. The group goes on to suggest application of this design in manipulation of molecular species concentration and in separation of molecular species in biological studies. Main capabilities of these devices are: controllable and precise analyte delivery across microchannels, and analyte separation across microchannels (such as analytes with opposing charges). Deficiencies of these devices are: if used in cell assays then there would be high shear stress acting upon them, only one concentration o fdrug or analyte could be made per microchannel, and potential incompatibility with inverted microscopes (if total device thickness is greater than about 500 μm).

Overall, microfluidic liquid handling presents many different physical mechanisms to provide precise fluid control. Microfluidics can have great potential in aiding biological assays, in HTS, and in HCS.

1.7 Open-Well Microfluidics

Most commonly, microfluidic devices for cell culture consist of closed chambers, with cell suspension and reagents delivered through microchannels. While these architectures are compatible with long-term cell culture and are capable of nanolitre scale dosages, they may not necessarily be compatible with established cell culture protocols and equipment for well-plates. In recent years, there have been efforts to address this issue by designing microfluidic cell culture devices with open chambers. In particular, our work builds upon previous microfluidic devices that were designed by P.R. Selvaganapathy *et. al*.

In the study carried out by P.R. Selvaganapathy *et. al.* [Selvaganapathy PR, 2010], they used a polycarbonate nanoporous membrane to deliver dyes, DNA, and proteins via an applied electric field to a rectangular slab of hydrogel. It was proposed the hydrogel slab would serve as a single continuous scaffold for cell culture; having a chamber-less culture area was advantageous since it promoted cell-to-cell communication and minimized surface tension forces imposed by chamber walls, as opposed to the relatively small chambers of well plates. Three different types of devices were fabricated; all the devices consisted of a bottom PDMS layer of microchannels, a middle layer of a patterned polycarbonate nanoporous membrane, and a top layer of PDMS with an open rectangular chamber. In the open chamber, a mixture of agar powder and de-ionized (DI) water was poured and allowed to cure into a gel. The first device had two microchannels with an open-pore area over each. The purpose of this device was to validate the electrokinetic delivery mechanism using the dyes trypan blue and methylene blue (simulated drug molecules). It was demonstrated that the dyes did not diffuse through the nanoporous membrane into the gel layer of a period of one hour; this

was due to the high flow resistance and high diffusion time brought upon by the narrow diameters of the pores (100 nm) relative to the thickness of the membrane (around 8 μm). Conversely, when a voltage of 30V was applied across the membrane, a dye spot was created in the gel layer within 30 seconds. These qualitative findings validated that electrokinetic flows dominated over diffusion when dealing with very small (100 nm) pores and a relatively large (8 μm) membrane thickness.

The second device consisted of 4 microchannels and 6 open-pore areas, and its purpose was to validate control of dye delivery independently between 3 different locations on the gel layer. Independent drug delivery was demonstrated by applying a potential of 30V at 2 locations and 0V at 1 location for 10 minutes. Once the power supply was turned off, the locations at 30V had each a dye spot while the location at 0V had no dye spot formed. Subsequent tests were made to measure the increase in drug spot size over time when the applied electric field was on and when the drug spot increased in size by diffusion only. At an applied voltage of 30V for 5 minutes, it was found that the dye spot increased in size rapidly for about the first 2 minutes, then at a decreased rate for the remaining 3 minutes. Afterwards, the dye spot was allowed to diffuse in the gel for about 1 hour; the dye spot increased in size at a much slower rate than compared to when the electric field was applied. Furthermore, for a fixed applied voltage of 30V, the amount of dye delivered to the gel was calculated to increase linearly with time; this meant that, depending on the drug properties and membrane pore dimensions, the dosage of drug delivered could perhaps be predicted for a certain applied voltage.

The third device consisted of a printed nanoporous membrane with open-pore areas to create potential dye spot densities of 44 spots/cm^2 and 156 spots/cm^2. The purpose was to demonstrate simultaneous dye delivery at an array of multiple open-pore locations. Spot arrays were demonstrated with trypan blue, bovine serum albumin, and 20 base-pair DNA. It was shown that the spots of the array could increase in size by increasing the duration of the applied voltage. A potential problem is spot-overlap, since there was no barrier to prevent diffusion over a defined distance. To address this problem, a new design was simulated in software. The simulation showed that the rate of lateral spot diffusion could significantly be reduced by making a ring-shaped depression in the gel surrounding the open-pore area.

Although these devices bring major advantages, such as compatibility with existing cell culture protocols and simulation of *in-vivo* conditions, there could be difficulty being imaged with high-magnification (20X) objectives of inverted microscopes. The distance from the bottom of the devices to the cells is relatively thick (>1mm), while the working distances of high-magnification and high numerical aperture objective lenses are relatively short. Automated microscopes for high-content and

high-throughput screening of well-plates are commonly in the inverted configuration.

A similar example, by the work of N.A. Melosh *et. al.* [Melosh NA, 2011], uses diffusion as the mechanism of delivery instead of an applied electric field. The device design consists of a bottom layer containing PDMS microchannels, a polycarbonate nanoporous membrane for the middle layer, and a PDMS top layer which has a rectangular opening for the cell culture chamber. The microchannel is 1000 μm wide and runs under the culture chamber; upstream from the channel is a concentration gradient generator that can produce up to 6 different concentrations, which is then sent down the main microchannel. The nanoporous polycarbonate membrane surface is made hydrophilic via exposure to oxygen plasma, to aid in cell attachment and cell culture; the pores are 750 nm in diameter and the membrane is 24 μm thick. The properties of the membrane are such that diffusion occurs rapidly across it, unlike the membrane in the previous example. With a concentration gradient of fluorescent dyes in the microchannel and cells cultured on the polycarbonate membrane, the dyes had diffused through the membrane and stained the cells in about 45 seconds. The quick diffusive delivery is due to the short distance traveled by the dyes, which is the thickness of the membrane (24 μm); this is faster than devices that use lateral diffusion to reach the chambers, which can be on the order of 100 μm or greater.

The device has the advantage over well-plates since the diffusive delivery mechanism better mimics *in-vivo* conditions. Furthermore, the device can be imaged with inverted microscopes since the distance from the bottom of the device to the cell monolayer is less than 500 μm. However, the deficiencies of this device are: horizontal mixing between different concentrations of analyte, and limitation on the number of concentration that could be made depending on the mixing generator and the width of the microchannel.

Another open-concept microfluidic device, by Li Z. *et. al.* [Li Z., 2011], had a similar configuration to a 96 well-plate but made from PDMS. This device was applied toward siRNA and DNA transfection of mammalian cells, via electroporation. The layer between the upper PDMS wells and above the glass substrate was a thin film of flexible paraylene, with printed patterns of gold electrodes. Adherent mammalian cells would attach and grow on top of the parylene, but would not adhere to the electrodes. The main capabilities of this device are: compatibility with robotic fluid handlers, compatibility with inverted and automated microscopes, and an independent applied electric field could be established for each individual well. The main deficiencies of this device are: no concentration gradient generator within the device (can only be made with robotic liquid handlers), and limitation of the effective well area

for cell attachment because the electrodes are situated on the bottom of the well.

These examples illustrate the advantages and controllability of open-well microfluidics; since these devices can mimic *in-vivo* conditions and are compatible with existing cell culture protocols, they could perhaps eventually replace well-plates for early-stage drug discovery and for cell-based assays.

1.8 Cell Attachment and Proliferation in Culture

Many studies in cell biology and in cell-based assays deal with the culture of established cell lines. Cell lines are formed by sub-culturing cells of the original host tissue (such as a human patient) and selected for their ability to proliferate and/or attach to a substrate. In two-dimensional cell culture, the cell must attach to a non-biological substrate such as plastics and polymers. These substrates are usually pre-treated, typically changing the surface energy (making more hydrophilic). Often, cells will secrete attachment bio-molecules to the substrate first, and then the cells themselves will attach to the bio-molecules. Hence, substrates are often pre-coated with attachment bio-molecules such as fibronectin. [Freshney RI, 2006]

P. Schiavone *et. al.* studied cell attachment on Polydimethylsiloxane (PDMS) substrates. The un-modified surface of PDMS is hydrophobic, mainly due to methyl groups; when the PDMS surface was modified by exposure to either Ar or O_2 plasma, the methyl groups were removed and the surface became hydrophilic. Afterwards, the PDMS surfaces were treated with 3.5 $\mu g/cm^2$ fibronectin, and seeded with Murin 3T3 fibroblasts at 6500 $\mu g/cm^2$, and incubated for 1 hour. After 1 hour, around 120 cells were measured for attachment for each PDMS sample. It was found that hydrophobic PDMS had around 1-2% cell attachment and hydrophilic PDMS had around 30% cell attachment. [Schiavone P, 2008]

Another example in cell attachment is of the microfluidic device designed by A. Folch *et. al*. This microfluidic device consisted of an open well that was 5 mm in diameter. The well substrate was a thin (<10 μm), nanoporous polyester membrane with a pore diameter of 400 nm. The well walls were made of PDMS. The substrate and walls were pre-sterilized with ultra-violet light and then treated with poly-D-lysine. After washing the surfaces with phosphate-buffered saline, the membrane was treated with 10 mM fibronectin for several hours in an incubator. The membrane was seeded with NIH-3T3 fibroblasts at a density of 600,000 cells/mL and left to attach for 3-4 hours. Afterwards, the cells were observed to attach and spread throughout the entire membrane surface. [Folch A., 2010]

Most cell lines in culture will go through a typical growth cycle, after which a fraction of the cells must be removed and placed in a new chamber called a passage or sub-culture. When a new culture of cells is seeded onto a substrate, the cells will first go through a lag phase. The lag phase is when the newly seeded cells attach to the substrate and initially look rounded and eventually spread out as they become more attached; the lag phase takes around 12-24 hours after seeding and there is typically no proliferation during this phase. Immediately after the lag phase is the log phase, where the attached cells proliferate until the entire substrate is covered in a monolayer. Depending on the substrate surface area and initial seeded cell density, the cells may double in population several times before becoming a monolayer. The doubling time depends on the type of cell line, how frequent the old cell media is replaced by new cell media, and the constituents of the cell media. Once the cells become a monolayer, they reach the plateau phase where the cells typically do not proliferate but remain viable. For making a new sub-culture, it is not desirable to passage the cells during the plateau phase but during peak proliferation during the log phase; by passaging during the peak of the log phase, the new sub-culture will have a minimal lag phase. Lastly, it is important to keep track of the number of passages made for cell lines with a finite life span. For these cell lines, there is a limit to the number of times the population can double before reaching senescence. [Freshney RI, 2006]

Chapter 2: Multi-Well Drug Delivery Microfluidic Device

A multi-well microfluidic drug delivery device is to be designed and experimentally validated. The main goal of the microfluidic device is to deliver drugs in a concentration gradient to mammalian cells in culture, and to be compatible with current high-content screening (HCS) systems in academia and in industry.

Current HCS systems mainly utilize 96 well plates for cell-based assays, with a single concentration of a drug per well. The proposed design of the microfluidic system had 16 micro-wells within the area of a well in a 96 well plate. Ideally, each micro-well would have a unique drug concentration delivered to it; the resulting dose-response curves would then have 16 times more data points in the equivalent area of a single well in a 96 well plate. The drug delivery concept builds upon previous multiple drug spot devices developed by S. Upadhyaya and R. Selvaganapathy [Selvaganapathy R, 2010]. In the previous study, S. Upadhyaya developed a gel-based drug delivery device in which the cells would grow on a single open platform with no physically separated chambers. However in this study, the chambers are to be physically separated in order to mimic well plates and to be compatible with HCS well plate automated imaging systems.

Unfortunately due to time limitations, only preliminary validation studies have currently been completed for this project. As such this chapter outlines a conceptually proposed design, as well as materials to be used, experimental setup, and fabrication process flow. Finally, the need for validation studies is addressed.

2.1 Design Criteria

Before a design could be visualized, several parameters needed to be established: the duration of drug delivery, the cell population per well, and the overall device configuration. Drug delivery would ideally take as little time as possible, up to a maximum of about 10 minutes. There should be at least 100 viable cells in each well to have sufficient statistical analysis; as such, the well diameter should have an area large enough to accommodate these cells. If the diameter of a single MCF-7 cell is about 10 μm in diameter, then the minimum area required to hold 100 cells would be 0.008 mm^2. Since the device would be compatible with robotic liquid handlers for dispensing of cells and media, the wells should be in an open configuration.

2.2 Design Overview

The proposed design has 16 wells within the equivalent area of a well from a 96 well plate [Figure 2.1]. There is a single microchannel that runs along the far ends of each well. This microchannel is to contain the drug or analyte to be used in a cell-based assay. Based on validation studies of cell attachment and proliferation in various micro-well diameters, discussed in Chapter 4, the proposed range of well diameters is 0.35 to 1.2 mm. A well diameter of 0.75 mm was shown to be the smallest diameter to have a similar cell proliferation profile as coverslip glass controls.

Aside from the coverslip glass substrate, the microfluidic device consists of three layers [Figure 2.2]. The bottom layer contains both the microfluidic channels and the bottom halves of the wells. The microchannel contains the drug or dye and has a width of 0.1 mm in order to fit within the device dimensions while being as wide as possible to deliver the drug rapidly; the microchannel has a height of 0.3 mm to coincide with the height of the wells and for ease of mould fabrication. A single layer mould is fairly simple to fabricate, since only one photolithographic step is needed. The bottom halves of the wells contain the cells to be analyzed; the wells have a height of 0.3 mm in order to contain an adequate volume of cell media so that the cells remain viable.

The middle layer is a nanoporous polycarbonate membrane, which serves as a barrier between the drug and the cells. Based on previous electrokinetic delivery studies [Selvaganapathy R, 2010; Bohn PW, 2001] an externally applied electric field will transport the drug across the membrane and into the well above. The pore diameters are 100 nm in order to be larger than the particle size of any analytes used; the membrane is also hydrophobic to prevent any diffusion of drug or cell media across it.

The top layer consists of only the top halves of the wells. These wells contain additional cell media and physically separate the individual micro-wells. The top halves of the wells are 0.5 mm in height to prevent any delivered drug from potentially diffusing into adjacent cell chambers; the wells are 1.35 mm in diameter to contain the microchannels and the bottom halves of the wells.

Finally, potential failings in the device are difficult alignment of microfluidic layers, evaporation of liquid in wells, cell attachment and growth in the wells, and long diffusion times for drugs to reach the cells. The device layers need to be precisely aligned and as such, may not be practical when it comes to device fabrication. If this problem is true, then a simpler version of the design would need to be made. Each well uses microlitre-scale volumes; this could lead to rapid evaporation of the liquid, especially in an incubator (35°C). A potential solution could be to use a

protective lid, similar to those used in high-density well-plates. Since PDMS is naturally hydrophobic, cell attachment and growth could either not happen at all or at a reduced percentage compared to well-plates; potential solutions could arise in surface modification to make PDMS hydrophilic, using larger diameter wells, and by initially seeding cells at a relatively low concentration. Diffusion times of molecular species (in this case, drug molecules) usually scale with the square of the distance travelled, leading to very long diffusion times at the millimeter scale. A solution to this problem would be to design the total diffusion distance to be less than one millimeter.

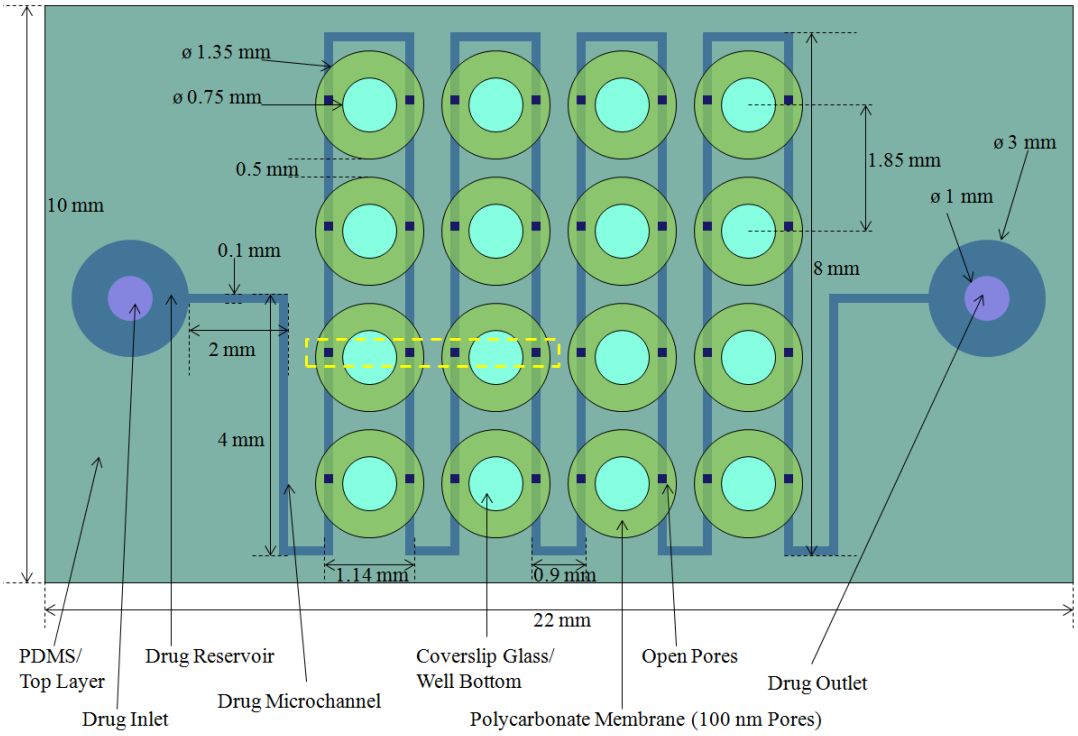

Figure 2.1: Top view of a conceptual microfluidic device, capable of both cell culture in micro-wells, and drug delivery through a nanoporous membrane. The cross-section of the highlighted region in yellow is shown in Figure 2.2. Dimensions shown are not to scale.

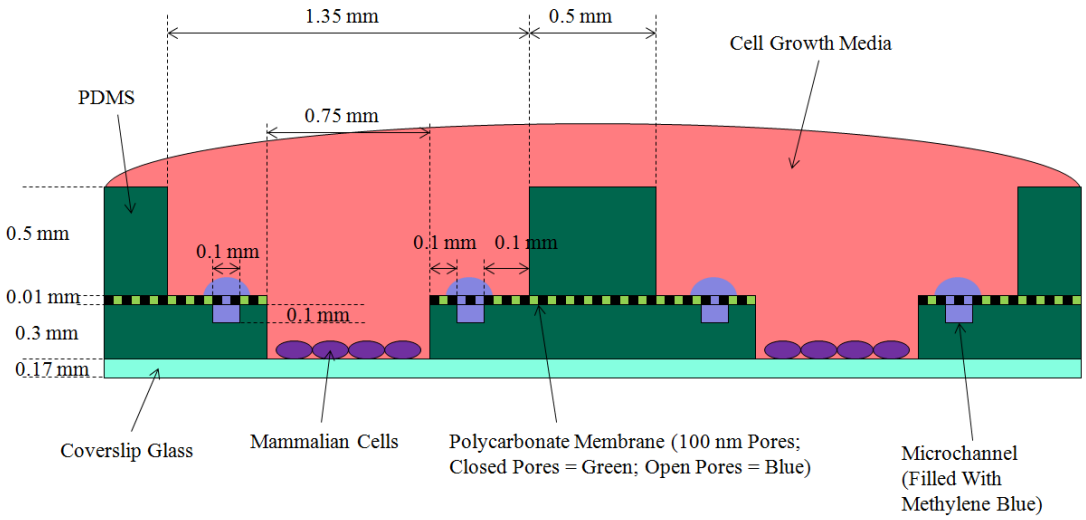

Figure 2.2: Cross-section of a conceptual microfluidic device, capable of both cell culture in micro-wells, and drug delivery through a nanoporous membrane. Dimensions shown are not to scale.

2.3 Materials

SU8 100 Photoresist

SU8 100 (MicroChem) is commonly used in microfluidic moulds and in microelectronics as solid structures. It is a negative photoresist, meaning the exposed portions, during the photolithography process, will eventually become solid structures. Typical structure heights can range from around 90 µm to 240 µm, depending on maximum spin speed, duration, and initial volume of photoresist used. The photoresist is epoxy based and is transparent to wavelengths above 360 nm. Once exposed to UV (ultra-violet) light, an acid is formed within the photoresist. Once heat is applied to the post-exposed photoresist, such as on a hot plate, the acids initiate a cross-linking reaction between epoxy molecules, eventually forming a solid structure. A liquid developing agent then dissolves any unexposed photoresist. [Micro Chem, 2002]

Polydimethylsiloxane (PDMS)

PDMS (Dow Corning, Sylgard 184 Elastomer Kit) is a chemically inert, transparent elastomer that is commonly used in soft lithography for microfluidic devices. When purchased from the manufacturer, PDMS comes in liquid form as a base and curing agent. Solid PDMS is formed by mixing a curing agent to base ratio of 1:10, then curing on a hot plate at

around 70°C. Although a 1:10 ratio is most common, other ratios may be used as well. If less curing agent is used, then the cured PDMS will become more flexible; conversely if more curing agent is used, then the cured PDMS will become more rigid. Initially the PDMS surface is hydrophobic, but can be temporarily changed to a hydrophilic surface by exposure to oxygen plasma. Hydrophilic PDMS is useful for biological applications, such as cell culture and cell-based lab-on-a-chip devices.

Polycarbonate Track Etched Membrane (PCTE)

PCTE membranes (GE Water Process Technologies) are flat, smooth, and transparent; they are suitable for use in a variety of applications such as water filtration, cell culture, and microscopy. These membranes have also been used in lab-on-a-chip devices for drug delivery to cells, either by diffusion [Melosh NA, 2011] or by electrokinetic pumping [Selvaganapathy PR, 2010]. Normally hydrophobic, the polycarbonate membranes can be surface treated with polyvinylpyrrolidone (PVP) to become hydrophilic. A hydrophilic surface aids aqueous solutions to pass through the pores via capillary action, and aids cells to attach and proliferate on the surface. Membranes come in many different pore diameters (ranging from 20 μm to 10 nm) and thicknesses (ranging from 5 μm to 12 μm). Membrane parameters chosen for this study were: 100 nm pores, 4×10^8 pores/cm^2, 10 μm thickness, 25 mm diameter membranes, and hydrophilic surfaces.

Methylene Blue

Methylene blue (Sigma Aldrich) is a blue dye that was used in this study to imitate a drug compound. It has a molecular weight of 319.85 g/mole and a chemical formula of $C_{16}H_{18}ClN_3S$. In solution, methylene has a pH between 5 and 9, a net charge of +1, and its diffusion coefficient in solution at 25 °C can be approximated to be 5×10^{-6} cm^2/s [Melosh NA, 2011]. The dye was chosen for this study because it can be used in absorption measurements, is relatively inexpensive, and becomes a positively charged ionic solution when dissolved in water (for electrokinetic pumping). It has been commonly used in both cell studies and microfluidic studies.

Phosphate Buffered Saline (PBS)

PBS (Sigma Alrich) is an optically transparent, inexpensive, ionic solution that is commonly used in cell culture. It is generally used to wash mammalian cells while passaging. PBS contains sodium chloride (0.9%), Sodium dihydrogenorthophosphate monohydrate (0.22%), and Sodium monohydrogen phosphate, heptahydrate (0.025%) in aqueous solution, and has a pH of ~7.4. In this study, PBS was used as the liquid medium of the well in the microfluidic dye delivery device.

Silver Wires

Silver wires were used in this study as electrodes for electrokinetic pumping because they have with a thin diameter (around 75 μm) and can fit inside the inlets of the microfluidic device.

Acetone and Methanol

Acetone (100%, $(CH_3)_2CO$) and methanol (100%, CH_3OH) are flammable, organic compounds that were used in this study for cleaning silicon wafers, as a precursor to depositing photoresist.

2.4 Proposed Experimental Setup

To facilitate cell culture, the top polydimethylsiloxane (PDMS) surfaces of the lab-on-a-chip device may be modified to be hydrophilic (PDMS is usually hydrophobic). Hydrophilic surfaces aid in filling of the wells when cell culture media is dispensed onto the device. If surface modification of PDMS is needed, the device should be placed in a plasma etcher and subjected to oxygen plasma at a power of 40W for 60 seconds. The applied power and duration should be low enough and short enough that any exposed polycarbonate membrane would remain intact. Once exposed, the microfluidic device should be placed in a container and submerged in de-ionized (DI) water; this should retain hydrophilic properties for several hours. Ideally, the surface modification procedure should be performed on the same day as the cell seeding.

Before seeding the cells on the lab-on-a-chip device, observe the previously cultured cell in pitri dishes under a microscope and check to see if they are healthy. If the previously cultured cells are healthy, bring cell media, cells, the lab-on-a-chip device, trypsin, and any other cell culture supplies to the biosafety cabinet. Remove the old media from the pitri dish, wash the cells with phosphate buffered saline (PBS), aspirate the PBS, and then add 1 mL of trypsin. Once the trypsin has lifted off the

cells, add 5 mL of cell media and aspirate the cells into a test tube. Count the number of cells and calculate the cell density using a grid-based cell counting device with an established protocol.

Once the cell density is known, dilute down to the desired cell density which will depend on the well area and well diameter. Generally, a smaller well area would require a lower seeded cell density. With the desired cell density established, pipette the cells onto the microfluidic device so that all the wells are filled. After seeding, place the device in the incubator for 4 hours to allow the cells to attach to the bottom of the wells. Check if the cells are attached by looking under a microscope. If the cells are attached, then replace the old media with new media. Place the device back in the incubator, and wait 24 hours to allow the cells to form colonies. Check under the microscope to see if the cells are healthy and are at the required density to commence with the experiment. If the cell density is too low, then replace the cell media with fresh media and leave the device in the incubator for another 24 hours. Keep checking the cells and replacing the media every 24 hours until the cells reach the required density.

Bring the seeded device to the biosafety cabinet and insert tubing into the inlet and outlet. Fill a 1 mL syringe to the inlet tubing. Place the end of the outlet tubing inside a test tube, which will serve as the waste. Use the syringe to fill the entire microfluidic channel with the dye or drug. Remove the syringe and place a silver wire electrode in the inlet tubing; place another silver wire electrode over the first well. Attach both electrodes to a direct current (DC) power supply. Deliver a certain concentration of dye or drug by applying the required voltage and duration. Required voltages and durations would be previously calibrated to obtain desired dye or drug concentrations from validation studies. Deliver different concentrations of dye or drug to the remaining 15 wells by replacing a new silver wire electrode for each well. Once the dye/drug delivery is complete, place the lab-on-a-chip device in the incubator and wait for the specified amount of time for the dye or drug to diffuse into the cells. Take the device out of the incubator and place it under an inverted microscope (either widefield or confocal).

Take images of the entire field-of-view and of each individual well. For example, a 4X objective may be needed to view the entire area of a well, and a 20X objective may be needed to view a portion of a well in detail. The images may either be in brightfield, fluorescence, or a compilation of both. If working with a widefield microscope, then deconvolution post image processing may be required to subtract any out-of-focus light. In this case, several z-sections need to be taken above and below the plane of focus. ImageJ is free image processing software that is capable of deconvolving image stacks. Time-lapse imaging may also be needed, and ImageJ also has a plugin catered to those types of assays.

Once imaging has been completed, the lab-on-a-chip device should be disposed of by first eradicating the cells by washing with bleach and then placing the device in a biohazard level two waste bin.

2.5 Proposed Fabrication Process Flow

In the clean room, any surface particulates are removed from the silicon wafer by submerging in 100% acetone for 15 seconds, submerging in 100% methanol for 15 seconds, and submerging under flowing de-ionized (DI) water for 15 minutes. Any moisture remaining on the surface is removed by blowing nitrogen gas.

On the vacuum spinner, ~3 mL of SU-8 negative photoresist is poured on the silicon wafer. The silicon wafer is then spun to achieve a photoresist thickness of 300 µm. After spinning, the photoresist is pre-baked on a hot plate for 10 minutes at 65 °C. The temperature is then increased 10 degrees per minute, up to 95 °C; the photoresist is then baked at 95 °C for 30 minutes.

Once pre-baked, the photoresist is exposed, through the photomask of the bottom layer, to UV light at a power density of 646 mJ/cm^2 for 127 seconds.

Once exposed, the silicon wafer is placed back on the hot plate for post-exposure baking. The wafer is baked at 65°C for 3 minutes, and then the temperature is increased 10°C per minute up to 95°C. The wafer is then baked at 95°C for 10 minutes. After post-baking, the wafer is left to stand at room temperature for 5 minutes.

For the developing process, the wafer is submerged in Microchem SU-8 developing solution until solid structures appear on the wafer (may take about 10 minutes, depending on the photoresist thickness). After development, the photoresist is then rinsed with isopropyl alcohol (IPA) to check if all unexposed photoresist is removed. If the IPA leaves a white residue on the wafer, the developing process is repeated.

For the top layer mould, the process will be similar to the bottom layer mould. The exceptions are that a different photomask is used (contains the outline of the top layer features) and the spun thickness of the SU-8 photoresist is 0.5 mm instead of 0.3 mm.

Once both silicon wafer moulds are fabricated, they are placed in a vacuum chamber where 1 g of paralyene is vapour-deposited on their top surfaces. Paralyene reduces adhesion between the surfaces of the moulds and PDMS; the cured PDMS can then be easily peeled off the moulds.

Liquid polydimethylsiloxane (PDMS) is prepared by mixing a 1:10 ratio of cross-linking agent to base polymer. Once prepared, the liquid PDMS is poured over both moulds of the lab-on-a-chip device. To ensure through-holes, excess PDMS is blown off with compressed air until the PDMS lies just below the mould structures. The PDMS is then cured by

placing the silicon wafers on a hotplate at 80°C for two hours. After curing, the PDMS layers are peeled off the silicon wafers [Figure 2.3 A and C].

A micro-contact printing method is used to bond the nanoporous polycarbonate membrane to the top of the PDMS bottom layer. 1 mL of 1:10 liquid PDMS is spun at 3000 rpm for 60 seconds, leaving a very thin layer (<10 μm). The thin layer of liquid PDMS serves as a kind of glue to bond the membrane and solid PDMS layers together. The bonding side of the solid PDMS layer is exposed to oxygen plasma at 40W for 60 seconds. Exposure to oxygen plasma will render the solid PDMS hydrophilic, which will aid in bonding with the liquid PDMS. The hydrophilic side of the solid PDMS is placed on top of the liquid PDMS, and then lifted off. A thin layer of liquid PDMS is then bonded to the hydrophilic side of the solid PDMS. The polycarbonate membrane is placed on top of the hydrophilic side of the solid PDMS, forming a bond [Figure 2.3 B]. The thin layer of liquid PDMS is cured by placing the device on a hot plate at 50°C for two hours.

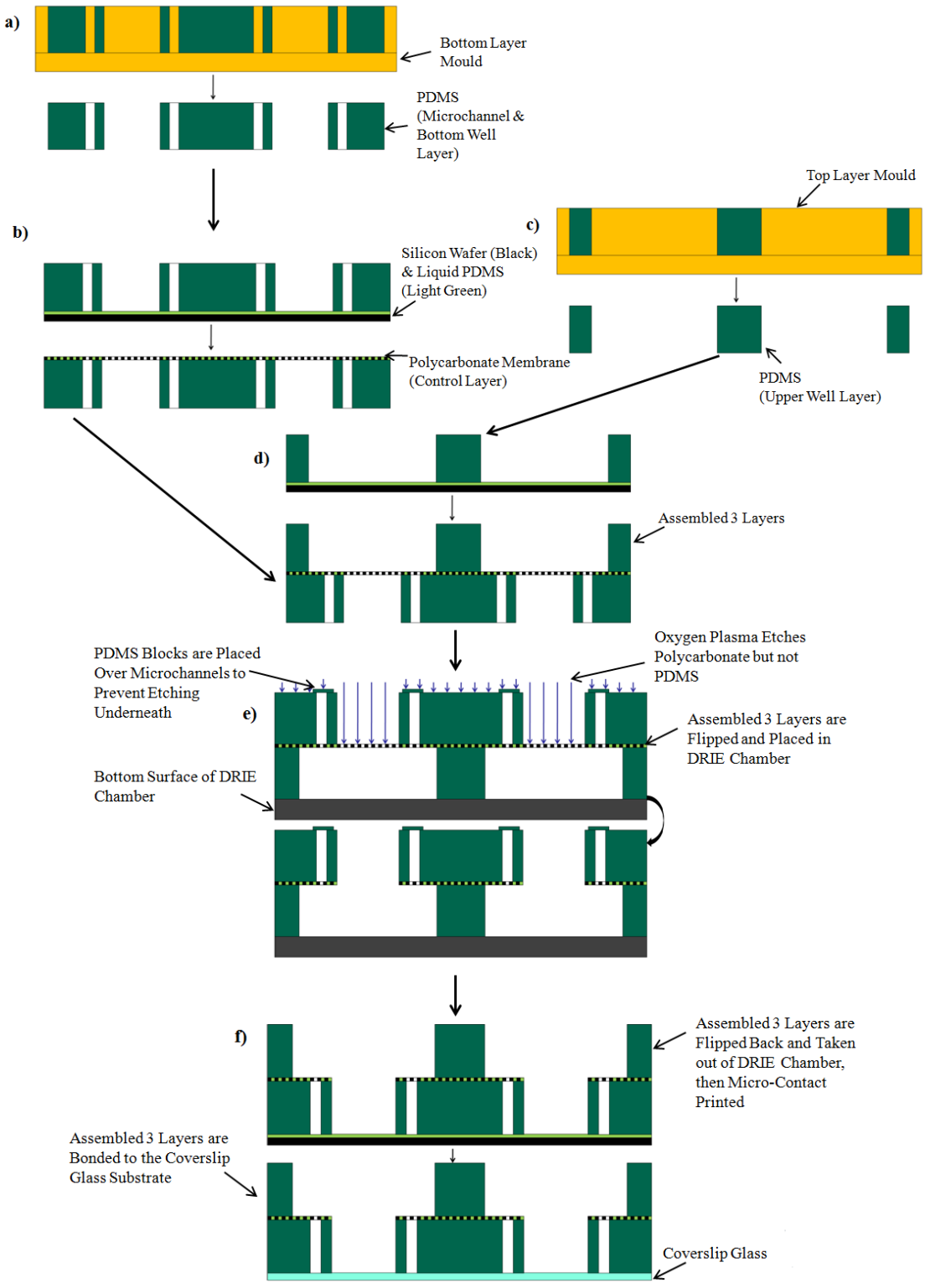
a)
Bottom Layer Mould
PDMS (Microchannel & Bottom Well Layer)
b)
Silicon Wafer (Black) & Liquid PDMS (Light Green)
Polycarbonate Membrane (Control Layer)
c)
Top Layer Mould
PDMS (Upper Well Layer)
d)
Assembled 3 Layers
PDMS Blocks are Placed Over Microchannels to Prevent Etching Underneath
Oxygen Plasma Etches Polycarbonate but not PDMS
e)
Assembled 3 Layers are Flipped and Placed in DRIE Chamber
Bottom Surface of DRIE Chamber
f)
Assembled 3 Layers are Flipped Back and Taken out of DRIE Chamber, then Micro-Contact Printed
Assembled 3 Layers are Bonded to the Coverslip Glass Substrate
Coverslip Glass

Figure 2.3: Proposed process flow fabrication of a 16 well lab-on-a-chip drug delivery and cell culture device. a) Liquid PDMS is poured and cured on the silicon wafer mould of the bottom layer. b) The nanoporous polycarbonate membrane is bonded on top of the bottom PDMS layer via micro-contact printing. The bonding side of the PDMS layer is placed, then peeled off, a thin (< 10 μm) layer of liquid PDMS on a silicon wafer. The polycarbonate membrane is placed on the printed side of the PDMS layer, filling the membrane pores with PDMS. The liquid PDMS is then cured by heating on a hot plate at 50°C for two hours. c) Liquid PDMS is poured and cured on the silicon wafer mould of the top layer. d) The PDMS top layer is bonded on top of the polycarbonate membrane by micro-contact printing. e) Areas where the polycarbonate membrane is overlapping the wells are removed via oxygen plasma deep reactive ion etching (DRIE). Oxygen plasma will selectively etch any exposed polycarbonate, but not PDMS. f) The entire bottom of the lab-on-a-chip device is bonded to coverslip glass via micro-contact printing. Dimensions are not to scale.

The top layer of the lab-on-a-chip device is bonded to the nanoporous polycarbonate membrane, using the micro-contact printing method described above [Figure 2.3 D].

All areas of the membrane that overlap the wells must be removed. The device is placed top-downwards in a deep reactive ion etching (DRIE) machine. Exposed areas of the polycarbonate membrane are etched away by oxygen plasma at a power of 100 W for 60 minutes. The oxygen plasma will selectively etch polycarbonate while leaving the PDMS intact. Any exposed areas of polycarbonate that are not to be etched are covered by placing solid PDMS blocks over top [Figure 2.3 E].

Finally, the bottom of the assembled lap-on-a-chip device is bonded to a piece of coverslip glass, using the micro-contact printing method previously described [Figure 2.3 F].

2.6 Validation of Device Modalities

There are two major issues that need to be addressed before moving on to the proposed design: drug delivery in multiple wells, and cell proliferation and viability in PDMS micro-wells.

Electrokinetic drug delivery through a nanoporous membrane needs to be studied in a simpler format than the 16 well design. Initial validation tests are to be carried out for a single well, and then subsequently for multiple wells. A challenge for multiple well devices would be to deliver

different concentrations of drug independently to each well. These validations will be outlined and discussed in Chapter 3.

Cell proliferation and viability in PDMS micro-wells must be validated to determine if they are similar to coverslip glass controls. A range of diameters that are similar to controls is needed for potentially different device designs that may be required for future studies. As well, hydrophilic and hydrophobic PDMS well side-walls should be compared to determine if they have an impact on cell attachment. These validations will be outlined and discussed in Chapter 4.

Another issue that needed to be addressed, but sadly was not reached by the end of the project, was the effect of an electric field on mammalian cells. DC Electric fields can be used to open pores in the outer membrane of mammalian cells. With the membrane pores temporarily open, the cells can be easily transfected. However, these electric fields are usually pulsed as to not significantly perturb the cells, either by thermal ablation or by rupture of the outer membrane. Previously known microfluidic devices that used pulsed electric fields for electroporation of cells had voltage potentials up to 80V [Li Z, 2010]. With the electrode applying the electric field within a micro-channel on HEK-293 mammalian cells, Li *et. al.* were reported to achieve an overall cell viability of 60%.

Chapter 3: Characterization of Drug Delivery Through a Nanoporous Membrane

It has been demonstrated that nanoporous membranes could selectively pass fluids with high spatial and temporal control, when an external DC electric field was applied across them. [Selvaganapathy PR, 2010] Hence, polycarbonate nanoporous membrane is chosen as the mechanism for drug delivery in a microfluidic device capable of delivering drug compounds to cells, while being compatible with current high-content screening equipment.

In this chapter, we describe the design and fabrication process of a microfluidic device integrated with nanoporous polycarbonate and performance validation of spatial and temporal control of drug delivery. A single well device was chosen as the starting point, since that modality would be the simplest to characterize. This work forms the foundation for designing subsequent, multi-well devices such that we proceed step by each step with increased complexity.

3.1 Theory

Electroosmotic flow occurs when a thin mobile layer of ions near the channel walls move in response to an applied electric field, and through viscous forces, drags the bulk fluid along with it. This type of flow occurs in system when the Reynold's Number is less than one; meaning that the viscous forces of a system dominate over inertial forces.

When an aqueous solution fills a channel, the adjacent molecules of the channel wall ionize. Ions of the opposite polarity in the bulk liquid are attracted to, and associate with, the ions at the channel wall. The associated counter-ions form a double layer: the Stern layer and the diffuse layer. The Stern layer consists of an unmovable, single layer of counter-ions that are directly adjacent to the channel wall ions. The diffuse layer is thicker than the Stern layer and consists of counter-ions that are capable of moving. The thickness of the double layer is characterized by the Debye Length:

$$K^{-1} = (3.29zC^{1/2})^{-1} \quad \text{(Eq. 3.1)}$$

According to P.W. Bohn *et. al.*: K^{-1} is in nm, z is the charge of the counter-ions, and C is the counter-ion concentration of the bulk liquid in mol/L [Bohn PW, 2001]. As can be seen from equation 3.1, the Debye Length is inversely proportional to the counter-ion concentration [Bohn PW, 2001].

When an external electric field is applied across the channel, the counter-ions in the diffuse layer move toward the oppositely polarized electrode. As the diffuse layer moves, a shear force plane is created between it and the Stern layer; the voltage potential at this shear plane is called the zeta potential. As previously stated, the moving diffuse layer exerts viscous forces on the bulk liquid, which moves along with the diffuse layer [Bohn PW, 2001].

From the 2001 study of P.W. Bohn *et. al.*, Electroosmosis ultimately dictates transport of liquids across nanoporous membranes when an external electric field is applied and there are low counter-ion concentrations (around 10 mM) in the bulk liquid. The channel wall material (and hence the ionic charge of the channel wall) along with external electric field polarity, determine the direction of electroosmotic flow [Bohn PW, 2001].

Electrophoretic flow is the bulk movement of ions in an aqueous solution, in response to an applied external electric field. Like electroosmotic flow, electrophoretic flow occurs in a system where viscous forces dominate over interial forces (Reynold's Number less than one).

The velocity of ions or charged particles in the bulk solution is dependent on their molecular weight, on the magnitude of their charge, and on the magnitude of the external applied electric field. Electrophoretic flow does not depend on the charge of the channel walls. A common application of electrophoretic flow is in biology; DNA and proteins in a hydro-gel are subjected to an external electric field and thus are separated according to molecular weight. The charge of the ions or particles will move to the opposite electrode, determining the direction of flow.

From the 2001 study of P.W. Bohn *et. al.*, electrophoresis ultimately dictates transport of liquids across nanoporous membranes when an external electric field is applied, there are high ion concentrations in the bulk liquid (around 1M), and that the membrane is hydrophobic (Figure 3.1). Liquids resist binding to hydrophobic channels, and must be forced through by electrophoretic flow [Bohn PW, 2001].

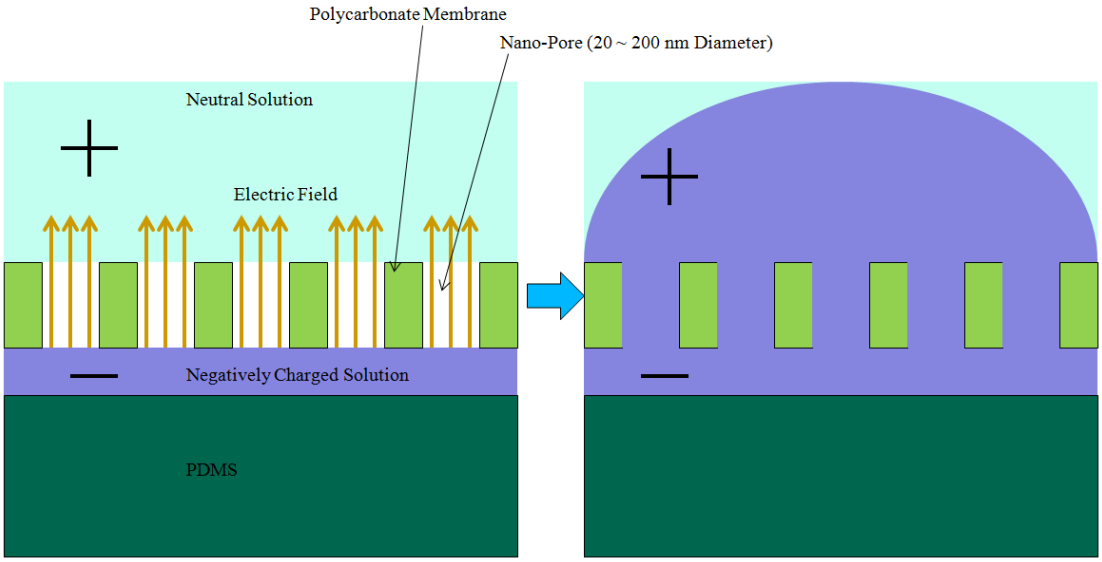

Figure 3.1: Working concept of electrokinetic transport of an ionic solution through the nanoporous polycarbonate membrane. An external electric field is established across the membrane, causing electrophoretic and electroosmotic flow.

On the scale of a single small particle, diffusion is the random displacement of the particle from one moment in time to the next moment in time. On the scale of many identical particles interacting with each other, diffusion is the flux of those particles in the general direction from the highest concentration to the lowest concentration (when a concentration gradient is present). This relationship is described in Fick's First Law of Diffusion [Ursell TS, 2007]:

$$\vec{J} = -D\nabla C \quad \text{(Eq. 3.2)}$$

Where $\vec{J}$ is the flux vector of the diffusive species, D is the diffusion constant (species dependent), and ∇C is the concentration gradient of the diffusive species. The negative sign on the right side of Equation 3.2 indicates that the direction of the flux is opposite to the direction of the concentration gradient (lowest to highest).

In an ideal case, the time taken for a group of particles to diffuse from one point to another is the square of the distance travelled, as shown in Equation 3.3:

$$t \propto x^2 \quad \text{(Eq. 3.3)}$$

Where t the time taken in seconds, and x is the diffusion distance in meters.

Likewise with electroosmosis and electrophoresis, diffusion transport dominates at low Reynold's Numbers (less than one). Viscous forces dominate over inertial forces, and hence laminar flows characterize the fluidic system instead of turbulent flows. In laminar fluidic systems, mixing of fluids is by diffusion rather than by convection.

In the context of cell-based microfluidics, drug delivery is usually accomplished by diffusion. Fluid flows over cells are avoided because they exert shear forces which may perturb cell function, such as mitosis [Melosh NA, 2011]. For example, N.A. Melosh *et. al.* designed a microfluidic drug delivery device which used diffusion through a nanoporous polycarbonate membrane to deliver drugs and dyes to the cells above. However, they also reported that diffusion through the nanoporous polycarbonate membrane is altered from the ideal case by geometrical factors such as: nanometer-scale diameter of cylindrical channels, high density of channels with close relatively close proximity to one another, the exit from the cylindrical channels to a large chamber [Melosh NA, 2011].

Diffusive transport through a nanoporous membrane dominates over electroosmosis and electrophoresis when the analyte concentration is high (around 1M), and the nanoporous membrane material is hydrophilic [Bohn PW, 2001]. Likewise, diffusion is the only type of transport possible across nanoporous membranes when there is no applied external electric field; conversely, diffusion is virtually non-existent through nanoporous membranes that are hydrophobic.

3.2 Design Criteria

The following parameters for the design of a drug-delivery validation device were: an open well configuration, a well diameter suitable for monitoring drug delivery, and a method to control fluid flow. An open well configuration was chosen in order to easily dispense liquids, other than the drug, with a pipette. A 6 mm well diameter was used because it would provide a large maximum drug spot size with which to study the drug spot growth rate, both by direct pumping and by diffusion. A nanoporous membrane was chosen to control fluid transport into the well, as it could be easily integrated into the drug delivery device, and if the surface was hydrophobic, could effectively separate two different fluids above and below the well.

3.3 Design

An initial design of a single well device to characterize drug delivery, both electrokinetic and diffusional, is shown in Figure 3.2A and Figure 3.3. The design was based off of the work by S. Upadhyaya and R. Selvaganapathy *et. al.* [Selvaganapathy PR, 2010], and serves for validation of the mechanism for drug delivery. All materials used are identical to the ones previously described in Chapter 2.

This device was built on a microscope slide (Figure 3.2A) because it served as a rigid base, and was optically transparent. All materials for this device were chosen to be optically transparent which facilitated observation through a microscope and for optical measurements, such as absorption. The device consisted of three layers: The first layer was made from PDMS and contained a mircochannel with a cross-sectional area of 400 μm x 100 μm (top view, Figure 3.3B). The function of the microchannel was to transport drug candidates underneath the wells in preparation for delivery. The second layer was the polycarbonate nanoporous membrane (100 nm pores, 10 μm thickness), which acted as a barrier between the mircochannel below and the well above. The third layer was made from PDMS and contained a 6 mm diameter open well, which was located directly above the middle position of the microchannel and above the nanoporous membrane (top view, Figure 3.3A). The well would contain a clear liquid, to observe the flux of drug candidates under different experimental conditions.

Electrokinetic transport, through the membrane, would be characterized by magnitude and duration of applied external voltage. Increasing variables such as electric field strength, membrane pore size, drug concentration, dielectric constant of the drug, zeta potential, and net ionic charge of drug molecules can increase electroosmotic flow and electrophoretic flow. Whereas increasing variables such as the drug dynamic viscosity, and coefficient of friction of the drug molecules can decrease electroosmotic flow and electrophoretic flow. For simplicity, all variables remained constant except for the electric field strength. The magnitude of the electric field is directly related to the applied voltage potential; as such, the voltage potential between the two electrodes is the primary controlling parameter for drug delivery. Diffusional transport would be characterized by growth rate of spot size of drug molecules in the well, when the applied voltage was turned off.

A 6 mm well was decided upon, so that measurements of spot growth rate could be easily monitored. The microchannel had a width of 400 μm and a height of 100 μm. However, the channel dimensions would have had to be scaled down for a device with a smaller well diameter.

Two silver wires, one in an inlet and one in the well, acted as the electrodes. When an external voltage was applied, an electric field was

established across the membrane. Figure 3.2B illustrates the electrical resistance circuit of the cross-section in Figure 3.2A. The total resistance (R_T) from the inlet electrode to the electrode in the well is the summation of: the resistance across half the channel length (R_C), the resistance across the polycarbonate membrane (R_M), and the resistance across the well (R_W). Depending on the ionic polarity of the drug, the location of the anode, and the location of the cathode: the drug would pass through open pores in the membrane, via electrophoretic and electroosmotic flow. The dye would then be transported passively throughout the well, via diffusion.

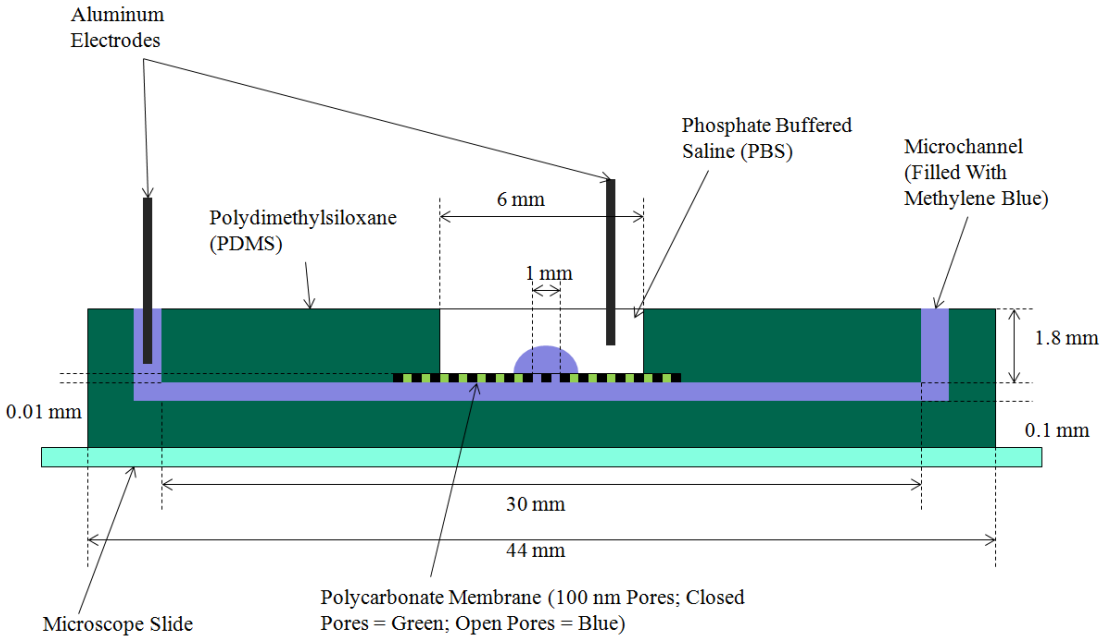

Figure 3.2A: Cross-section view of a single-well drug delivery device. Dimensions shown are not to scale.

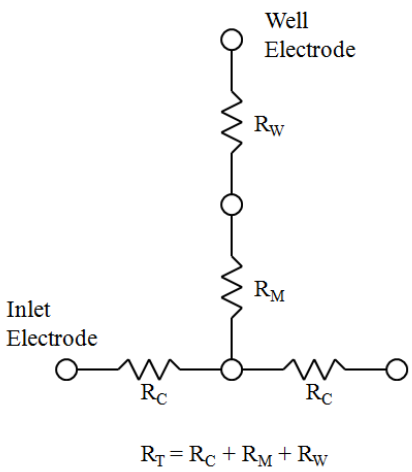

Figure 3.2B: Electrical Resistance circuit from the inlet electrode to the electrode in the well. R_C is the resistance across half of the channel, R_M is the resistance across the polycarbonate membrane, R_W is the resistance across the well, and R_T is the total resistance between the electrodes.

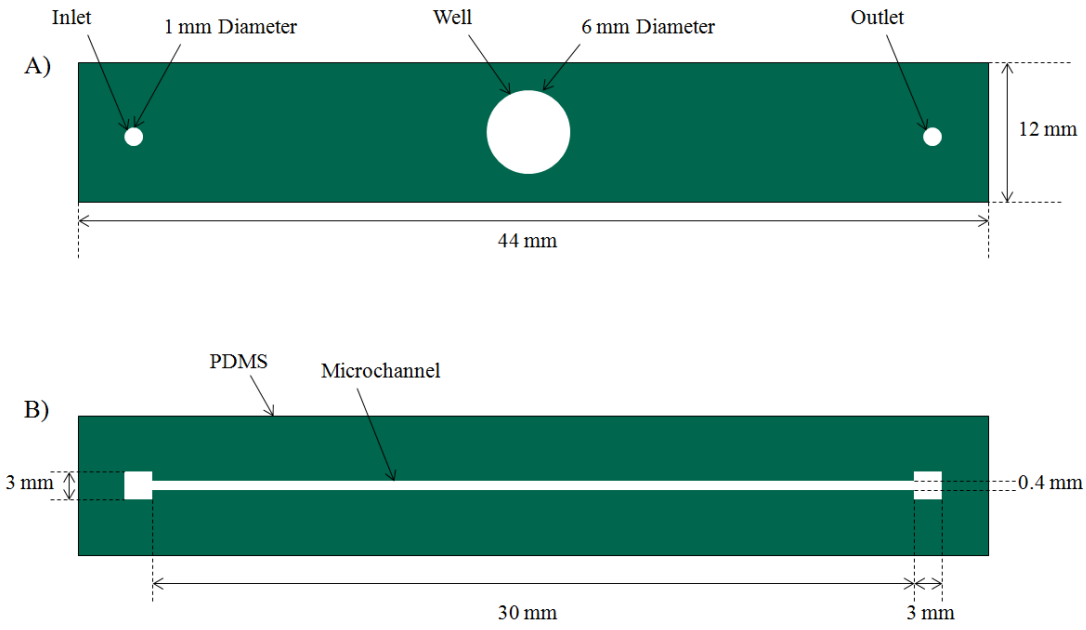

Figure 3.3: Top view of a single-well drug delivery device. A) Bottom microchannel layer. B) Top inlet/outlet and well layer. Dimensions shown are not to scale.

3.4 Experimental Setup and Procedure

Phosphate buffered saline (50 µL, 1X concentration) was dispensed into the microfluidic device's well. PBS was then injected into the microchannel with a syringe. A 3 cm long piece of silver wire was held in place over the well, with the tip suspended in the PBS. Another 3 cm long piece of silver wire was placed inside the microchannel inlet. Both silver wires were then connected to a DC power supply. The wire in the well acted as the cathode and the wire in the microchannel inlet acted as the anode. The DC power supply was also set to measure current. A constant 20 DC volts was applied between the electrodes for 5 minutes; this was to pre-fill the membrane pores with fluid, in order for subsequent dye delivery tests to flow more easily into the well.

Once the power supply was turned off, PBS was taken out of the microchannel and replaced with 1340 µM methylene blue dye. A flat LED platform-light was placed underneath the microfluidic device, which was the only light source for subsequent absorption measurements. The device and LED were then placed under a microscope; the electrodes were put back in their places, and connected to the DC power supply. The anode and the cathode were connected so that the dye would flow from the microchannel to the well; this would depend on the ionic polarity of the dye. Since methylene blue dye was positively charged, the cathode was in the well while the anode was in the microchannel inlet. Before measurements began, all light sources in the room were turned off except for the LED underneath the microfluidic device. With a digital camera mounted on top of the microscope, an image of the test area was taken before dye delivery had begun. The power supply was turned on at 100 V for 3 minutes; every minute, including the initial time, an image was captured and the current was recorded. After 3 minutes had passed, the power supply was turned off. While the dye was diffusing in the well, an image was taken at every minute for 10 minutes; after the first 10 minutes, images were taken at 20 minutes, 30 minutes, 40 minutes, 50 minutes, and 60 minutes. Absorbance data was then measured with a custom-made MATLab program (the program is displayed in the Appendices).

The camera settings (Nikon Coolpix P600) were as follows: monochrome; ISO (International Standards Organization) sensitivity = 64; shutter speed = 1/5 second; aperture = F7.2; manual focus = 1; zoom = 1X; image quality = fine; image size = 4224 x 3168 pixels; metering = matrix; flash exposure compensation = 0.0; flash control = off; noise reduction = auto; distortion control = off; wide-angle converter = off.

3.5 Device Fabrication

3.5.1 Mould Fabrication Process Flow

At the wet bench in the clean room, a 76 mm (3 in) diameter silicon wafer was cleaned by washing in acetone, methanol, and de-ionized water. The silicon wafer was submerged in acetone for 15 seconds, then submerged in methanol for 15 seconds, and then placed under flowing de-ionized water for 5 minutes (Figure 3.4A). Excess water on the surfaces was dried with nitrogen gas, and then the wafer was placed on a hot plate at 110°C for 2 minutes. To further clean the surface, the wafer was placed in a barrel etcher and subjected to oxygen plasma at a power of 50W for 1 minute.

The silicon wafer was placed on a vacuum spinner, and then 3 mL of SU-8 100 photoresist was dispensed on the wafer's surface. According to the manufacturer's protocol, there should be around 1 mL of SU-8 per inch of substrate diameter. [Micro Chem, 2002] SU-8 100 was spun on the wafer to 500 rpm in 5 seconds, and then held for 5 seconds. The speed was ramped up to 3000 rpm in 8 seconds, and continued spinning for 22 seconds at that speed. After spinning, the layer of SU-8 100 should be around 100 µm in thickness (Figure 3.4B). The wafer was prebaked for 10 minutes at 65°C. The temperature was increased 10 degrees per minute, up to 95°C, and then baked at the final temperature for 30 minutes.

At the photolithography station, the ultraviolet (UV) lamp was allowed to warm up for 30 minutes. Once the UV lamp was ready, the microchannel mask and silicon wafer were placed in their respective holders. The silicon wafer was exposed to UV light with energy per unit area of 500~650 mJ/cm^2 for about 130 seconds (Figure 3.4C). Once exposed, the wafer was post-baked on a hot plate at 65°C for 3 minutes. The temperature was increased 10 degrees per minute, up to 95°C, and then baked at the final temperature for 30 minutes. The wafer was left to stand at room temperature for 5 minutes (Figure 3.4D).

The silicon wafer was submerged in a beaker of SU-8 developer agent [Micro Chem, 2002] until microchannel features appeared (estimated time was about 10 minutes). Besides the developer agent from Micro Chem, ethyl lactate or diacetone alcohol could also be used (Figure 3.4E). The wafer was rinsed with isopropyl alcohol (IPA) to ensure complete removal of any unexposed SU-8. If the IPA left a white residue on the wafer, the developing process would have been repeated (Figure 3.4F).

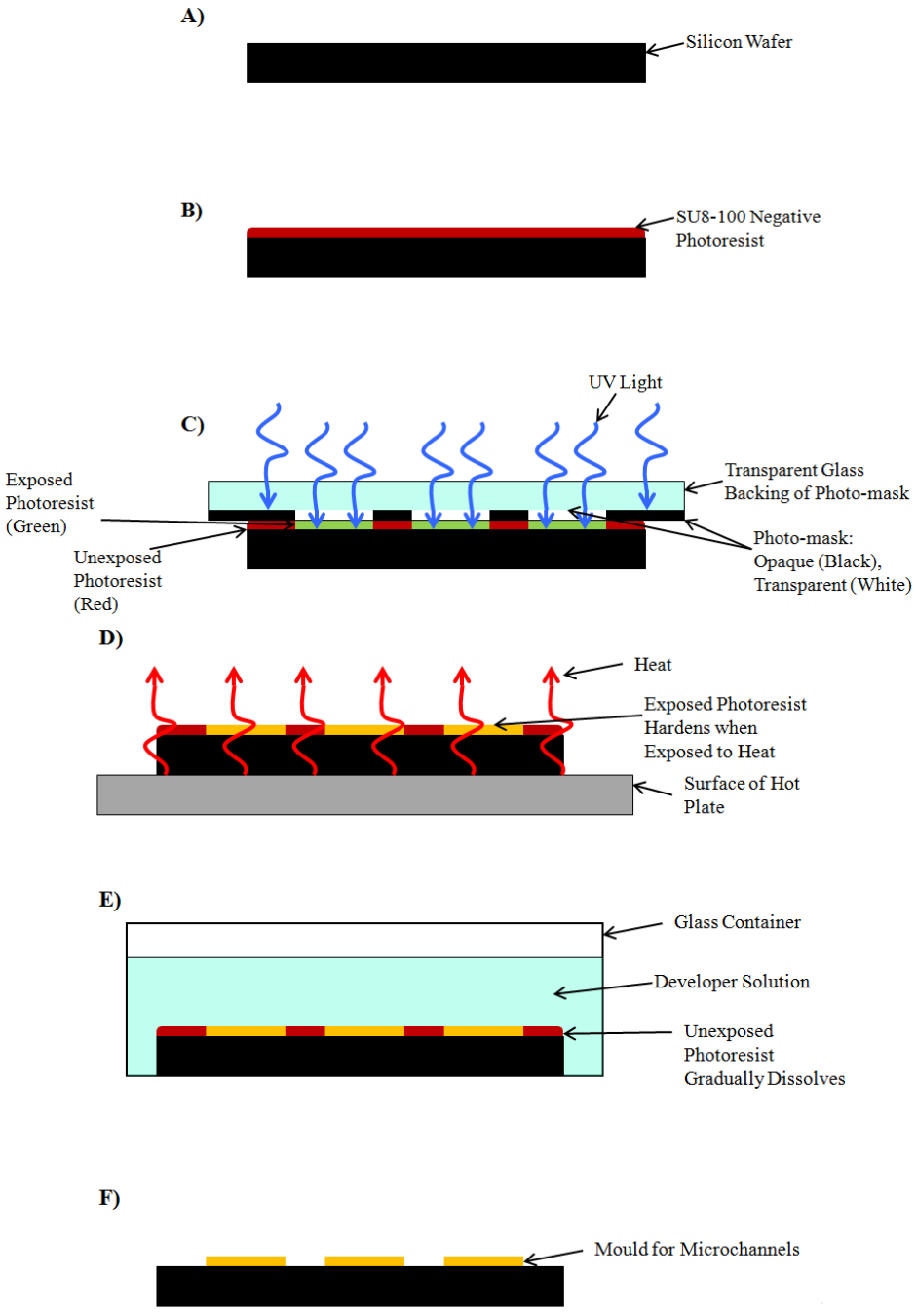

Figure 3.4: Mould fabrication process flow for microchannels of the mircofluidic dye delivery device. A) A 3 inch (7.6 cm) diameter silicon wafer was cleaned with acetone and methanol for 15 seconds each, and then rinsed for 5 minutes in running DI water. B) 3 mL of SU-8 100 was dispensed on the silicon wafer, and then was placed upon a vacuum spinner, and the SU-8 100 was

spun to a thickness of around 100 µm. C) After the pre-bake stage, the silicon wafer was exposed to UV light, through a photo-mask, at 646 mJ/cm^2 for 127 seconds. D) Exposed SU-8 100 structures were hardened during the post-bake stage, on a hot plate. E) Any SU-8 100 that was not exposed was removed via a liquid developing agent. F) The finished microchannel structures were ready to be used as a mould.

3.5.2 Device Fabrication Process Flow

Liquid PDMS was prepared by mixing the curing agent with the base elastomer in a 1:10 ratio. Bubbles in the PDMS were degassed by placing in a vacuum chamber for 30 minutes. The PDMS was poured into two pitri dishes, one empty and one with the silicon wafer microchannel mould, to a height of 3 mm. Both pitri dishes were placed on a hot plate at 95°C for 60 minutes, to cure the PDMS. The cured PDMS was peeled off the two pitri dishes. The microchannels in the PDMS were each cut out in a 4 cm by 1.5 cm area. The featureless PDMS was to become the well layer; the PDMS was cut into 4 cm by 1.5 cm areas, to match the microchannels. In the well layer, inlet holes were created with 0.5 mm diameter biopsy punch; a 6 mm diameter biopsy punch was used to create the center well.

In the clean room, 3 mL of 1:10 liquid PDMS (used as glue for micro-contact printing) was poured on a bare silicon wafer then spun at ~8000 rpm for 60 seconds; the liquid PDMS would be less than 10 µm thick. The bonding surfaces of the microchannel and well layers needed to be hydrophilic to increase surface adhesion to the liquid PDMS when micro-contact printing. Microchannel layer and well layer bonding surfaces were placed in a barrel etcher and exposed to oxygen plasma, at 60 W for 1 minute.

For micro-contact printing, the microchannel surface and the well layer surface were gently placed on the liquid PDMS glue wafer. The microchannel surface was gently peeled off, then a polycarbonate nanoporous membrane (100 nm diameter pores) was placed on the center location of the microchannel (Figure 3.5B). Done properly, the microchannel outline could be seen through the polycarbonate membrane. A 15 mm^2 PDMS block, with a 1 mm^2 hole, was used to block the pores of the polycarbonate membrane, via micro-contact printing. With the PDMS block, all the pores of the membrane would be blocked, except for 1 mm in the center of the microchannel. A very thin layer of liquid PDMS was applied to the solid PDMS block, and then printed down on the nanoporous membrane. The well layer was gently peeled off and placed, glue side down, on top of the polycarbonate membrane. Careful attention was given to properly align the inlets and well, over the correct

microchannel locations. Once assembled, the device was cured on the hot plate at 60°C for around 40 minutes (Figure 3.5C).

Outside the clean room, the device was placed on a clean microscope slide. To bond the device to the microscope slide, drops of 1:10 ratio liquid PDMS were placed around the perimeter of the device. The device was placed on a hot plate at 65°C for 60 minutes, to cure the liquid PDMS; the cured PDMS formed a strong bond between the device and the microscope slide (Figure 3.5D).

Two 4 cm long pieces of #20 AWG (0.813 mm inner diameter, 1.42 mm outer diameter) PTFE tubing were cut. The tubing was placed in the inlets, up to just before the end of each inlet hole. A very small amount of 1:10 liquid PDMS was placed around the interface between the inlet tubes and the top surface of the device. The device was placed on a hotplate at 65°C for 60 minutes, to cure the liquid PDMS.

Two pieces of 1 cm long, 3 mm inner diameter tubing were cut. Small amounts of 1:10 liquid PDMS were glued around the bottom of the tubing, and then placed over top the inlet tubing with the liquid PDMS side down. The device was placed on a hotplate at 65°C for 60 minutes, to cure the liquid PDMS. The 3 mm inner diameter tubing was filled with liquid PDMS, and then cured on a hotplate at 65°C for 60 minutes. The larger diameter tubing was filled with PDMS to secure the smaller inlet tubing in place.

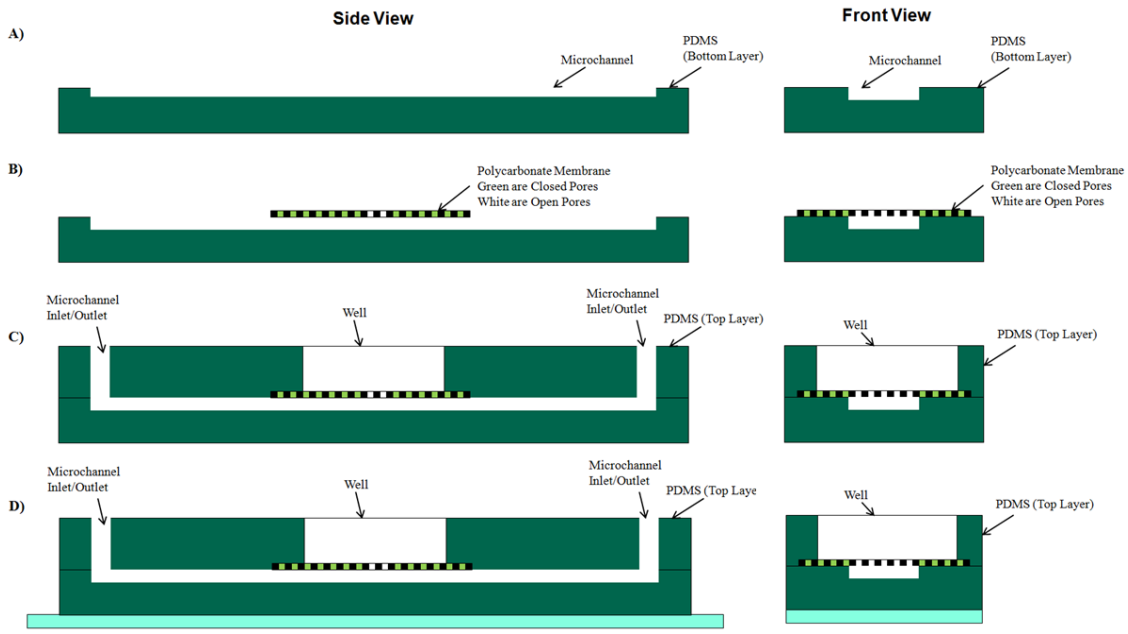

Figure 3.5: Microfluidic dye delivery device fabrication process flow. PDMS, with a 1:10 agent to base ratio, was dispensed into 2 separate pitri dishes; a plane pitri dish and a pitri dish containing the microchannel mould. Layers of PDMS were cut out and exposed to oxygen plasma for bonding. The exposed sides of the PDMS layers were then printed onto a thin layer (less than 10 µm) of liquid PDMS. A) The bottom PDMS layer, containing the microchannel, was laid microchannel-side up on the working bench. B) The nanoporous polycarbonate membrane was placed over the center of the microchannel layer, bonding it to the bottom PDMS layer. A PDMS block, with a 1 mm^2 hole and liquid PDMS covering the underside, was contact printed over the polycarbonate membrane. The nanoporous membrane only then had open pores along 1 mm of the microchannel length. C) The top well PDMS layer was aligned and bonded. D) The assembled device was bonded to a glass slide placing liquid PDMS around the perimeter of the bottom device layer, and then curing the liquid PDMS on a hot plate.

3.6 Characterization of Drug Delivery

3.6.1 Diffusion Through Membrane

Transport of compounds through the nanoporous membrane should have a high degree of spatial and temporal control. Control could be achieved by manipulation of an external electric field, which in turn would determine the overall electrokinetic flow rate. Because of the need for a high degree of control, compounds should not be able to pass through the membrane without any user input. Since diffusion through the membrane pores had very little controllability, that type of transport needed to be prevented. However, previous works have demonstrated the degree of control of passive diffusion through a porous membrane. [Melosh NA, 2011] Diffusion could be controlled by the surface hydrophobicity of the membrane, and of the membrane's pore size.

A qualitative test of controllability was carried out for hydrophobic, 100 nm diameter pores (Figure 3.6). Methylene blue was filled in the microchannel, with PBS in the well, and then left for 1 hour to see if the dye would passively transport though the membrane. After 1 hour, no diffusion was observed. However, when an external electric field was applied, the dye was transported across the membrane within 1 minute.

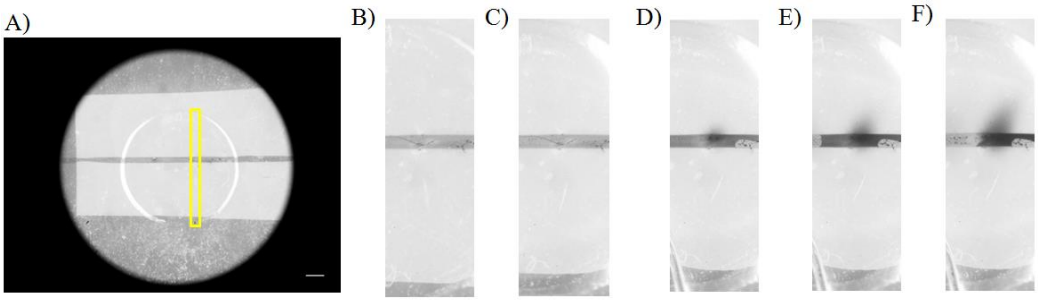

Figure 3.6: Qualitative demonstration of flux of methylene blue dye through the nanoporous polycarbonate membrane. A) Full view of the well and highlighted test area. B) Dye was initially loaded into the microchannel below the membrane. C) After 60 minutes with zero applied voltage, diffusion of dye could not be detected by eye. Once an external voltage of 150V was applied across the membrane, migration of dye into the well above could be detected after: D) 1 minute, E) 2 minutes, F) 3 minutes. Scale bar is 1 mm.

3.6.2 Spot Diameter Growth Rate

First tests were to determine if controlling the electric field could have an effect on the initial dye spot size. Larger spot sizes, once electrokinetic pumping was turned off, were desirable since it would have taken less time for the dye to diffuse homogeneously throughout the well.

A theoretical analysis of the diffusion of methylene blue in the device well was calculated to determine the maximum expected diffusion times. The analysis used a worst-case scenario of a dye spot starting in the middle of the well, with a radius of almost zero. The equation used was based off Einstein-Stokes diffusion relationship:

$$\tau = x^2/2D \quad \text{(Eq. 3.4)}$$

Where τ is the diffusion time for a group of molecules with a diffusion coefficient of D, to migrate across a distance, x. The diffusion coefficient of methylene blue was 5 x 10^{-6} cm^2/s, and the diffusion distances ranged from 0.01 cm to 0.6 cm. As can be seen from Figure 3.7, the theoretical time taken for methylene blue to diffuse from the center of the device well to the edge (0.3 cm) was around 9000 seconds. It was expected, however, that the actual diffusion time across the same distance to be less than the theoretical time. This is because the experimental scenario takes into account the variation in concentration gradient with time (magnitude of diffusive flux), and an initial spot radius greater than zero. Furthermore, there is a region between 0 and 0.1 cm, where diffusion times could be practical for microfluidic applications. If experimental diffusion times are less than these theoretical values, then diffusive drug delivery at these distances could be viable.

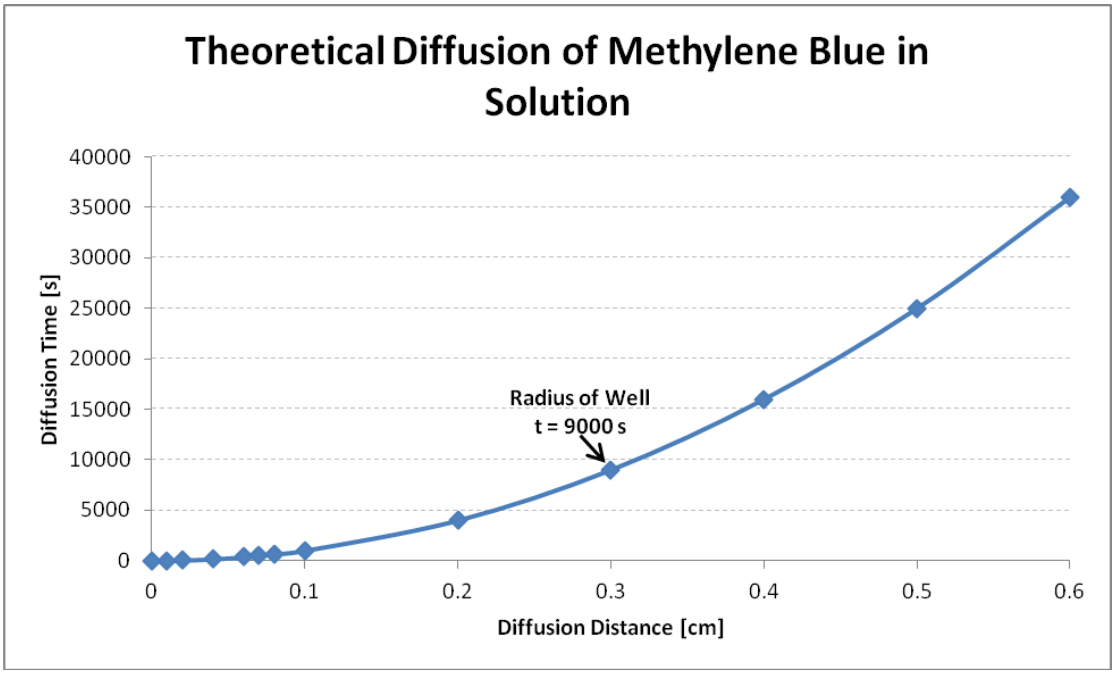

Figure 3.7: Theoretical analysis of the diffusive behaviour of methylene blue in the well of the dye delivery device. There is a squared relationship between diffusion distance and time. For methylene blue to diffuse to the edge of the device well, it would take approximately 9000 seconds. There is also a region between 0 cm and 0.1 cm where diffusion times are low enough for diffusion drug delivery to become viable.

Absorbance of the dye spot was measured as arbitrary gray values. Background values represented the absorbance of the well (with 50 µL of PBS inside) and PBs in the channel below. For a single applied DC voltage, the absorbance profile of the dye spot had increased every minute (Figure 3.8). The dye spot could then be controlled by duration of the applied voltage, when all other parameters remained constant (such device materials, device dimensions, and magnitude of applied voltage). Although absorbance outside the channel walls increased with time, they were not correlated with dye concentration until a later test.

Measured spot diameters were compared with different applied voltages. For the three voltages tested (150 V, 125 V, and 100 V), the rate of increase of the dye spot were similar (Figure 3.10). If this relationship hold true, then dye spot size could perhaps be interpolated for voltages and durations that were not tested.

The second test was to measure the time taken for dye spots to diffuse to the walls of the well, after electrokinetic pumping. After 3 minutes, the power supply was turned off. Absorbance measurements

were made every minute for 10 minutes, then every 10 minutes for 60 minutes. A timeframe was needed for how long diffusion transport would take, and determine if it was suitable for any drug delivery application.

After pumping at 150V for 3 minutes, the absorbance profile of the dye spot was measured over time. As expected, the absorbance values closer to the channel (around 0.6 mm from the center) decreased over time, while the absorbance values father from the channel (greater than 0.6 mm from the center) increased over time (Figure 3.9). At 5 minutes the absorbance profile, excluding over the channel, was fairly level (about a 30 gray value difference). A level profile would indicate a homogeneous dye concentration throughout the well. For this study's application, a homogeneous concentration is required for each well. Every well would have a unique concentration for testing on mammalian cells.

Increases in dye spot diameters, due to diffusion, were measured over time for three different applied voltages: 100 V, 125 V, and 150 V. The initial time (0 minutes) was when the power supply was turned off, after the dye was continuously pumped into the well for 3 minutes. For 150 V pumping voltage, the dye spot had reached the edges of the well in 2 minutes; for 125 V the time was 3 minutes, and for 100 V the time was 4 minutes (Figure 3.11). These results indicate, within applied voltages between 100 V to 150 V, the dye could be distributes throughout the well within 5 minutes. Drug delivery studies could potentially be viable for this device configuration, if the minimum required timeframe was 5 minutes or greater. Furthermore, if the device dimensions and/or materials were changed, these same tests could be implemented to determine a required timeframe for drug delivery.

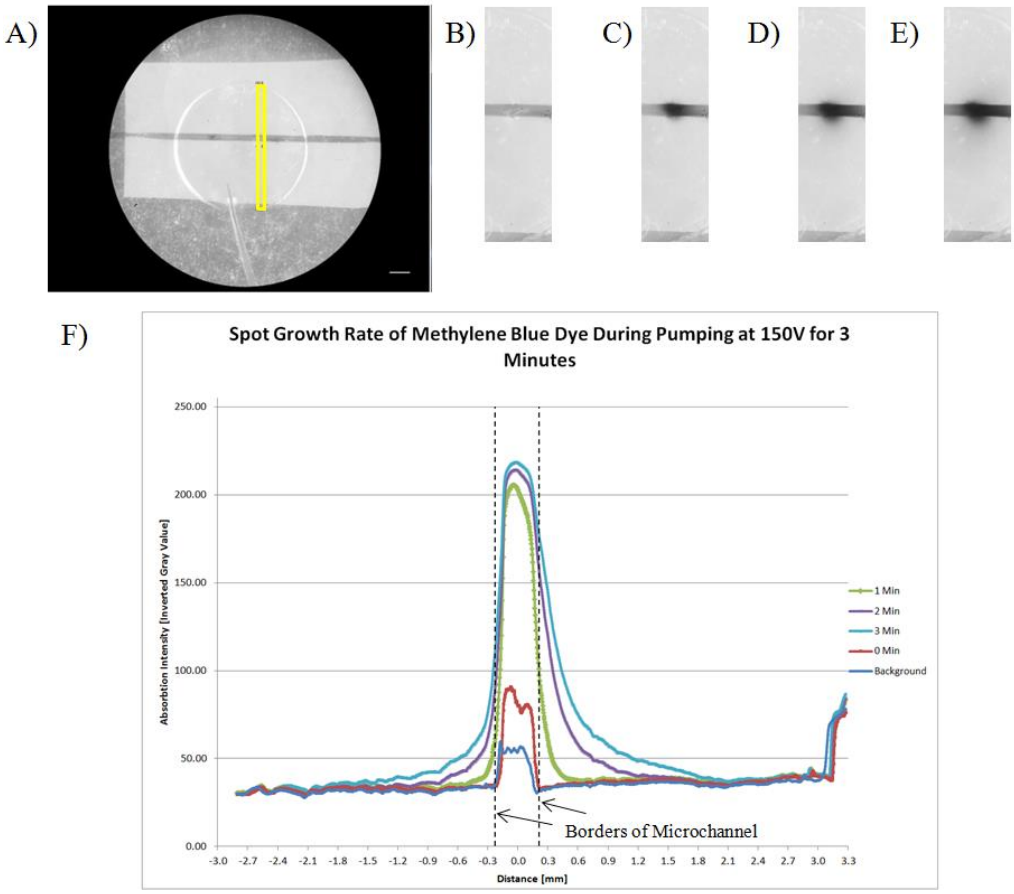

Figure 3.8: Active electrokinetic pumping of dye at 150V, over a time period of 3 minutes. A) Full view of the well and highlighted test area. Area analyzed was 6 mm by 0.4 mm. B) Before the voltage was applied. C) 1 minute. D) 2 minutes. E) 3 minutes. F) Absorbance plot profiles from the center of the channel. Spot size can be measured when the absorbance equals the background value. Scale bar is 1 mm.

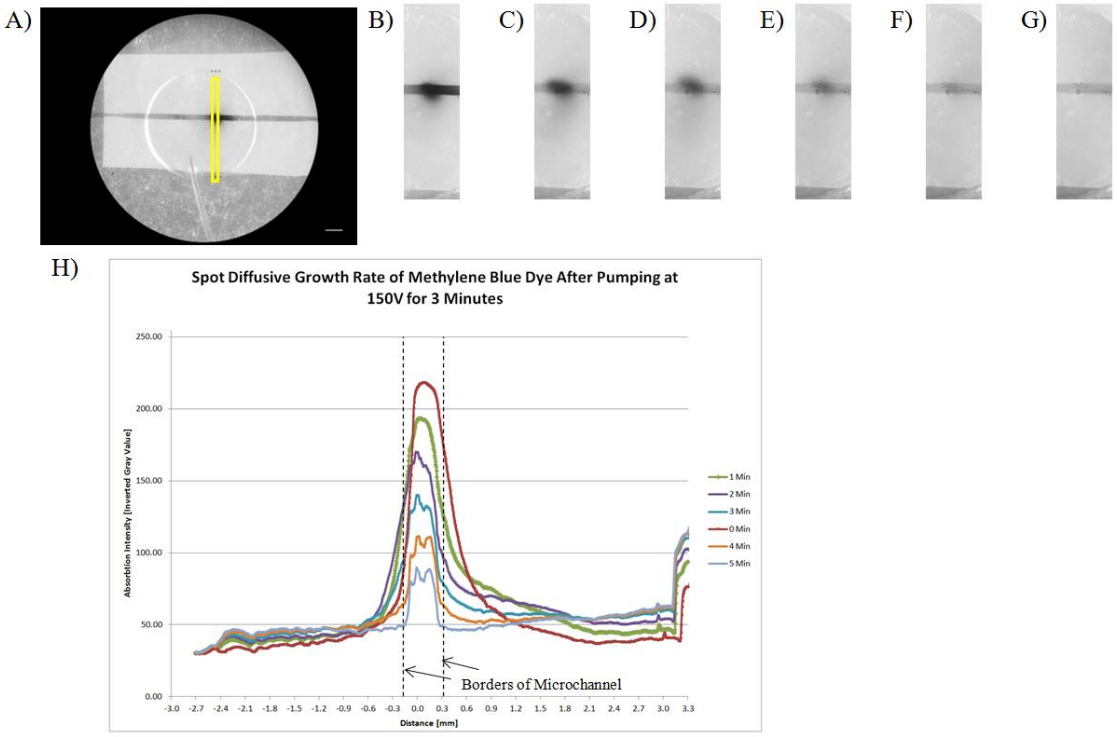

Figure 3.9: Passive diffusion of dye, after electrokinetic pumping, over a period of 5 minutes. A) Full view of the well and highlighted test area. Area analyzed was 6 mm by 0.4 mm. B) Immediately after active pumping had stopped. C) 1 minute. D) 2 minutes. E) 3 minutes. F) 4 minutes. G) 5 minutes. H) Absorbance plot profiles from the center of the channel. Spot size can be measured when the absorbance equals the background value. Scale bar is 1 mm.

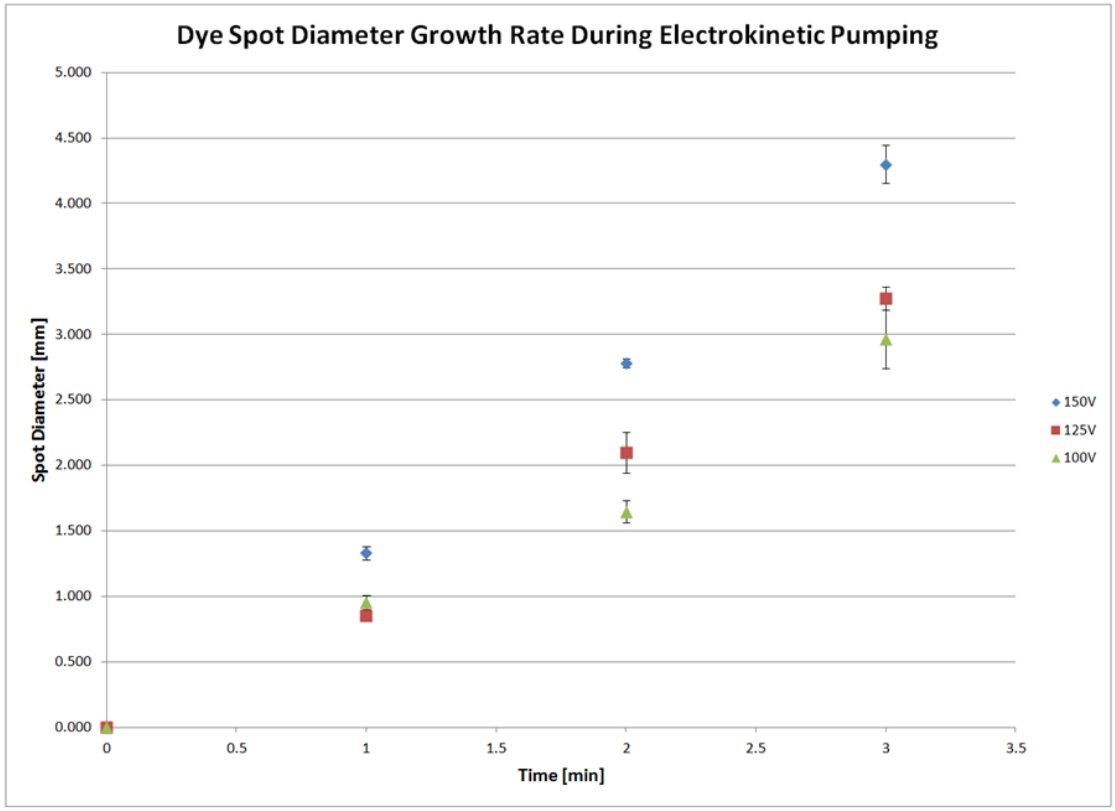

Figure 3.10: Growth of the dye spot over time, as a result of electrokinetic pumping into the well. Voltages, ranging from 100V to 150V, were applied across the nanoporous membrane for 3 minutes each. At each time point, high voltages had yielded large spot diameters; however, 125V and 100V measurements seemed to overlap in the first and third minutes. Error bars represent the standard deviation of 5 measurements taken per time point.

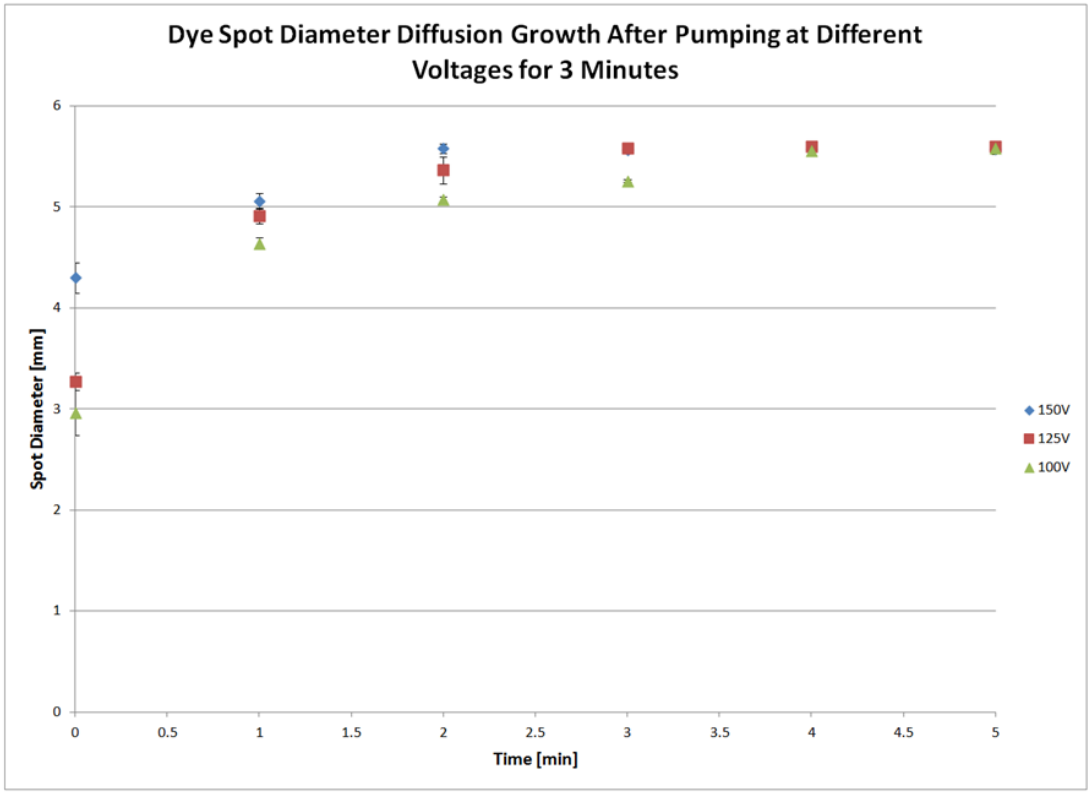

Figure 3.11: Growth of the dye spot over time, as a result of diffusion transport after electrokinetic pumping had ceased. For all voltages, the dye had diffused to the measured limits of the well within 5 minutes. Error bars represent the standard deviation of 5 measurements taken per time point.

3.6.3 Drug Dose Control

Using arbitrary absorbance values, the concentration needed to be determined in order to relate end application dosage of drug delivery. Calibration measurements were made by preparing several known concentration of Methylene blue dye, then dispensing 50 µL of a single concentration into the well of the device. For each concentration, two images were taken with a Nikon Coolpix camera for exposure times of 0.3 and .25 seconds. The images were imported to a custom MatLAB program, which could analyze each image as a matrix of gray values, with each value representing a pixel. Gray values were set by the camera, and were represented as arbitrary numbers between 0 and 255. A gray value of 0 was white and a gray value of 255 was black. The MatLAB program averaged the gray values over a 1400 by 100 pixel area in the center of and perpendicular to the microchannel. Each averaged value (one per

image) was exported as an Excel file. In Excel, the gray values were plotted against the known methylene blue concentration. There seemed to be a linear relationship between the averaged gray value and known concentration (Figure 3.12). However, with absorbance as the method of measurement, it was difficult to distinguish concentrations of 10 μM or less; this was true for both camera exposure times. For future considerations, there could be greater sensitivity to concentration differences if fluorescent measurements were taken instead of absorbance.

We wanted to determine the amount of dye (in mass units) delivered during active pumping, and if it could be controlled by changing the applied external electric field. During active pumping for 3 minutes, the dye spot diameter was measured every minute. With the absorbance profile, and the diameter of the dye spot known, an average gray value was then calculated. The average gray value was then converted to a concentration value, by interpolation along the calibration curve. Since the volume of the spot was known, the amount of dye (in nano grams) was calculated from the averaged concentration value. Duration of electrokinetic pumping, for a single DC voltage, seemed to have an exponential relationship to the amount of dye delivered (Figure 3.13). It can be seen that 100 V and 125 V yielded similar results, while 150 V could be distinguished at 2 minutes. The reason as to why 100 V and 125 V are so similar may have arisen from sources of error such as: too small and area analyzed, the contrast of absorbance measurements between concentrations was too low, or the shape of the dye spot was irregular.

Besides the amount of dye delivered over time, the final concentration in the well needed to be determined. For the end application of drug delivery, there would be a single concentration of drug per well. After electrokinetic pumping for 3 minutes, the dye spot was left to diffuse for 5 minutes, in order to spread throughout the well. After 5 minutes of diffusion transport, absorbance measurements were taken of the dye. Gray values were taken over a 1400 by 100 pixel area, minus the area of the channel. The gray values were averaged along the rows first, then the remaining column; a single averaged value then resulted. Averaged gray values were then compared with 150 V, 125 V, and 100 V applied voltages (Figure 3.14). 150 V yielded the greatest concentration, while 125 V and 100 V had similar concentrations. The similarity between 125 V and 100 V could have been attributed sources of error, such as: the diffusion time was too short, or the contrast of the absorbance measurements was too low. However, some degree of control was demonstrated by variation of the applied voltage. Furthermore, the dye concentration could also be controlled by variation of the pumping duration.

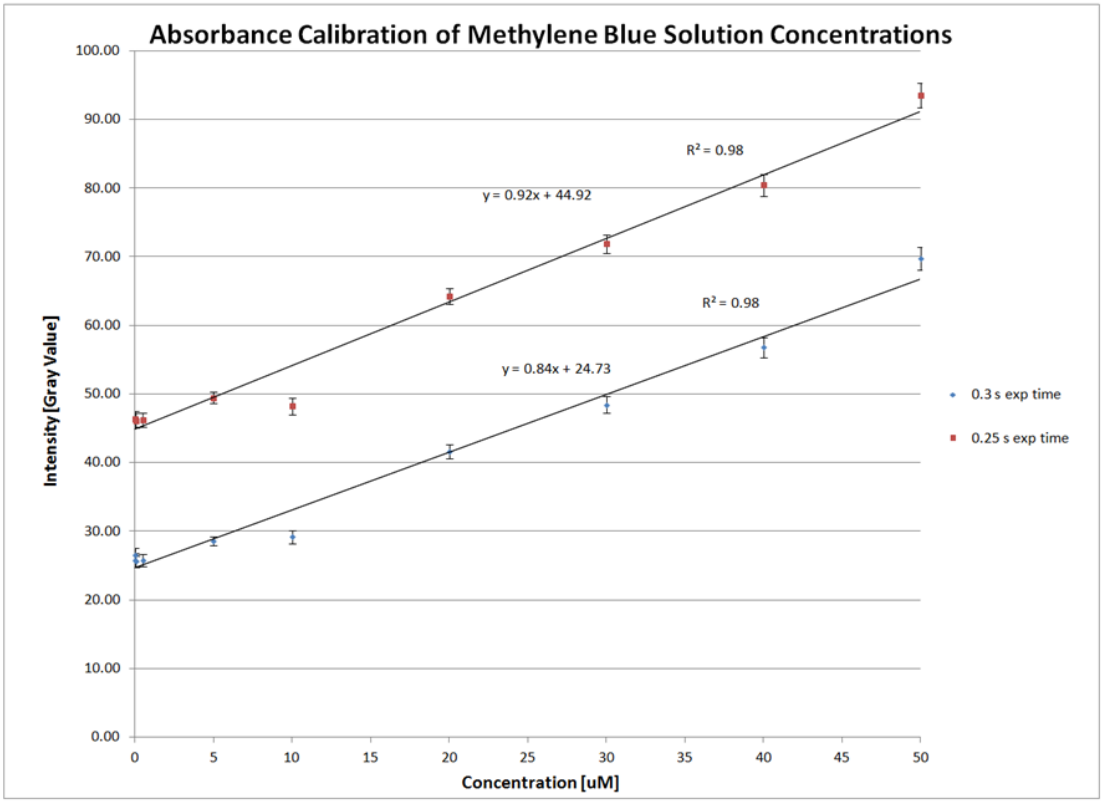

Figure 3.12: Absorbance values calibrated to various concentrations of methylene blue dye. Known concentrations of methylene blue were manually prepared, then dispensed directly into the well of the device. The two plots represent different exposure times of the camera: 0.25 seconds and 0.3 seconds. Error bars represent the standard deviation of 340 measured pixels.

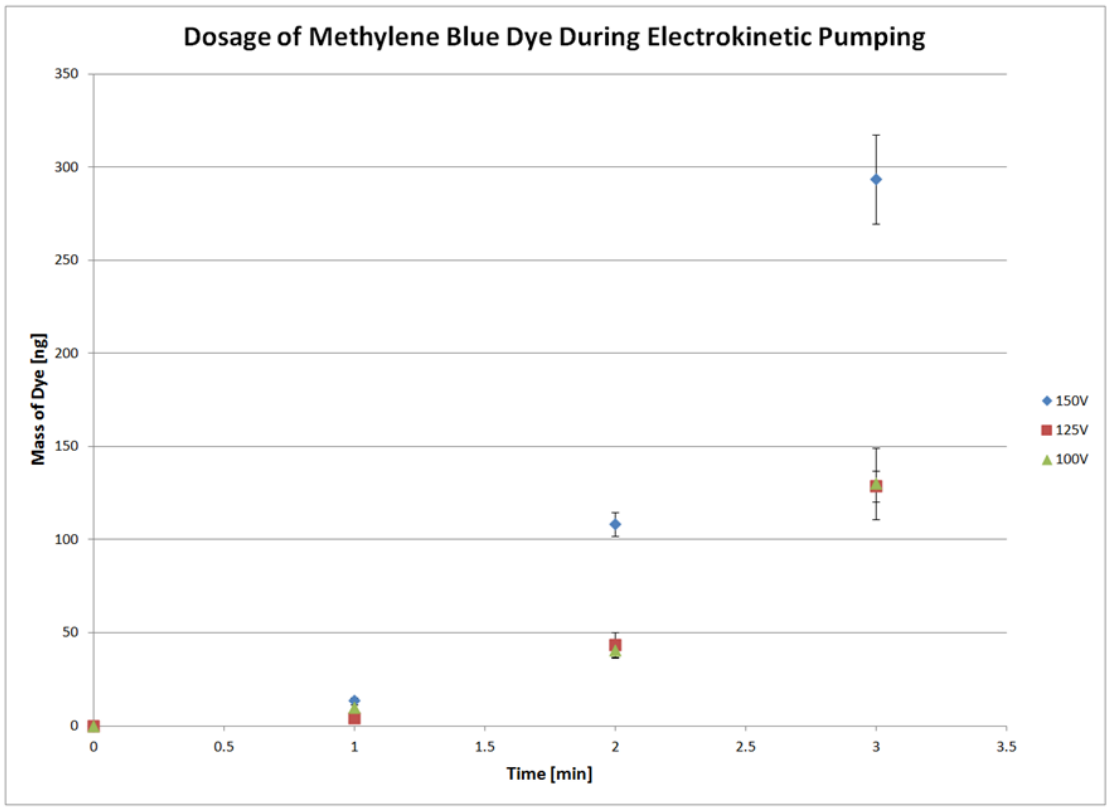

Figure 3.13: Amount of dye, in nano grams, that had been delivered to the well over time for various voltages. Absorbance values were averaged across the measured area, except along the microchannel. The calculated absorbance values were then compared to the calibration curve, and converted into micro molar concentration values. With the molar mass of methylene blue known, concentration values were converted to units of nano grams. Error bars represent the standard deviation of 5 measurements per time point.

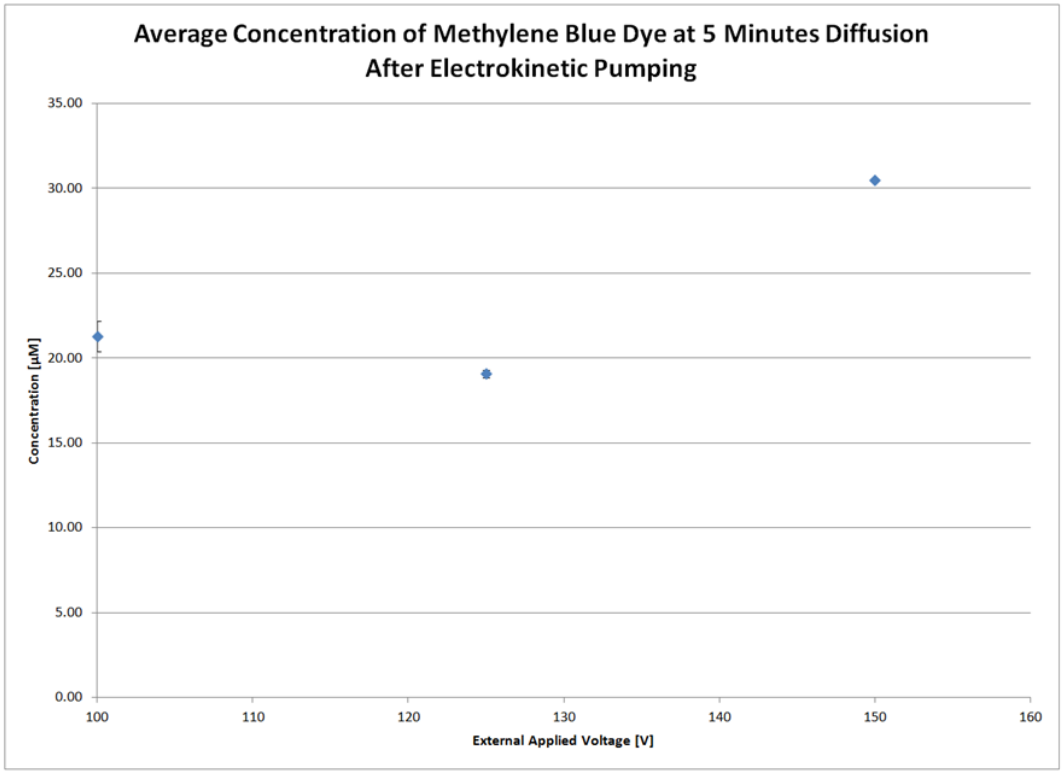

Figure 3.14: Average concentration of dye, in µM, after 5 minutes of passively diffusing in the well. Absorbance values were averaged across the measured area, except along the microchannel. The calculated absorbance values were then compared to the calibration curve, and converted into micro molar concentration values. Error bars represent the standard deviation of 5 measurements per voltage.

Chapter 4: Cell Seeding in Multi-Well Devices

Most HTS and HCS cell-based assays are carried out with multi-well plates. These well plates usually come in 96, 384, or 1536 well configurations; each increase in number of wells results in a subsequent decrease for each well volume.

For proper use in cell biology studies, well plates must not have a negative impact on cell biology. As such, PDMS multi-well microfluidic devices were seeded with cells and characterized in terms of cell viability and cell growth. Characterized parameters were then determined if they were comparable with plain coverslip glass controls. Since surface characteristics of PDMS could have an effect on cell attachment, both hydrophobic and hydrophilic PDMS was also characterized.

4.1 Design Criteria

The following parameters for the design of a multi-well cell culture device were: an open well configuration, a mammalian cell line, a wide range of well diameters, and the material of the wells. An open well configuration was needed since the cells and culture media would be dispensed by pipette, and it would be potentially compatible with robotic liquid dispensers. A mammalian cell line was needed that would be currently used in drug discovery studies; MCF-7 breast cancer cells were chosen because they are actively used in research, and are an adherent cell line. For a range of well diameters, the minimum was defined to hold at least 100 cells, and a maximum would be similar to those used either in well plates or similar to diameters used in microfluidic cell culture. PDMS was chosen as the material for the well walls since it is chemically inert, and its surface can be modified from hydrophobic to hydrophilic which effectively provides two different testing conditions. Coverslip glass was the chosen material for the well bottom, since it is thin enough (0.17 mm) for high-magnification microscopes and it is often used as a cell culture substrate.

4.2 Design

PDMS micro-well devices each had an array of 9 wells, with diameters ranging from 0.35 mm to 1.2 mm, with a 25 mm diameter coverslip glass as the culture substrate. The smallest diameter roughly represented the minimum area to contain 100 cells, which is the set minimum number of cells each well is required to hold. The largest diameter had a cell culture area similar to previously developed microfluidic devices from other groups. [Quake SR, 2007]. All PDMS well diameters tested were less than the diameter of a well of a 384 well plate

(2.67 mm); the 0.75 mm PDMS wells were roughly equivalent in diameter to a well of a 1536 well plate (0.74 mm).

The total device area is equivalent to the area of a well in a 96 well plate (Figure 4.1). Since the Perkin Elmer Opera automated microscope and robotic liquid dispensers can both be configured for a 96 well plate format, the PDMS micro-well devices could be compatible with each. The Opera microscope and the robotic liquid dispenser were not directly used in experiments; even so, future studies could include these pieces of equipment if the PDMS micro-wells were mass replicated in a 96 well plate fashion.

To enter the wells, cells are seeded from a cell media solution in a pitri dish and pipetted directly onto the PDMS micro-wells (Figure 4.2). The cells precipitate down to the bottoms of the micro-wells; as a downside, the distribution of cells was expected to be very random and non-uniform. A future design could perhaps incorporate a mechanism capable of a uniform and predictable cell loading distribution. For example, Lee *et. al.*'s group had used microchannels with varying resistances to load an 8x8 array of cell culture chambers; with a fixed flow rate and cell density, the cells had exhibited a predicted Poisson distribution and the number of cells was independent of chamber location. [Lee LP, 2005] MCF-7 breast cancer cells would be analyzed via imaging with an inverted widefield microscope, in phase contrast mode, through the coverslip glass.

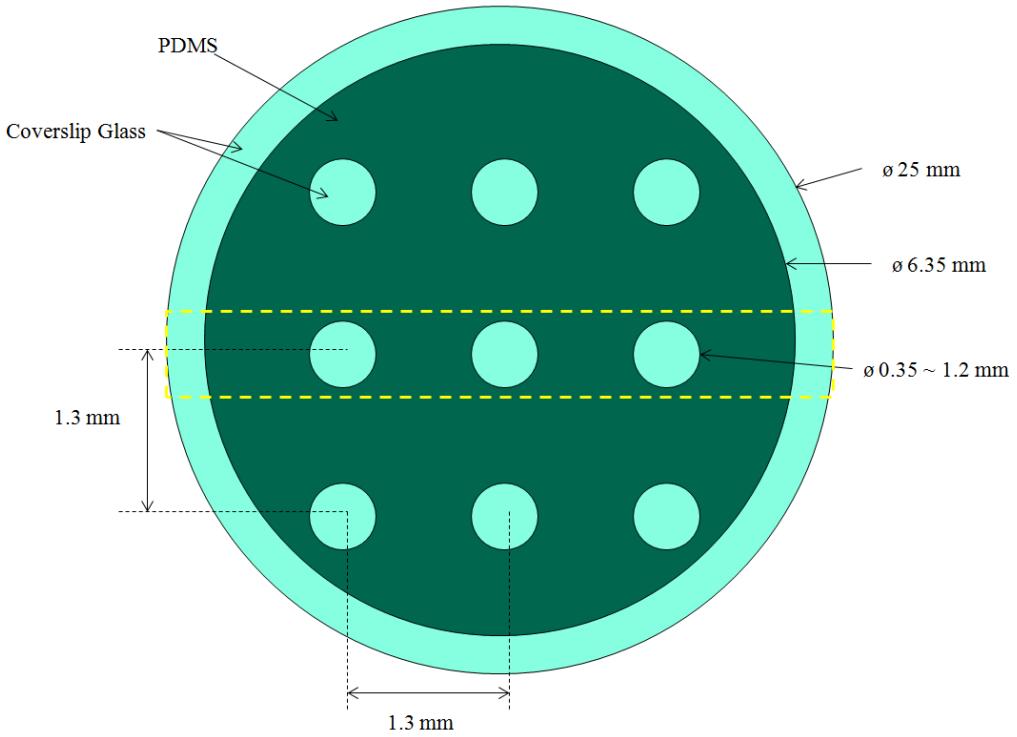

Figure 4.1: Top view of the multi-well micro cell culture device. The cross-section of the highlighted region in yellow is shown in Figure 4.2. Dimensions shown are not to scale.

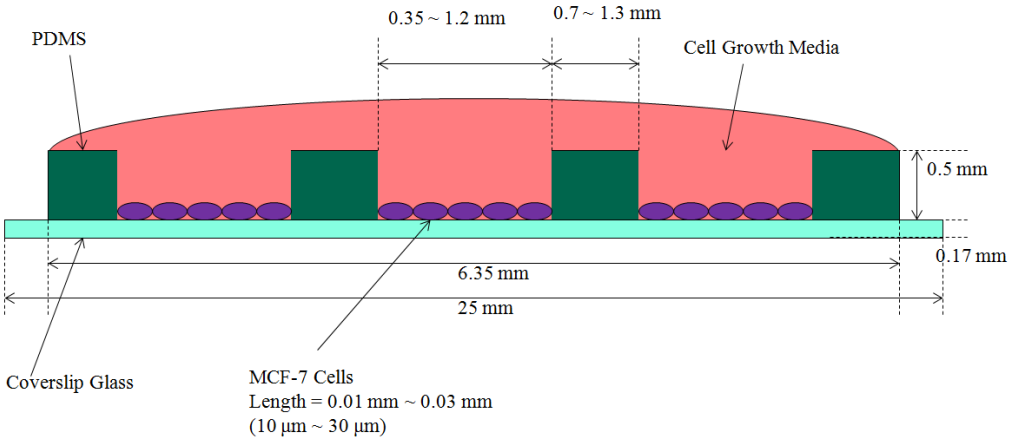

Figure 4.2: Cross-section of the multi-well micro cell culture device. Dimensions shown are not to scale.

4.3 Materials

Coverslip Glass

For achieving images with high optical quality under an inverted widefield microscope, 170 µm (0.17 mm) thick coverslips were used. Coverslips were implemented as the substrate of all multi-well culture devices fabricated. Diameters of the coverslips were 25 mm, made of borosilicate glass, had an untreated surface, and were amenable to cell culture.

Trypsin

Trypsin is an enzyme used in *in-vitro* cell culture to breakdown proteins that anchor cells to the culture surface. Once the anchoring proteins have broken down, the cells can be lifted off the culture surface by gently aspirating with a pipette.

To reduce the reaction rate of breaking down proteins, trypsin would be typically diluted 1 to 10 with PBS.

Cell Media

Keeping cells healthy and proliferating in culture requires media containing a mixture of nutrients. Media used for cell culture was α-MEM (Minimum Essential Media), supplemented with 10% fetal bovine serum and 1% penicillin. Fetal bovine serum provided extra nutrients to further promote health and division of cells, while penicillin acted as an anti-biotic against potential pathogens such as mycoplasmas.

MCF-7 Cells

MCF-7 cells are a breast cancer cell line that have estrogen receptors in their cell cytoplasm, and as such are called estrogen receptor positive. The line was originally extracted and isolated from a Caucasian woman, who was 69 years old, in 1970. The Michigan Cancer Foundation had then subsequently discovered the cell line in 1973. These cells were used in this study because they were adherent to cell culture surfaces, grew in a monolayer, and had been used in many different molecular screens such as siRNA gene silencing.

Trypan Blue

Trypan blue is a highly visible dye that is often used in cell-based assays as an indicator of viability. Membranes of healthy cells prevent trypan blue from passing through, while the dye can pass through compromised membranes of dead and unhealthy cells. Under a light microscope, viable cells would appear somewhat transparent, and dead and compromised cells would appear blue or dark. Trypan blue dye used in experiments was from Sigma Aldrich and had a concentration of 0.4%, dissolved in 98.73% water; other solvents included were sodium chloride and dipotassium hydrogenorthophosphate at concentrations of 0.81% and 0.06%, respectively.

4.4 Experimental Setup and Procedure

Assembled micro-well devices were brought into a biosafety cabinet (BSC). MCF-7 cells were placed into the BSC, along with media, phosphate buffered saline (PBS), and trypsin. After approximately 3 minutes, the trypsin had lifted the cells off the pitri dish surface. Cells were then aspirated off the petri dish; 5 mL of the cell suspension was dispensed in a test tube. Using a pipette, the cell suspension was aspirated up and down in the test tube, to remove any clumps and create a homogeneous distribution.

Before the cell suspension could be seeded on the micro-well devices, the initial cell density and initial cell viability needed to be determined. 0.5 mL of the cell suspension was removed and dispensed into a 1 mL test tube, which was then combined with 0.5 mL of 0.4% v/v trypan blue solution. The cell suspension/trypan blue mixture was aspirated up and down in the 1 mL test tube, until homogenously distributed. A grid-based hemocytometer, with two separate chambers, was used for cell counting. The counting chambers and glass lid of the hemocytometer were sterilized with 70% ethanol, and then dried with Kimwipes. 10 µL of the cell suspension/trypan blue mixture was dispensed into each of the two chambers of the hemocytometer. Counting was performed under an inverted light microscope, with a 4X objective. Following a protocol for a grid-based hemocytometer [Roberts PE, 1998], the initial cell density was measured; initial percent cell viability was calculated for each chamber by dividing the number of non-blue cells to the total number of cells. With the initial cell density known, the original 4.5 mL cell suspension was diluted with cell media to approximately 0.75×10^6 cells/mL. The new cell suspension was then brought into the BSC.

In the BSC, DI water was aspirated from the PDMS well devices. 100 µL of 70% ethanol solution was used to sterilize each of the PDMS micro-well devices. After 3 to 5 minutes, the 70% ethanol solution was

aspirated from the devices. 50 µL of cell suspension was seeded on each PDMS micro-well device. For control measurements, 50 µL of cell suspension was dispensed on 2 plain coverslip glasses. All micro-well devices and controls were placed in 6-well plates. The devices and controls were then stored in the incubator for around 30 minutes to allow attachment of cells to the bottom of the micro-wells. Afterwards, the micro-well devices and controls were brought back to the BSC, and then 2 mL of fresh media were dispensed into each device.

Once seeded with cells, the micro-well devices were brought to the widefield microscope (Leica DMI 6000 B). Images were taken of every well, in each device, using 4X and 20X objectives. Once finished, all devices were placed back in the incubator. Images were taken every 24 hours, for up to 5 days (0, 24, 48, 72, 96, and 120 hours). After imaging, cell media was replaced with fresh media for each device. After imaging at the end of 5 days, the cell media of each device was replaced with 100 µL of 1:1 cell media to trypan blue solution. Under the widefield microscope, the final % cell viability was calculated for each well, with the method previously stated.

Cell proliferation rate was measured by counting the approximate number of cells at each time point; cells were counted in one well for each diameter and surface condition (hydrophilic, hydrophobic, and polycarbonate membrane). The cell number was automatically determined using a particle counting plugin in ImageJ. The region of interest was defined as the inner perimeter of each well. For coverslip glass controls, the region of interest was defined as a 1.2 mm diameter circle, in the center of the image. Manual counts for hydrophilic 1.2 mm diameter wells at each time point were used to validate automated counts.

4.5 Fabrication Process Flow

Three-dimensional moulds for each multi-well device (1.2 mm, 1.0 mm, 0.75 mm, 0.5 mm, and 0.35 mm) were drawn in Adobe Inventor. Each mould represented the inverted structures of the devices (Figure 4.3A). All designed moulds were then fabricated in a three-dimensional printer, using acrylic polymer as the material.

PDMS was prepared by mixing 10 mL of base with 1 mL of curing agent; a 10:1 base to curing agent ratio was used. The PDMS mixture was stirred for around 1 minute, to ensure that the cross-linker was distributed homogeneously throughout the PDMS base. If bubbles were degassed in the lab, then the mixture was placed in a vacuum chamber for around 5 minutes. If bubbles were degassed in the clean room, the mixture was left to sit at atmospheric pressure for about 30 minutes. Once the mixture was ready, about 1 mL of liquid PDMS was dispensed onto each device mould (Figure 4.3B). To make the liquid PDMS flush with the surface of the

mould, a small sheet of plastic laminate and a microscope slide were placed on top of the PDMS side of the moulds, while another microscope slide was placed under the bottom side of the moulds. Clips held the mould, laminate, and microscope slides into place. The liquid PDMS was made flush with the mould surface to prevent a membrane forming over the wells, once the PDMS was cured (Figure 4.3C). Liquid PDMS in the moulds were cured on a hot plate at 50°C for 24 hours (Figure 4.3D). Clips, microscopes slides, and laminate sheets were then removed from the moulds. Tweezers were then used to gently peel off the PDMS micro-wells (Figure 4.3E). The micro-well devices were then stored in a petri dish, before being taken to the clean room.

At the wet bench in the clean room, 10 coverslip glasses (8 devices, 2 controls) were cleaned by washing in acetone, methanol, and de-ionized water. The coverslips were submerged in acetone for 15 seconds, submerged in methanol for 15 seconds, and then placed under flowing de-ionized water for 5 minutes (Figure 4.3F). Excess water on the surfaces was dried with nitrogen gas. Liquid PDMS, at a ratio of 10:1, was spun on a clean silicon wafer at 4000 rpm for 120 seconds, to get a thickness of around 1 μm or less. The silicon wafer was then transferred over to the wet bench. In order to bond the PDMS devices to coverslip glasses, the bonding surfaces needed to be hydrophilic. The coverslip glass surfaces were made hydrophilic by exposing them to oxygen plasma at 40 W for 60 seconds in a barrel etcher (Figure 4.3G). Aside from coverslip hydrophilic surfaces, a thin layer of liquid PDMS was applied between the cured PDMS layer and the coverslip glass to aid in bonding. The bottom surface of the solid PDMS was placed on the silicon wafer, containing liquid PDMS, and left on for about 10 seconds. The solid PDMS was gently peeled from the wafer with tweezers. If a device used a polycarbonate membrane: a piece of the 100 nm pore, polycarbonate membrane was placed on top of the glued PDMS surface; another layer of liquid PDMS was applied to the underside of the membrane. The glued side of the PDMS (or polycarbonate) was gently contact-printed onto the hydrophilic coverslip glass surface, which formed a bond (Figure 4.3H). All assembled devices were placed on a hot plate, at 80°C for 20 minutes; once the liquid PDMS had cured, a strong and permanent bond was formed between the PDMS micro-well devices and the coverslip glasses.

Before the devices were used for cell culture, the top surfaces and side-walls needed to be hydrophilic. The devices were exposed to oxygen plasma at 40 W for 60 seconds, in a barrel etcher (Figure 4.3I). Finished micro-well devices were placed in clean petri dishes (or any other containers), and then filled with de-ionized water (Figure 4.3J). Hydrophilic surface properties of the PDMS would remain for about several days.

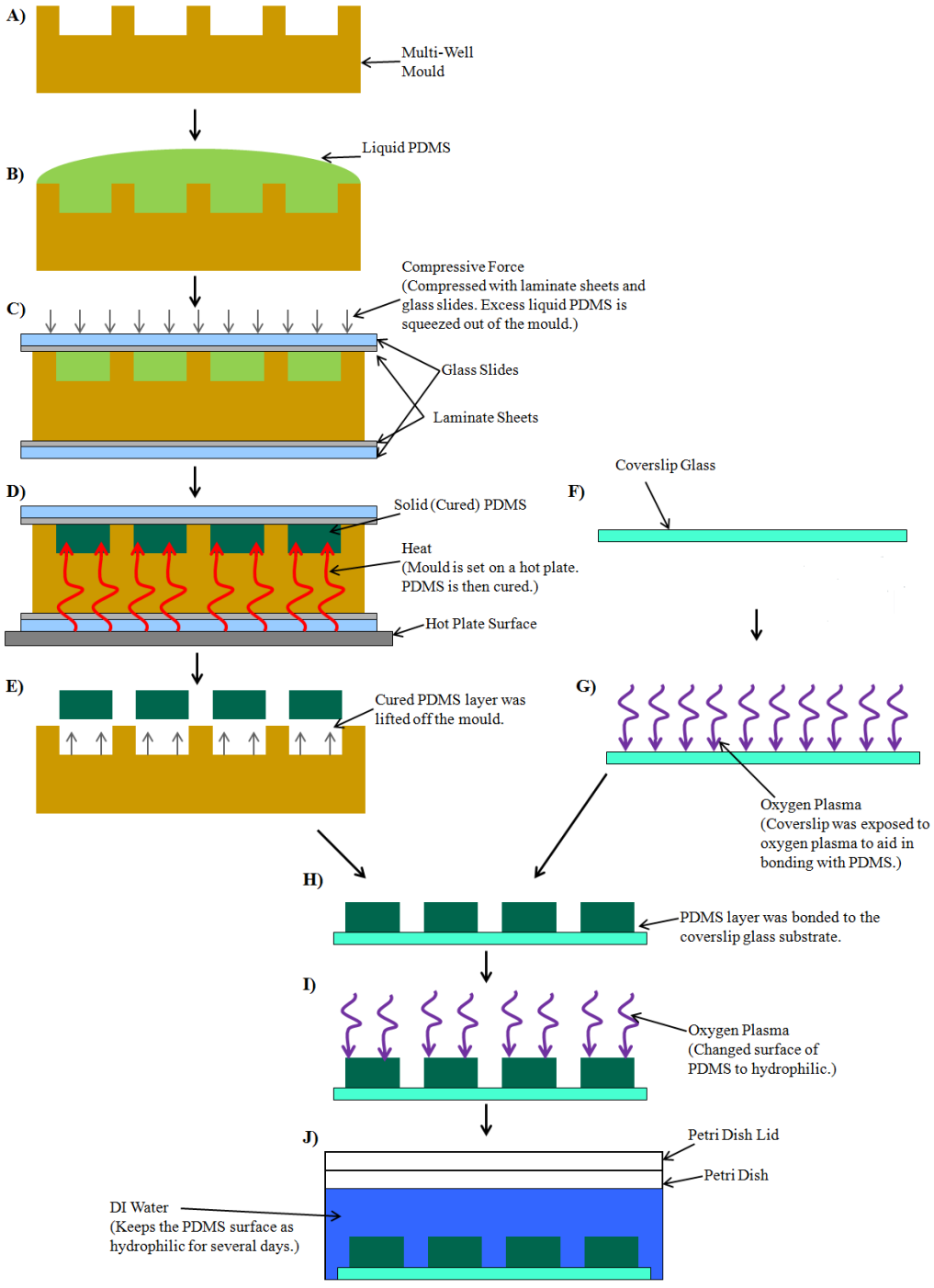

Figure 4.3: Process flow for the fabrication and preparation of multi-well cell culture devices. A) Inverted structures in a polymer mould. B) Liquid PDMS poured over the mould structures. C) Laminate

sheets and microscope slides act as a clamp, to displace any excess liquid PDMS by compression. D) The PDMS was cured on a hot plate at 50 °C for 24 hours. E) Cured PDMS was gently peeled off the mould. F) Coverslip glass was cleaned in acetone and methanol for 15 seconds each, and then rinsed in flowing DI water for 5 minutes. G) Coverslip glass was exposed to oxygen plasma to aid in bonding with PDMS. H) The PDMS well layer and the coverslip glass were bonded together by contact- printing. I) The PDMS surface was modified to become hydrophilic, by exposing it to oxygen plasma at 40 W for 60 seconds inside a reactive ion etcher. J) Lastly, the entire device was placed in a petri dish, and stored in DI water. The DI water would help the PDMS surface stay hydrophilic for several days.

4.6 Discussion

MCF-7 cells had attached to the bottoms of the wells (i.e. the coverslip glass surface) within 4 hours after initial seeding. All test conditions had cells attached to the bottom of the wells, except for 0.5 mm diameter and 0.35 mm (which had 1 well each with cells). Upon observation with a 4X objective microscope, the cells had appeared spheroid in shape. After 24 hours of incubation, the attached cells had stretched themselves along the well bottom, and had formed small groups/colonies; under the microscope, the cells had appeared elongated in shape. Within 120 hours time, the cells had proliferated until each well was overgrown (Figure 4.4, Figure 4.5); the cells had appeared to cover the entirety of each well bottom.

Cells grown in 0.75 mm and 1.2 mm diameter wells taken with a 4X objective (Figure 4.5) and a 20X objective (Figure 4.6) had similar qualitative cell growth patterns. For controls and for both types of wells, the cells had appeared spheroid in shape after 4 hours of incubation. At 24 hours, the cells had spread out along the bottom of the wells and had appeared elongated in shape. After 120 hours of culture had passed, the cells had been overgrown throughout the wells.

A similar cell growth comparison was made between 0.35 mm and 05 mm (Figure 4.7). Only images taken with a 20X objective were shown because both well diameters could be taken within the field of view. For the 0.35 mm device, unlike the other well diameters, only a single well of the 9 wells had cells growing inside it. This may be due to experimental sources of error, such as: the diameter may have been too small for the cell media to initially fill wells during seeding; perhaps during initial cell seeding, air bubbles had formed within the wells; the cells may have preferentially attached onto the top PDMS surface. More tests should be carried out at this diameter, along with untreated hydrophobic PDMS.

For 1 mm diameter wells, comparisons were made between hydrophilic PDMS, hydrophobic PDMS, and hydrophilic PDMS with polycarbonate membrane on top (not covering the wells). At 4 hours (Figure 4.8), the hydrophilic PDMS with and without the membrane had similar cell attachment to controls; hydrophilic PDMS had cells attached to the bottom of the well, but had clustered more closely to one another in a corner of the well. At 24 hours (Figure 4.9), all cases appeared to have their cells elongated but with approximately the same number of cells. For all cases, the cell confluency increased at 48 hours (Figure 4.10) and at 72 hours (Figure 4.11). Full confluency was reached, for hydrophilic DPMS with and without the polycarbonate membrane, at 96 hours (Figure 4.12); for the hydrophobic PDMS, the cluster of cells had expanded but had not yet covered the entire well bottom. Although both hydrophilic PDMS cases had reached full confluency, the cells continued to proliferate over top one another when observed at 120 hours (Figure 4.13); the cells in the hydrophobic PDMS well had grown on top of one another, however the entire cell cluster had reached full confluency of the well bottom.

In the case of the PDMS with the polycarbonate membrane, the top surface was originally hydrophobic but was changed to hydrophilic via oxygen plasma during the fabrication process. For the final multi-well design, it is desirable that the cells do not grow on the membrane; if the cells do grow on the membrane, then they may block the nanopores over the microchannels and thereby stop any drug delivery into the well. However, it has been observed that the cells indeed grow on top of the membrane (Figures 4.8 to 4.13). This could be rectified by not surface modifying the PDMS during the fabrication process.

To provide a quantitative measure for the growth rate of cells in the micro-wells, the approximate number of cells was counted at each time point. For ease of counting, the automated particle counting plugin for ImageJ was used. Cell counts via manual counting and automated counting were compared against one another for the 1.2 mm diameter and controls at the 4 hour and 96 hour time points (Figure 4.14; Table 4.1). It was found that the automated counts were within an acceptable margin of error from the manual counts; hence, automated counting was validated to be used to measure the cell number for all experimental conditions. Sources of error for manual and automated counts were: cells along the edges of the well may have not been counted; cells too that appeared to dim in the micrograph may not have been counted; groups of closely packed cells could have been counted as a single cell; since MCF-7 cells are a cancerous cell line, at confluency they would grow on top of one another and hence these cells would most likely be unable to be counted. [Campbell NA, 2005, pg. 231] Based on these sources of error, it can be speculated that the cell number may be greater than what was counted (especially when the cells had reached confluency).

Table 4.1: Validation of Automated Counting by Comparison with Manual Counting

Method	Condition	Time [Hours]	Average Count	Error
Manual	Control	4	479	N/A
Automated	Control	4	444	55
Manual	1.2 mm	4	741	N/A
Automated	1.2 mm	4	811	53
Manual	Control	96	2820	N/A
Automated	Control	96	2882	81
Manual	1.2 mm	96	2336	N/A
Automated	1.2 mm	96	2442	146

Based on the automated counts, the cell population growth over time was plotted for all experimental conditions (Figure 4.15). Except for the 0.35 mm and 0.5 mm diameters, all cases displayed a similar growth profile: an initial lag phase, followed by an exponential growth phase, and then lastly a leveling-off phase once the cells reached confluency. Non-cancerous cell lines typically show this type of growth behaviour, and do not grow on top of each other after reaching confluency *in-vitro*; however, MCF-7 cells are a cancerous cell line. As such, it can be speculated that the cell number would continue to increase after the exponential growth phase but at a reduced rate.

Table 4.2: Theoretical Maximum Number of Cells per Micro-Well

Well Diameter	MCF-7 Cell Diameter	Well Area	MCF-7 Cell Area	Max. # of Cells
[mm]	[mm]	[mm2]	[mm2]	
0.35	0.01	0.096	0.0000785	1225
0.5	0.01	0.196	0.0000785	2500
0.75	0.01	0.442	0.0000785	5625
1	0.01	0.785	0.0000785	10000
1.2	0.01	1.131	0.0000785	14400

Except for the 0.35 mm and 0.5 mm diameters, the values shown in Figure 4.15 are averages of 9 wells with one standard deviation representing the error bars. The 0.35 mm and 0.5 mm diameters did not show a cell growth rate like the other conditions because only one well each had cells growing in them. Furthermore, images for 0.35 mm and 0.5 mm diameters from 24 hours onward show the cells undergoing apoptosis. Clearly, these had been unsuitable conditions for the MCF-7 cells; possible reasons for this behaviour are: initial seeded concentration was too high, replacement of cell media was too infrequent, the culture area was too small, and aversion to the well wall PDMS. With regards to PDMS, perhaps it had gradually become too hydrophobic over the first 24 hours.

It was observed that the hydrophobic PDMS had lower counts than hydrophilic PDMS for the first 72 hours, while the hydrophilic PDMS-with-membrane had overall lower counts than the hydrophilic PDMS. Hydrophobic PDMS had lowers counts perhaps due to the observation that the cells had typically clustered together, instead of being more evenly spread out like in hydrophilic PDMS wells. PDMS-with-membrane well had lower counts perhaps due to the cells preferentially attaching to the membrane surface rather than the well bottom; the wells may also have had lower counts perhaps due to the membrane overlapping the edges of the well, which may block the cells from reaching the bottom of the well. According to Table 2, the theoretical maximum number of cells was calculated for each micro-well diameter. With the diameter of a single MCF-7 cell to be about 10 μm, the area was calculated in square millimeters. The maximum number of cells, without overlap, was calculated by dividing the well area by the area of a single cell. Interestingly, according to Table 4.2, the maximum number of cells of a 0.5 mm diameter well (2500) is roughly equal to the number of cells measured at 120 hours for the 1.2 mm diameter hydrophilic PDMS well. The theoretical maximum number of cells for a 0.75 mm diameter well (5625) is

greater than any measured number of cells at the end of 120 hours (Figure 4.15).

For all devices, cell viability was tested with trypan blue at the end of 120 hours, and was determined to be around 99%. Since the viability of all conditions was approximately 99%, it could be speculated that these micro-wells could possibly be used in cellular assays as an alternative to well plates; however, the cells in all conditions exhibited apoptotic behaviour by the end of 120 hours. Perhaps the wells were too crowded, or the PDMS walls had reverted back to a hydrophobic state. The smallest diameter wells to exhibit a cell proliferation pattern similar to controls, 0.75 mm, was around the same size as a well from a 1536 well plate. Previous studies have used 1536 well plates reliably for cell assays; for example, cell-based compound activity of cyclic nucleotide phosphodiesterases (PDEs). [Zheng W, 2008] In conclusion, PDMS wells that were 0.75 mm in diameter and greater could be suitable for the drug delivery device in Chapter 2, if certain conditions are addressed to prevent apoptotic behaviour; these conditions include: a cell density that does not cover the entirety of the well bottom during the entire testing period, frequent changing of cell media (perhaps twice per day), and surface treatment of PDMS so that it remains hydrophilic longer than the testing period.

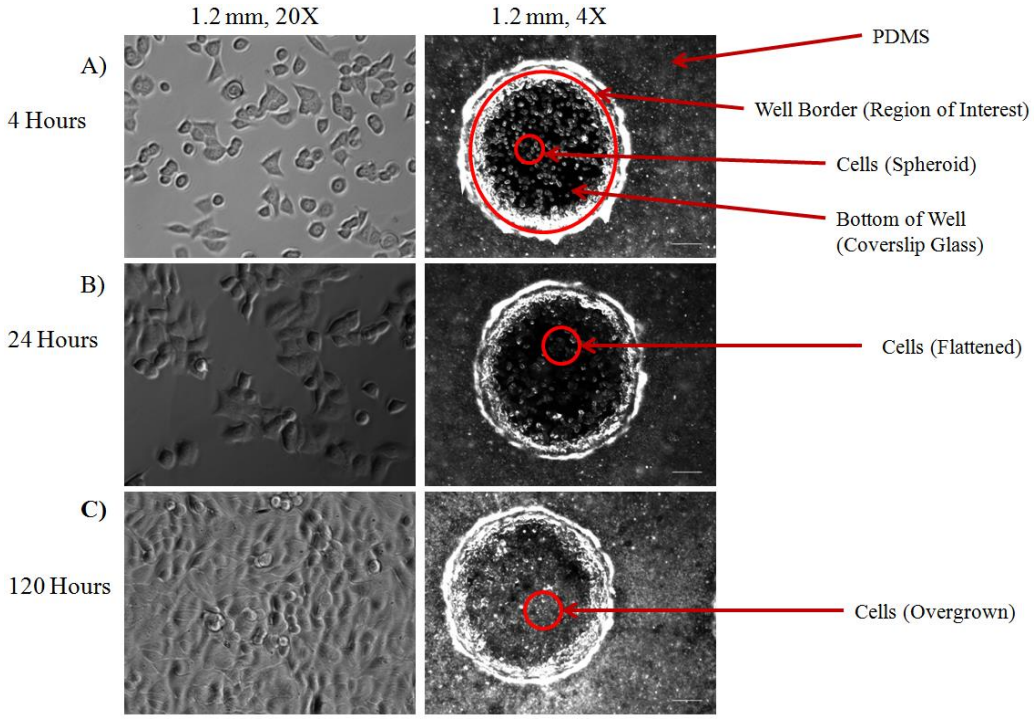

Figure 4.4: Cells seeded in a 1.2 mm diameter well, over a period of 120 hours (5 days). Images shown were of 1 well in a 9 well device. Images on the left column were magnified groups of cells taken with a 20X objective lens. Images on the right column were a view of the entire well taken with a 4X objective lens. A) Cells had attached to the coverslip glass and appeared spheroid in shape. B) At 24 hours, the cells had stretched out along the coverslip glass surface and appeared elongated in shape. C) Given time to proliferate, the cells had eventually covered the entire well bottom and had appeared to have grown on top of one another. Once the cells had overgrown, they were difficult to count. Images were captured with a 4X objective. Scale bars are 0.2 mm.

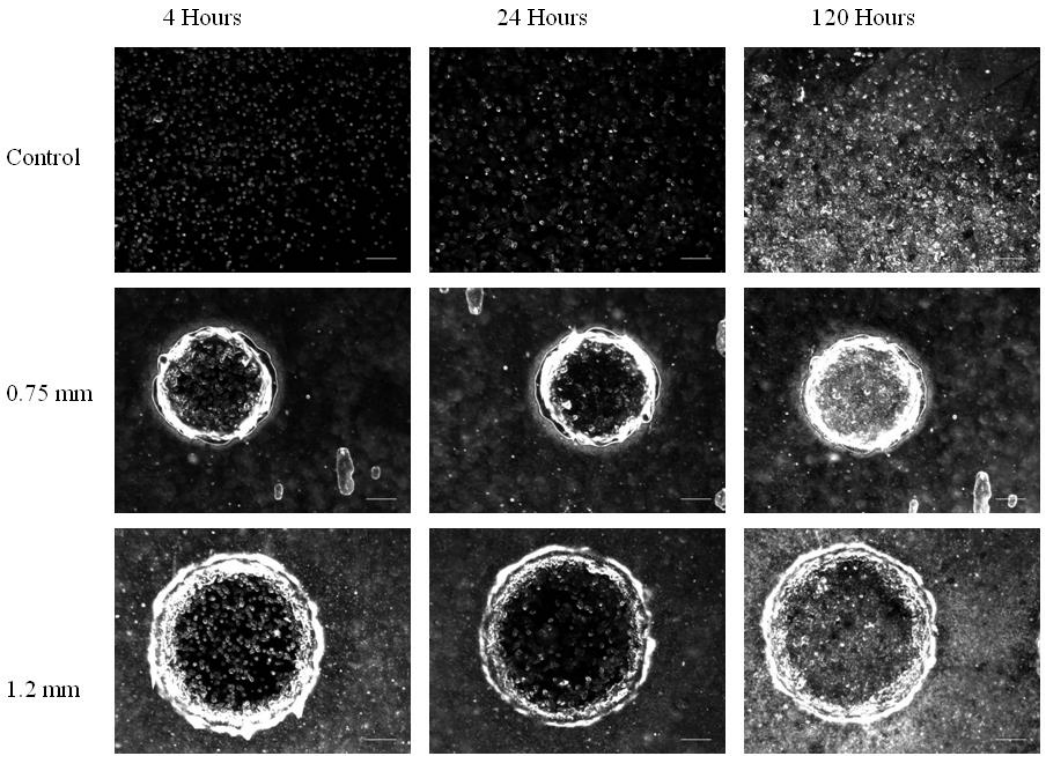

Figure 4.5: Micrographs of MCF-7 cells grown in different culture conditions over a period of 120 hours (5 days). Conditions shown are coverslip glass only (control), 0.75 mm hydrophilic PDMS well, and 1.2 mm hydrophilic PDMS well. Images were captured with a 4X objective. Scale bars are 0.2 mm.

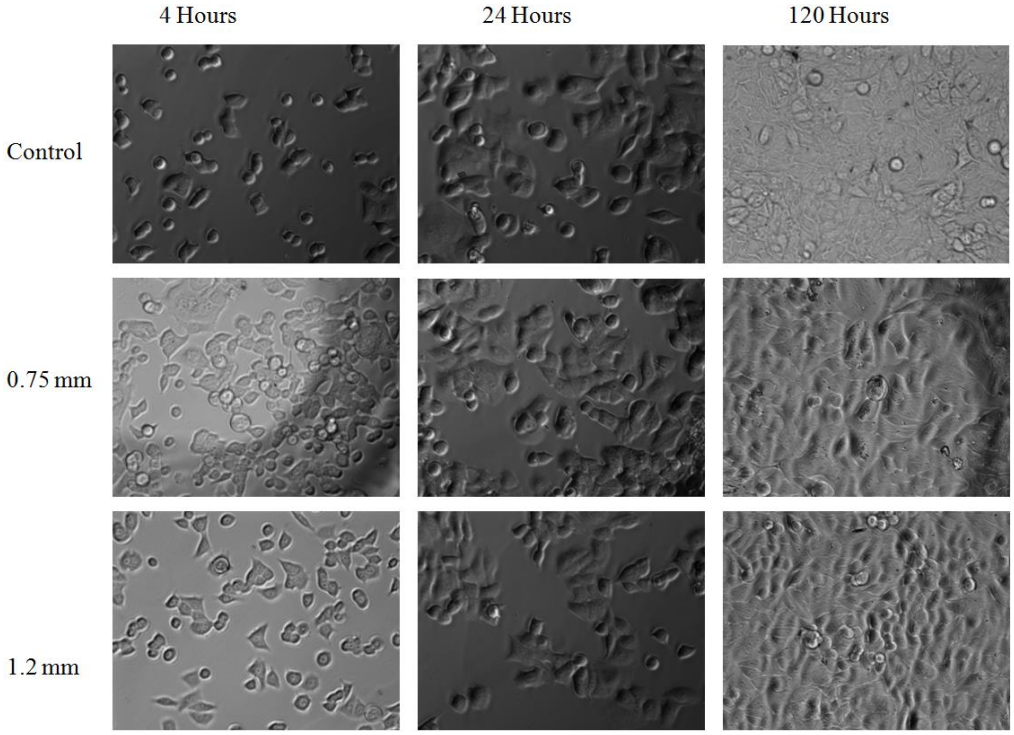

Figure 4.6: Micrographs of MCF-7 cells grown in different culture conditions over a period of 120 hours (5 days). Conditions shown are coverslip glass only (control), 0.75 mm hydrophilic PDMS well, and 1.2 mm hydrophilic PDMS well. Images were captured with a 20X objective. Scale bars are 0.2 mm.

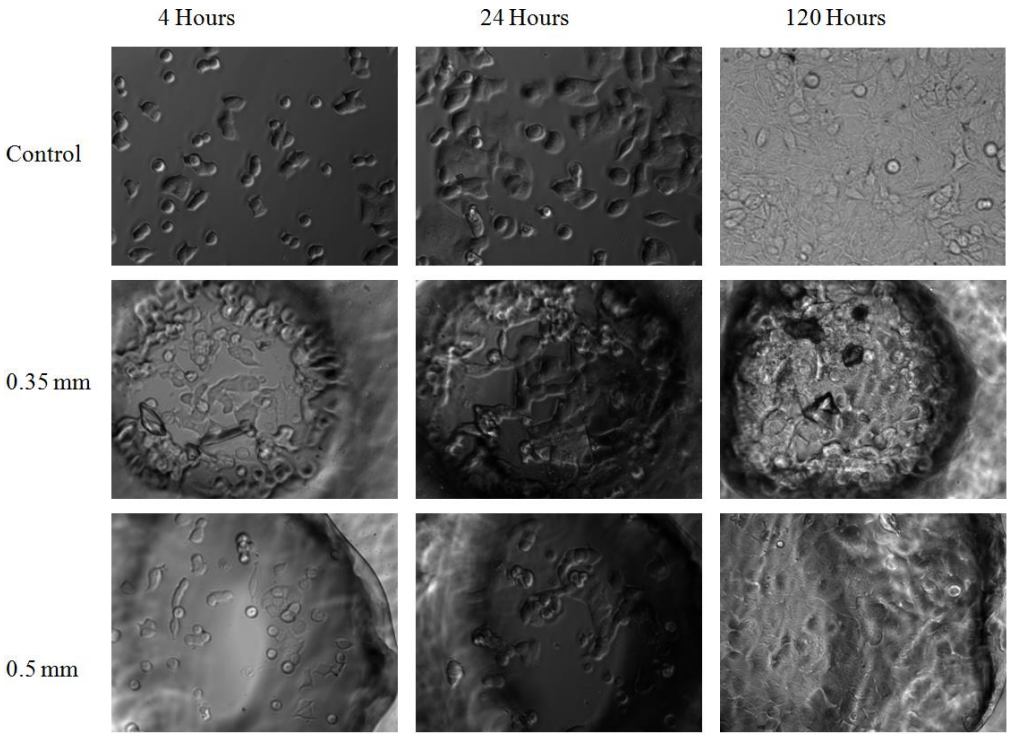

Figure 4.7: Micrographs of MCF-7 cells grown in different culture conditions over a period of 120 hours (5 days). Conditions shown are coverslip glass only (control), 0.35 mm hydrophilic PDMS well, and 0.5 mm hydrophilic PDMS well. Images were captured with a 20X objective. Scale bars are 0.2 mm.

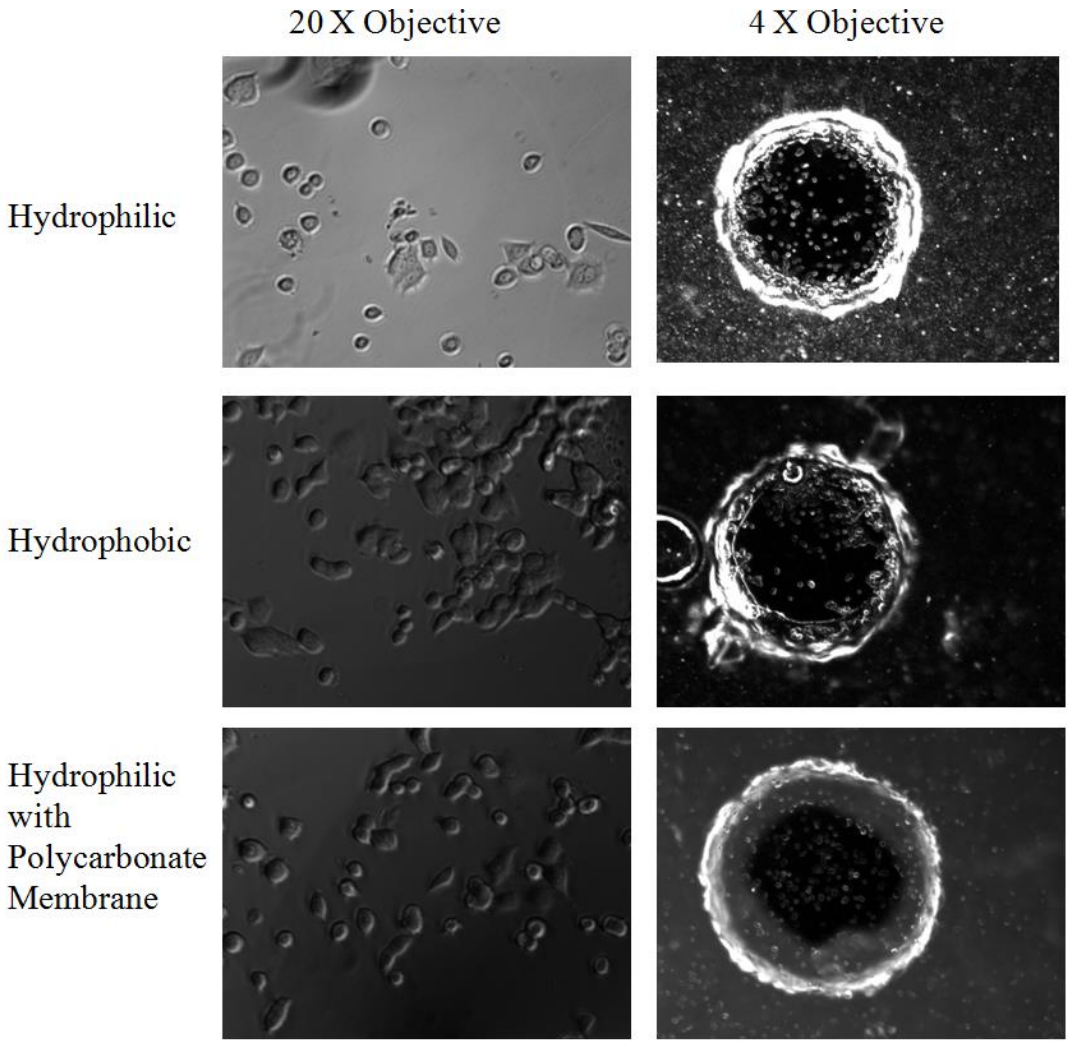

Figure 4.8: Comparison of micrographs of MCF-7 cells grown in different culture conditions over a period of 4 hours. Conditions shown are 1 mm hydrophilic PDMS well, 1 mm hydrophobic PDMS well, and 1 mm hydrophilic PDMS well with polycarbonate nanoporous membrane on top (not covering well). Images were captured with a 20X and a 4X objective.

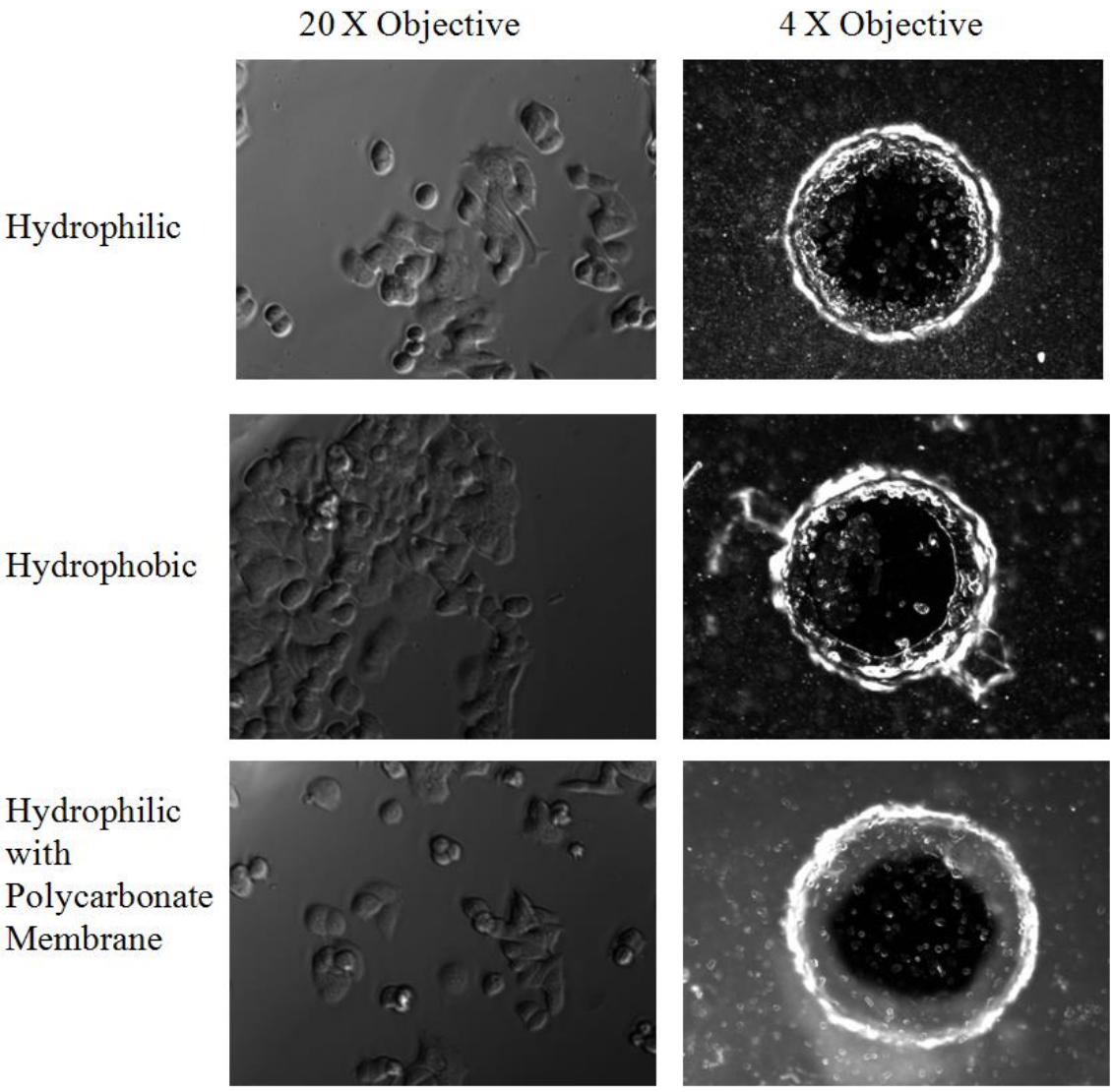

Figure 4.9: Comparison of micrographs of MCF-7 cells grown in different culture conditions over a period of 24 hours. Conditions shown are 1 mm hydrophilic PDMS well, 1 mm hydrophobic PDMS well, and 1 mm hydrophilic PDMS well with polycarbonate nanoporous membrane on top (not covering well). Images were captured with a 20X and a 4X objective.

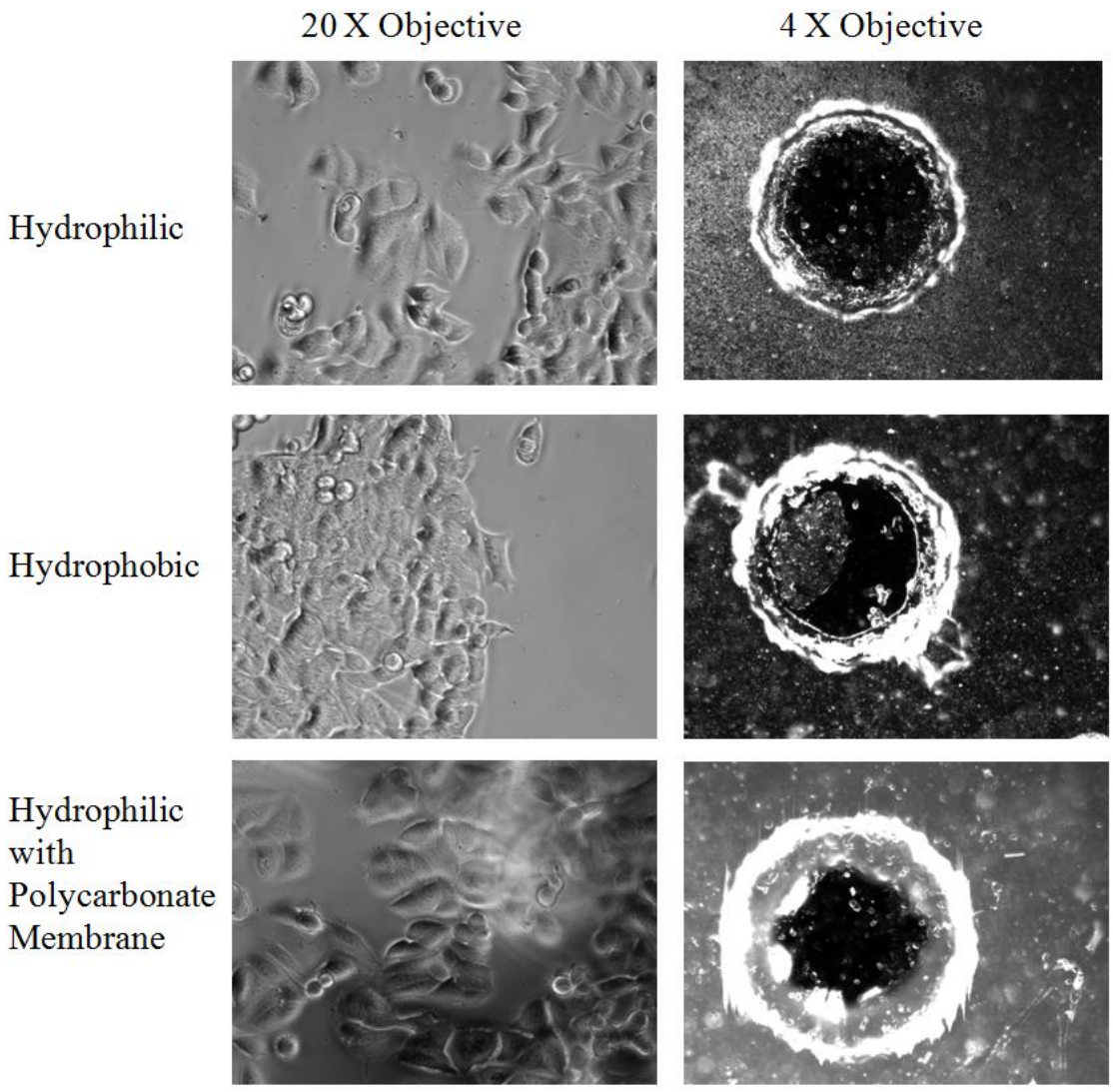

Figure 4.10: Comparison of micrographs of MCF-7 cells grown in different culture conditions over a period of 48 hours. Conditions shown are 1 mm hydrophilic PDMS well, 1 mm hydrophobic PDMS well, and 1 mm hydrophilic PDMS well with polycarbonate nanoporous membrane on top (not covering well). Images were captured with a 20X and a 4X objective.

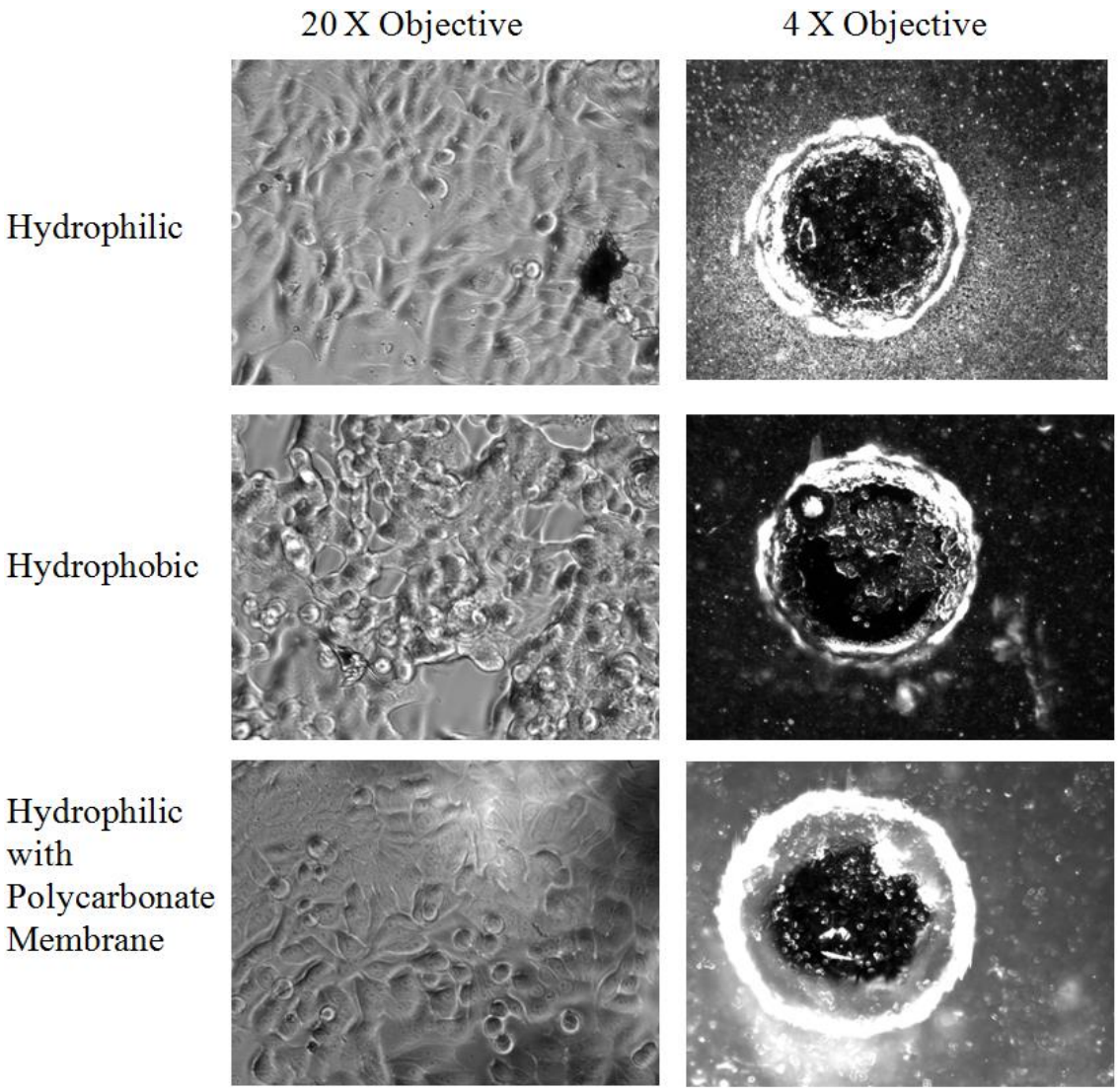

Figure 4.11: Comparison of micrographs of MCF-7 cells grown in different culture conditions over a period of 72 hours. Conditions shown are 1 mm hydrophilic PDMS well, 1 mm hydrophobic PDMS well, and 1 mm hydrophilic PDMS well with polycarbonate nanoporous membrane on top (not covering well). Images were captured with a 20X and a 4X objective.

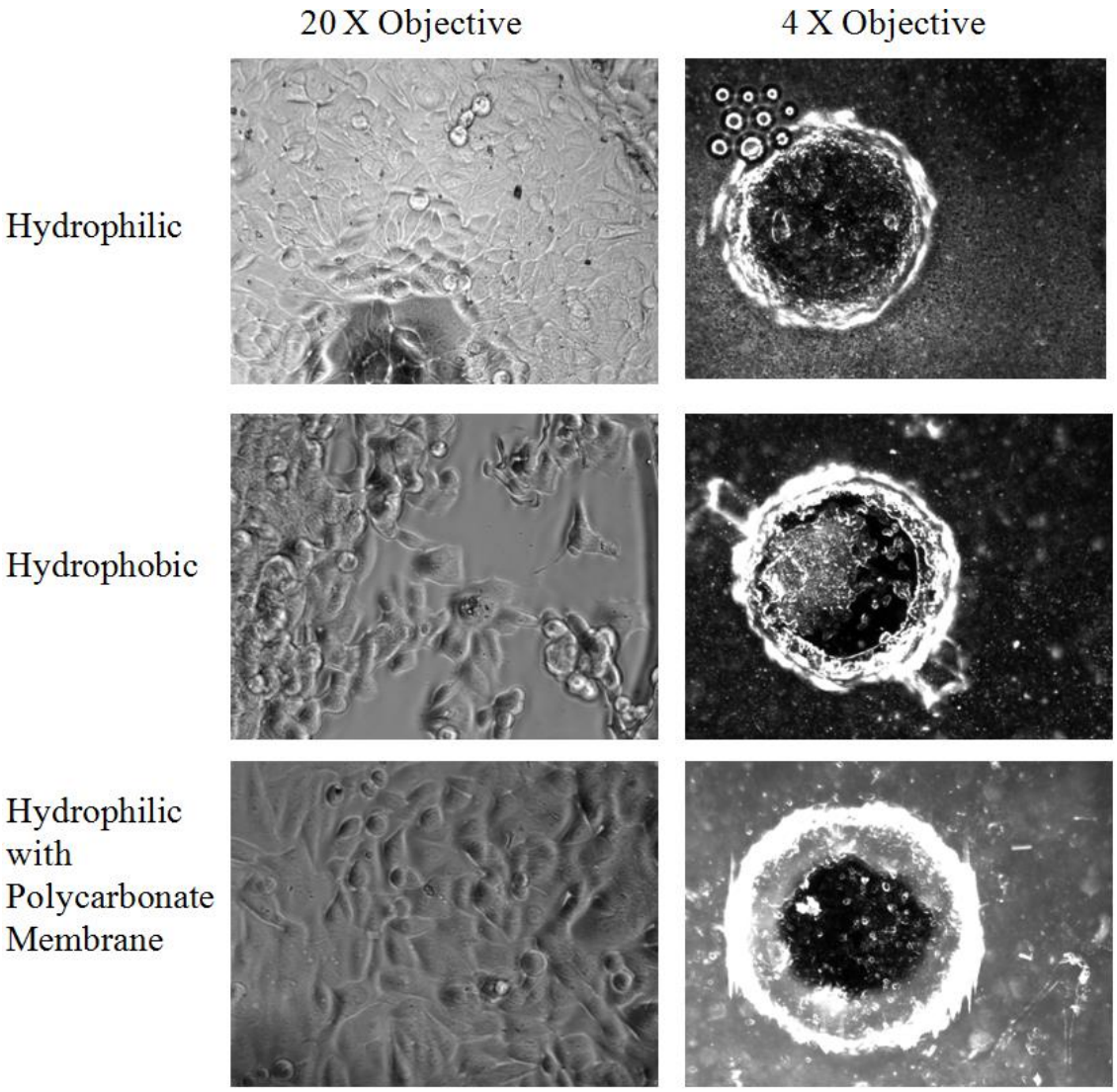

Figure 4.12: Comparison of micrographs of MCF-7 cells grown in different culture conditions over a period of 96 hours. Conditions shown are 1 mm hydrophilic PDMS well, 1 mm hydrophobic PDMS well, and 1 mm hydrophilic PDMS well with polycarbonate nanoporous membrane on top (not covering well). Images were captured with a 20X and a 4X objective.

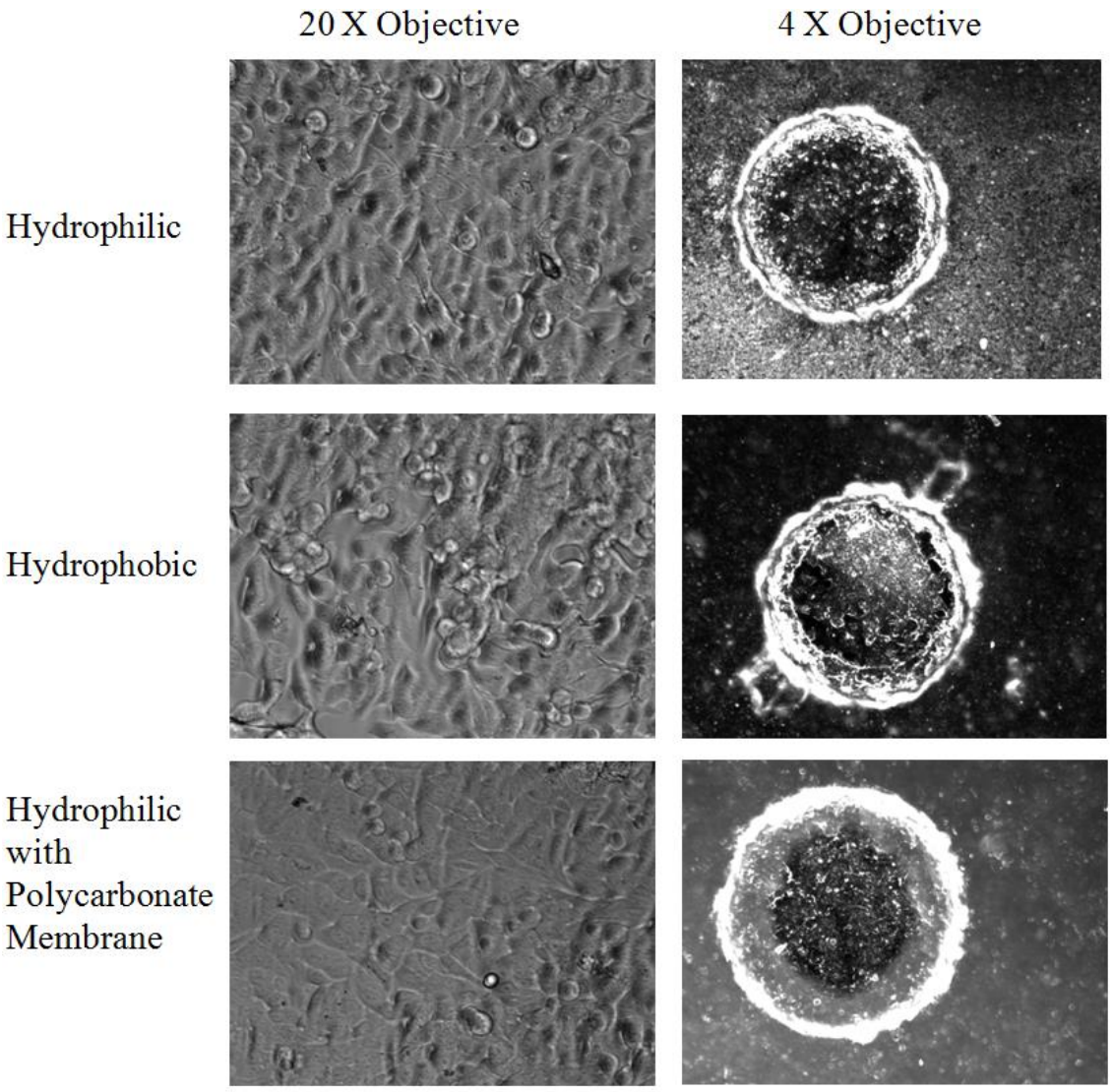

Figure 4.13: Comparison of micrographs of MCF-7 cells grown in different culture conditions over a period of 120 hours (5 days). Conditions shown are 1 mm hydrophilic PDMS well, 1 mm hydrophobic PDMS well, and 1 mm hydrophilic PDMS well with polycarbonate nanoporous membrane on top (not covering well). Images were captured with a 20X and a 4X objective.

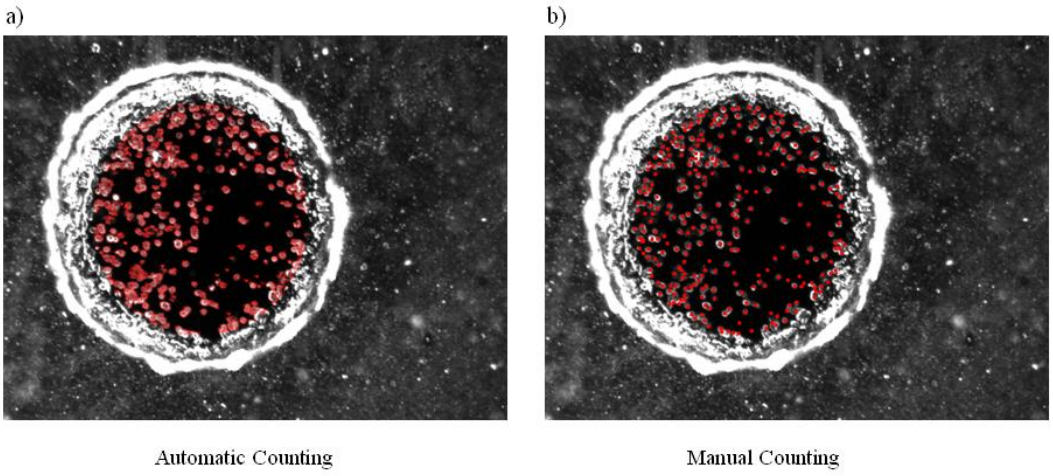

Figure 4.14: Automatic and manual counting in a 1.2 mm diameter well. Both methods were plugins from ImageJ. Images were captured at 4 Hours, with a 4X Objective.

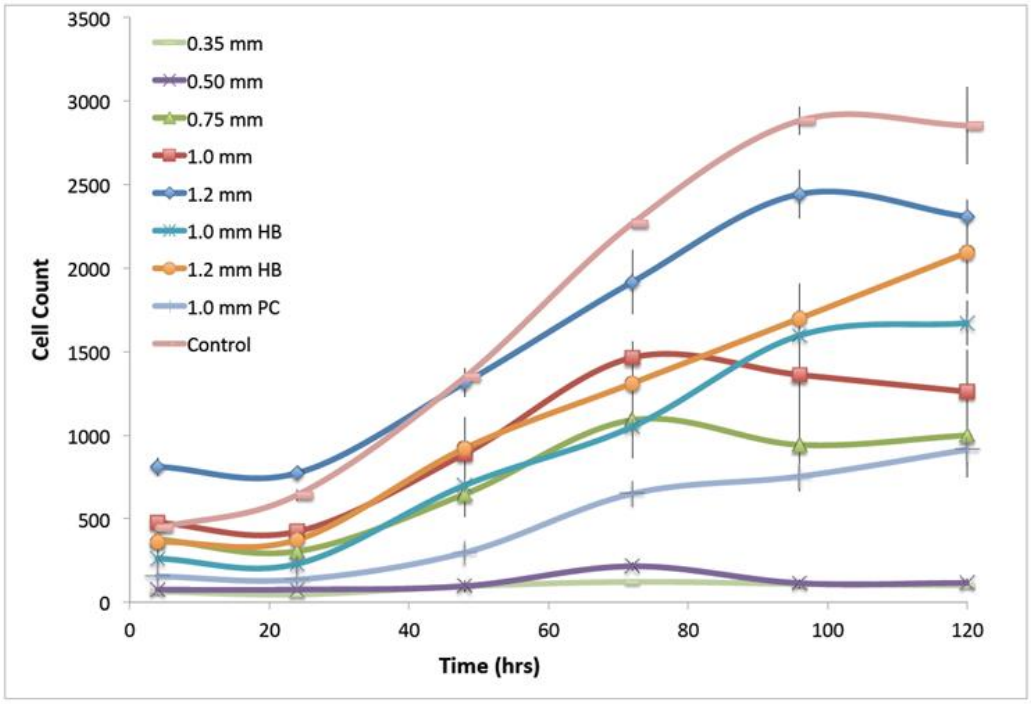

Figure 4.15: Proliferation rate of MCF-7 cells over a 120 hour (5 day) period. Culture conditions varied from 0.35 mm diameter to 1.2 mm diameter wells. Hydrophobic PDMS (HB), polycarbonate membrane (PC), and plain coverslip glass (control) were also compared. Except 0.35 mm and 0.5 mm diameter wells, all conditions exhibited an initial lag phase, followed by a sharp increase in cell number, and then finally leveling out. Error bars represent the standard deviation of 9 wells. In each case, cell viability was measured to be around 99% at the end of the 5 day period.

Chapter 5: Conclusion

5.1 Motivation and Objectives

In summary the project was aimed to address several needs in *in-vitro*, pre-clinical drug discovery: delivering drug dosages in a gradient to mammalian cells in a high-density format, but without having to overcome high surface tension forces present in existing high-density well-plates; attempt to mimic the *in-vivo* micro-environment in order to better predict the effects during clinical trials.

The objective of the project was to design a microfluidic device capable of: delivering drugs at different concentrations at a density of 16 wells within the equivalent area of a well in a 96 well-plate; culturing a single type of mammalian cell line in a high-density format; being compatible with the Perkin Elmer Opera automated microscope for high-content screening; have a high degree drug dose control via input parameters of an external applied electric field.

5.2 Summary of Findings and Conclusions

Chapter 2 laid out the potential final design of a lab-on-a-chip drug delivery device to mammalian cells in 16 separate wells. The proposed drug delivery mechanism was a nanoporous polycarbonate membrane, which was adopted from a drug delivery microfluidic device by R. Selvaganapathy *et. al*. A single microchannel was designed to snake around 16 separate wells and would hold the drug. The nanoporous membrane would separate the microchannel from the wells (Figure 2.1); based on the work of R. Selvaganapathy *et. al.*, the drug would cross the membrane and into the wells only when an external electric field was applied. It was proposed that the cells would be dispensed into the wells from the top, similar to a well-plate. The cells would rest on the bottom of the well, made of coverslip glass; coverslip glass is amenable to cell adherence and is thin enough (~170 μm) to be imaged with high magnification objective lenses (20X or greater) in inverted microscopes. A fabrication process flow and an experimental procedure were proposed. Based on the complexity of the design, 2 simpler devices were designed for validation purposes. The first was a single well device to test the drug dosage control. The second was a series of multi-well devices to validate cell attachment, proliferation, and viability for a single mammalian cell line.

The purpose of Chapter 3 was to validate drug delivery through a polycarbonate nanoporous membrane. For simplicity, a single well was used. The polycarbonate membrane chosen was hydrophobic in order to

prevent diffusion across it (Figure 3.2). Validation tests were based off the work by R. Selvaganapathy *et. al.*, which consisted of measuring the growth of the dye spot size during and after electrokinetic delivery, and measuring drug dose control. Three voltages were tested: 100 V, 125 V, and 150 V. Based on theoretical diffusion calculations, if the drug spot after electrokinetic delivery was zero, the drug would diffuse to the perimeter of the well (0.3 cm distance) in about 9000 seconds. However, the diffusion time was expected to be less than 9000 seconds because the dye spot would most certainly be greater than 0 mm, and the diffusion equation used did not account for the effect of the dye concentration gradient's effect on diffusive flux. It was observed that as the voltage was increased, the growth rate of the dye spot increased as well; when the voltage was turned off, for all 3 cases, the dye had diffused to the ends of the 6 mm diameter well within 5 minutes (300 seconds). As expected the experimental diffusion time was significantly less than what was theoretically calculated. For the dye dosage control study, it was found that the dye concentration increased almost linearly with the magnitude of the applied voltage and with the length of time that the voltage was applied.

For chapter 3, it is concluded that this design could be used for assays with a minimum drug delivery time of around 5 minutes, and that it could be viable for the integrated drug delivery device. However, it was not addressed how the magnitude of the electric fields used in this study could have an effect on cells in culture. It was speculated that the DC electric field, regardless of magnitude, would need to be pulsed in order to avoid harm to the cells; with greater electric field magnitude, the pulses should be most likely be shorter in duration.

Chapter 4 consisted of several multi-well devices at different diameters and PDMS surface properties. The purpose of Chapter 4 was to determine whether the cells would attach to the bottom, and remain viable, in PDMS micro-wells. Diameters tested were 0.35 mm, 0.5 mm, 0.75 mm, 1.0 mm, and 1.2 mm. Each device consisted of 9 wells of the same diameter (Figure 4.1). For 1.0 mm there were 3 different surface properties: hydrophilic PDMS, hydrophobic PDMS, and hydrophilic surface-treated polycarbonate membrane on top of PDMS. For 1.2 mm there were 2 different surface properties: hydrophilic PDMS and hydrophobic PDMS. All other diameters were tested with hydrophilic PDMS. Controls were plain coverslip glass. It was determined that all the devices except 0.35 mm and 0.5 mm had similar cell proliferation profiles as the controls. 0.35 mm and 0.5 mm diameters had only 1 of their 9 wells with cells growing in it. The hydrophobic PDMS wells had their cells clustering together, whereas the hydrophilic PDMS wells had their cells spread evenly. The polycarbonate membrane-topped wells had cells growing on top of the membrane and on the well bottom. All devices were measured to have 99% cell viability at the end of 120 hours in incubation.

For chapter 4, it was concluded that 0.35 mm and 0.5 mm diameters were unsuitable for the integrated device because of the unusual cell proliferation pattern, and from the apoptotic behaviour the cells had displayed after 24 hours of incubation. As well, the diameters 0.75 mm and greater could be suitable for the integrated device design if certain criteria were addressed, such as: a cell density that would not cover the entirety of the well bottom, replacement of the cell media often enough to keep the cells in healthy condition, and the PDMS well walls would remain hydrophilic throughout the testing period.

5.3 Contributions

Although mostly validative, this project had expanded upon practical application of electrokinetic molecular transport and microfluidic cell culture.

The architecture of the electrokinetic delivery device was simple, since it only consisted of a microchannel and a well; if the microchannel mould could be made with a 3D printer, the device could possibly be created without the use of a clean room. This could be useful to researchers who would like to have the capability of small-scaled chemical dosing, but do not have access to a clean room or do not want to use a device that has a complex operation. Another contribution was the validation of nanoporous membrane electrokinetic drug delivery into compartmentalized spaces. This study showed drug delivery dosage control into a well that contained liquid; in contrast, the work by R. Selvaganapathy *et. al.* demonstrated electrokinetic control of drug delivery into a large, open space that contained a hydro-gel. Example of previous work that have demonstrated control of drug delivery through a nanoporous membrane include: electrokinetic delivery from one compartment to another compartment, [Bohn PW, 2001] diffusion delivery from microchannel to compartment, [Melosh NA, 2011] and electrokinetic dye delivery from microchannel to microchannel. [Bohn PW, 2003] Possible applications of this study could be towards micro-environment control in tissue culture and to microfluidic-based micro-arrays such as the measurement of small molecule to protein interactions.

The study also contributed to the validation of PDMS-based micro-well plates. The micro-well cell culture device could aid other microfluidic researchers by integrating it into a more complex device, or as a micro-well layer in a multilayer device. These wells can also be inserted into the well of a 96 well-plate, increasing the number of effective wells without increasing the number of tall (1 cm) side-walls (such as with 384 and 1,536 well-plates). As well, the PDMS micro-wells could be rapidly

prototyped and customizable in terms of the shape of the wells, size of the wells, and spacing of the wells. Furthermore, fabrication could remain simple since hydrophilic surface modification may not be necessary for larger wells with a diameter of at least 1.0 mm (Figure 4.15). Open-well microfluidics could provide an alternative to closed-well microfluidics; advantages of open-well microfluidics are the potential compatibility with liquid-handling robots and that established cell culture protocols for well plates can readily be adopted.

Finally, based on the design in Chapter 2, the study has the potential to contribute to micro-environment control to multiple wells in parallel. If the design is demonstrated to work reliably in future studies, then the potential application could possibly be the replacement of well plates; if the device design is taken to industry, then these devices could be made out of similar materials as well plates such as hard plastics and borosilicate glass. Furthermore, the designed integrated device for small-scale dosage of drugs to cells could serve as a starting point towards an additional aid for automated high-content screening microscopes.

5.4 Future Directions

Since drug delivery to a single well device has been demonstrated, the next step would be to test drug delivery on a device with multiple wells. The number of wells should be designed in incremental steps; the end goal being 16 micro-wells within the equivalent area of a well (around 31.6 mm^2) of a 96 well plate. Issues such as independent drug delivery to each well, and the different electrical resistance to each well would need to be validated. Pertaining to the later, increased microchannel distance to each well would result in different electrical resistance, and hence a change in flux of drug to each well. However, the differences may not result in a significant change in overall drug dosage to each well. Since a variable in electrophoretic flow rate is electrical charge of a particle/molecule in solution, dosage of multiple dyes with different ionic charges should be calibrated.

A prototype combined microfluidic device, integrating drug delivery and cell culture, was designed in Chapter 2. Cells would be dispensed via pipetting, and would precipitate to the coverslip glass bottom. Drugs would enter the well from both microchannels by electrokinetic pumping, and then eventually reach the cells by diffusion. A predicted difficulty with the design is a chance that cross-contamination between wells could occur, since dispensed cell media would cover the tops of the wells. However, this problem could be circumvented if the well heights of the top layer are tall enough to slow or prevent diffusion. Lastly, two-dimensional

simulations of the electric field distribution and diffusion within each well will be completed in future work.

A problem addressed in the micro-well cell culture device was the lack of cells adhering to the bottom of wells with a diameter of 0.35 mm, when the cells were dispensed with a pipette. Hence, in addition to the design in Chapter 2, a second system of microchannels would need to be designed to deliver cells to wells that are less than or equal to 0.35 mm in diameter. For example, Lee L.P. et. al. had designed a microfluidic cell culture device that used microchannels to deliver cells to wells that were 0.28 mm in diameter. [Lee LP, 2005]

Other issues that would need to be investigated are the effects of applied external electric voltage on cell viability, and cell culture with multiple cell lines. Depending on the voltage amplitude, the cells could either have temporary open pores in their membrane, or have their membrane permanently damaged and kill the cells. Cell culture of multiple cell lines would be desirable since it could more closely mimic what happens *in vivo* than just a homogenous layer a single cell line.

Bibliography

- [Abraham VC, 2004]; Abraham, VC; Taylor, DL; Haskins, JR; High Content Screening Applied to Large-Scale Cell Biology; Elsevier Ltd.; TRENDS in Biotechnology; Vol. 22, No. 1; pp. 15-22; 2004.

- [Alanine AI, 2003]; Alanine, AI; Bleicher, KH; Bohm, HJ; Muller, K; Hit and Lead Generation: Beyond High-Throughput Screening; Nature Reviews, Drug Discovery; 2; pp. 369-378; 2003.

- [Bohn PW, 2001]; Bohn, PW; Sweedler, JV; Kuo, TC; Sloan, LA; Manipulating Molecular Transport through Nanoporous Membranes by Control of Electrokinetic Flow: Effect of Surface Charge Density and Debye Length; American Chemical Society; Langmuir; 17; pp. 6298-6303; 2001.

- [Bohn PW, 2003]; Bohn, PW; Sweedler, JV; Kuo, TC; Cannon Jr., DM; Shannon, MA; Hybrid Three-Dimensional Nanofluidic/Microfluidic Devices Using Molecular Gates; Elsevier Ltd.; Sensors and Actuators A; 102; pp. 223-233; 2003.

- [Campbell NA, 2005]; Campbell NA; Reece JB; Biology 7th Edition; Pearson Education Incorporated; ISBN 0-8053-7171-0; 2005.

- [Dickson M, 2004]; Dickson, M; Gagnon, JP; Key Factors in the Rising Cost of New Drug Discovery and Development; Nature Reviews; Drug Discovery; 3; pp. 417-429; 2004.

- [Eggert US, 2006]; Eggert, US; Mitchison, TJ; Small Molecule Screening by Imaging; Elsevier Ltd.; Current Opinion in Chemical Biology; 10; pp. 232-237; 2006.

- [Folch A., 2010]; Folch, A; Cate, DM; Sip, CG; A Microfluidic Platform for Generation of Sharp Gradients in Open-Access Culture; American Institute of Physics; Biomicrofluidics; 4; 044105; 2010.

- [Freshney RI, 2006]; Freshney, RI; Basic Principles of Cell Culture, in Culture of Cells for Tissue Engineering (eds G. Vunjak-Novakovic and R. I. Freshney); John Wiley & Sons, Inc.; Hoboken, NJ, USA.; doi: 10.1002/0471741817.ch1; 2006.

- [Lee LP, 2005]; Lee, LP; Lee, PJ; Hung, PJ; Rao, VM; Nanoliter Scale Microbioreactor Array for Quantitative Cell Biology; Biotechnology and Bioengineering; Vol. 94, No. 1; pp. 5-14; 2005.

- [Li Z., 2011]; Li, Z; Wei, Z; Li, X; Du, Q; Liang, Z; Efficient and High-Throughput Electroporation Chips; IEEE Transducers; Beijing, China, June 5-9; pp. 1825-1828; 2011.

- [Melosh NA, 2011]; Melosh, NA; VanDersarl, JJ; Xu, AM; Rapid Spatial and Temporal Controlled Signal Delivery Over Large Cell Culture Areas; Lab Chip; 11; pp. 3057-3063; 2011.

- [Micro Chem, 2002]; Micro Chem; Photoresist Working Guidelines; Nano SU-8 Negative Tone Photoresist Formulations 50-100; 2002.

- [Paul SM, 2010]; Paul, SM; Mytelka, DS; Dunwiddie, CT; Persinger, CC; Munos, BH; Lindborg, SR; Schacht, AL; How to Improve R&D Productivity: the Pharmaceutical Industry's Grand Challenge; Nature Reviews; Drug Discovery; 9; pp. 203-214; 2010.

- [Quake SR, 2007]; Quake, SR; Gomez-Sjoberg, R; Leyrat, AA; Pirone, DM; Chen, CS; Versatile, Fully Automated, Microfluidic Cell Culture System; Anal. Chem.; 79; pp. 8557-8563; 2007.

- [Roberts PE, 1998]; Roberts, PE; Mather, JP; Introduction to Cell and Tissue Culture: Theory and Technique; Springer; ISBN 0585275718, 9780585275710; 1998.

- [Schiavone P, 2008]; Schiavone, P; Fuard, D; Tzvetkova-Chevolleau, T; Decossas, S; Tracqui, P; Optimization of Poly-Di-Methyl-Siloxane (PDMS) Substrates for Studying Cellular Adhesion and Motility; Elsevier Ltd.; Microelectronic Engineering; 85; pp. 1289-1293; 2008.

- [Selvaganapathy PR, 2010]; Selvaganapathy, PR; Upadhyaya, S; Microfluidic Devices for Cell Based High Throughput Screening; Lab Chip; 10; pp. 341 – 348; 2010.

- [Shellman YG, 2005]; Shellman, YG; Ribble, D; Goldstein, NB; Norris, DA; A Simple Technique for Quantifying Apoptosis in 96-Well Plates; BMC Biotechnology; 5:12; 2005.

- [Thermo Fisher Scientific Inc., 2010]; Thermo Fisher Scientific Inc.; Off-Target Effects: Disturbing the Silence of RNA Interference (RNAi); Tech Review; 00082-06-F-03-U; www.thermoscientific.com; 2010.

- [Ursell TS, 2007]; Ursell, TS; The Diffusion Equation A Multi-Dimensional Tutorial; Department of Applied Physics, California Institute of Technology; Pasadena, CA 91125; October 2007.

- [Weinberg NA, 2007]; Weinberg, NA; The Biology of Cancer; Garland Science, Taylor & Francis Group, LLC; ISBN 0-8153-4076-1; 2007.

- [Zheng W, 2008]; Zheng, W; Titus, SA; Li, X.; Southall, N; Inglese, J; Brasch, M; Austin, CP; A Cell-Based PDE4 Assay in 1536 Well-Plate Format for High Throughput Screening; Journal of Biomolecular Screening; 13(7); pp. 609-618; 2008.

- [Zuck P, 2004]; Zuck, P; Murray, EM; Stec, E; Grobler, JA; Simon, AJ; Strulovici, B; Inglese, J; Flores, OA; Ferrer, M; A Cell-Based β-Lactamase Reporter Gene Assay for the Identification of Inhibitors of Hepatitis C Virus Replication; Elsevier Ltd.; Analytical Biochemistry; 334; pp. 344-355; 2004.

Appendices

Appendix 1: MATLab Program used to Measure Absorbance Values from Chapter 2

```
%Show an image, then specify coordinates using imrect function.

clc %Clear Command Window
close all %Close all objects (such as figures).
clear all %Clear all variables, etc.


% Template For Image Analysis


RGB=imread('(PG0005)150V3M.JPG'); %Read the image file matrix, and input
into workspace.
BW=rgb2gray(RGB); %Convert the image file from RGB to black and white.
BW2 = imrotate(BW,0.7,'bilinear','crop'); %Rotate the image.

% figure, imshow(BW); %Show the black and white image in a new window.

% h = imrect(gca, []); %Make an interactive rectangle on the image.
% figure, imshow(BW2); %Show the rotated image in a new window.
% h = imrect(gca, [10 10 100 100]); %Make an interactive rectangle on
the image.
% api = iptgetapi(h);
% api.addNewPositionCallback(@(p) title(mat2str(p)));
% fcn = makeConstrainToRectFcn('imrect',...
%                  get(gca,'XLim'),get(gca,'YLim'));
% api.setPositionConstraintFcn(fcn); %Record the position vector in the
title of the image.

X=BW2(750:2189,2366:2465); %Take the desired portion of the image file.

figure, imshow(X); %Show the desired portion in a new window.
Intensity_Avg=mean(X,2); %Average pixel values of each row. Produces a
column vector.
% figure, imshow(Intensity_Avg); %Show the averaged intensity in a new
window.

xlswrite('Intensity Plot', Intensity_Avg,'3 Min') %Write the numerical
matrix.



RGB=imread('(PG0004)150V2M.JPG'); %Read the image file matrix, and input
into workspace.
```

```
BW=rgb2gray(RGB); %Convert the image file from RGB to black and white.
BW2 = imrotate(BW,0.7,'bilinear','crop'); %Rotate the image.

% figure, imshow(BW); %Show the black and white image in a new window.
% figure, imshow(BW2); %Show the rotated image in a new window.

X=BW2(750:2189,2366:2465); %Take the desired portion of the image file.

figure, imshow(X); %Show the desired portion in a new window.
Intensity_Avg=mean(X,2); %Average pixel values of each row. Produces a
column vector.
% figure, imshow(Intensity_Avg); %Show the averaged intensity in a new
window.

xlswrite('Intensity Plot', Intensity_Avg,'2 Min') %Write the numerical
matrix.
```

Appendix 2: ImageJ Macro Used to Perform Automated Cell Counting from Chapter 3

```
//BG correct
run("Subtract Background...", "rolling=250");

//manually set threshold to include only cells
setThreshold(462, 3802);

//find maxima above threshold
run("Find Maxima...", "noise=100 output=[Segmented Particles] exclude above");

//select well area
makeOval(272, 185, 568, 619);

//set threshold for mask
setThreshold(129, 255);

//analyse particles
run("Analyze Particles...", "size=0-Infinity circularity=0.00-1.00 show=[Bare
Outlines] summarize add");
```